THE BARRIER PROPERTIES OF THE SKIN OF AQUATIC AND SEMI-AQUATIC VERTEBRATES

JULIA GAUBERG

A THESIS SUBMITTED TO
THE FACULTY OF GRADUATE STUDIES
IN PARTIAL FULFILLMENT OF THE REQUIREMENTS
FOR THE DEGREE OF
MASTER OF SCIENCE

GRADUATE PROGRAM IN BIOLOGY
YORK UNIVERSITY
TORONTO, ONTARIO

SEPTEMBER 2017

Abstract

Vertebrate skin is a heterogeneous organ that acts as a barrier to the external environment. A crucial structure for skin barrier function is the tight junction (TJ) complex that links skin epidermal cells. TJ proteins have been examined in mammalian skin but little is known about skin TJ proteins of vertebrates residing permanently or semi-permanently in water. This thesis provides new insights into the effect of abiotic and biotic factors on skin of fishes and amphibians using rainbow trout and the Australian green tree frog as models. The effects of water ion content and photoperiod on skin barrier properties and TJ proteins of trout are reported. Additionally, the effects of a deadly amphibian fungus, *Batrachochytrium dendrobatidis*, on skin TJ proteins of a frog are documented for the first time. This thesis provides novel information on skin TJ proteins of aquatic and semi-aquatic vertebrates and how they respond to environmental change.

Dedication and Acknowledgements

I would like to thank my supervisor Dr. Scott P. Kelly, whose guidance, advice and continual support has helped me develop into the scientist that I am today. Thank you for creating an environment where I could grow, take risks, and attend many, many conferences! I am certain that other Kelly Lab scientists will agree with me when I say that the Kelly Lab will forever hold a special place in our hearts!

Thank you to my advisor, Dr. Andrew Donini, whose kindness and willingness to help ensured my success in many of the experiments and award applications that I decided to undertake.

Thank you to Prof. Craig Franklin from the University of Queensland, for being my host supervisor in Australia during our 3-month collaboration. Thank you for trusting me to do good work and providing me with encouragement along the way!

I would also like to thank Drs. Tamara Kelly, Jean-Paul Paluzzi, and Carol Bucking for their support throughout my MSc.

Thank you to members of the Kelly Lab! Not only those who I was able to work with—Fargol, Anna, Chun, Sean, Sheralyn, and Connie—but also to Kelly Lab graduates Phuong Bui and Dr. Helen Chasiotis who provided valuable insights from afar!

A special thank you goes out to Ana Cuciureanu whose eagerness to learn has made my role as a mentor an easy one. I have likely learned from you as much as you have learned from me!

Thank you to members of the Franklin lab—Ross, Cameron, Niclas, Sam, Kathleen, Daniel and Harriet—for welcoming me with open arms and teaching me Australian slang! Special thanks goes out to Dr. Rebecca Cramp and Nicholas Wu: I would not have been able to complete my study abroad without you!

I want to also thank my partner Dr. Dennis Kolosov who has always believed in me, supported me and helped me grow as a scientist and as a person. Thank you for being beside me every step of the way! I hope that we can go on supporting each other in our careers for many years to come.

Finally, thank you to members of the Donini and Paluzzi labs for inspiring me to work hard each and every day!

List of Tables

List of Figures

List of Illustrations

LIST OF ABBREVIATIONS

11β-hsd – 11β-hydroxysteroid dehydrogenase

ADB - antibody-dilution buffer

ANOVA – analysis of variance

Bd – Batrachochytrium dendrobatidis

BMAL1 – Brain and Muscle ARNT-Like 1

bTJ – bicellular TJ

cDNA – cloned DNA

Cgn – cingulin

Cldn – claudin

CLOCK – Circadian Locomotor Output Cycles Kaput

Cry – Cryptochrome

DAPI - 4',6-diamidino-2-phenylindole

ECL – extracellular loop

FITC - fluorescein isothiocyanate

FW – freshwater

GR – Glucocorticoid receptor

GTF – green tree frog

IPW – ion-poor water

MARVEL - myelin and lymphocyte and related proteins for vesicle trafficking and membrane link

MR – Mineralocorticoid receptor

mRNA – messenger RNA

Ocln – occludin

PBS – phosphate-buffered saline

PEG – polyethylene glycol

Per – Period

PVDF - polyvinylidene difluoride

qPCR – quantitative real-time polymerase chain reaction

RNA – ribonucleic acid

RT-PCR – reverse transcriptase polymerase chain reaction

SDS-PAGE – sodium dodecyl sulphate polyacrylamide gel electrophoresis

SEM – standard error of the mean

SW – seawater

TAMP – tight junction-associated MARVEL protein

TJ(s) – tight junction(s)

Tric– tricellulin

tTJ – tricellular TJ

ZO-1 – zonula occludens 1

Statement of Contribution

Chapter One
This chapter was written by Julia Gauberg with valuable contributions from Dr. Scott P. Kelly. All illustrations were designed by Julia Gauberg unless otherwise stated.

Chapter Two
This chapter was written by Julia Gauberg with valuable contributions from Dr. Scott P. Kelly. Immunohistochemistry, qPCR, Western blot optimisation, permeability studies, and all other experiments were performed by Julia Gauberg. All illustrations were designed by Julia Gauberg unless otherwise stated.

Chapter Three
This chapter was written by Julia Gauberg with valuable contributions from Dr. Scott P. Kelly. Genomic search, cloning and characterization of rainbow trout clock and MMP genes and qPCR was performed by Julia Gauberg. 24-hour serum sampling was done by Julia Gauberg with valuable contribution from Laura Ana Cuciureanu. Muscle moisture content was measured by Laura Ana Cuciureanu. All illustrations were designed by Julia Gauberg unless otherwise stated.

Chapter Four
This chapter was written by Julia Gauberg with valuable contributions from Dr. Scott P. Kelly. Genomic search, cloning and characterization of Australian green tree frog TJ genes, immunohistochemistry, qPCR, Western blot optimisation, and permeability studies were performed by Julia Gauberg with guidance from Dr. Scott P. Kelly and Prof. Craig E. Franklin. Collection of experimental animals, slough monitoring, preparation of fungal inoculum and infection load measurements were performed by Nicholas Wu and Dr. Rebecca L. Cramp from The University of Queensland, Australia. Illustration was designed by Julia Gauberg.

Chapter Five
This chapter was written by Julia Gauberg. Illustration was designed by Julia Gauberg.

Chapter One: General introduction to the vertebrate skin and the tight junction complex

1. General introduction

1.1 The skin of vertebrates

All vertebrate species possess an integumentary system that covers the body surface and generally acts as a barrier to the external environment (Lillywhite, 2006). Due to its crucial role as a barrier tissue, the fundamental structure of vertebrate skin can be easily observed across all vertebrate species (Lillywhite, 2006). Different vertebrate species may possess skin modifications that serve a particular function, an obvious example being the flight feathers of birds, but the basic structure remains as: an epidermis that is in direct contact with the external environment, separated by a basement membrane from the underlying dermis (**Illustration 1.1;** Lillywhite, 2006). The vertebrate dermis is composed of connective tissue and collagen, and contains nerves, blood vessels, pigments, and other structures (e.g. scales, poison glands) (Elliot, 2000). The epidermis is composed mostly of epithelial cells with other species-specific cell types (e.g. mucous cells, alarm cells) interspersed among them (Lillywhite, 2006; Raker et al., 2010). The vertebrate epidermis can generally be subdivided into four distinct regions: the *stratum basale,* the *stratum spinosum,* the *stratum granulosum,* and the *stratum corneum* (Colville and Bassert, 2002**; Illustration 1.1a**). The *stratum basale* is made up of a single layer of skin precursor cells that divide and are pushed upwards to make up the other cell layers. The cells of the *stratum spinosum* begin to express keratin, a family of intermediate filaments that provide strength and water-resistance to the skin (Colville and Bassert, 2002). When cells enter the *stratum granulosum* layer, they begin to flatten, generate more keratin and, in terrestrial animals, their nuclei and organelles begin to disintegrate (Colville and Bassert, 2002). Finally, by the time that cells reach the *stratum corneum*, they are

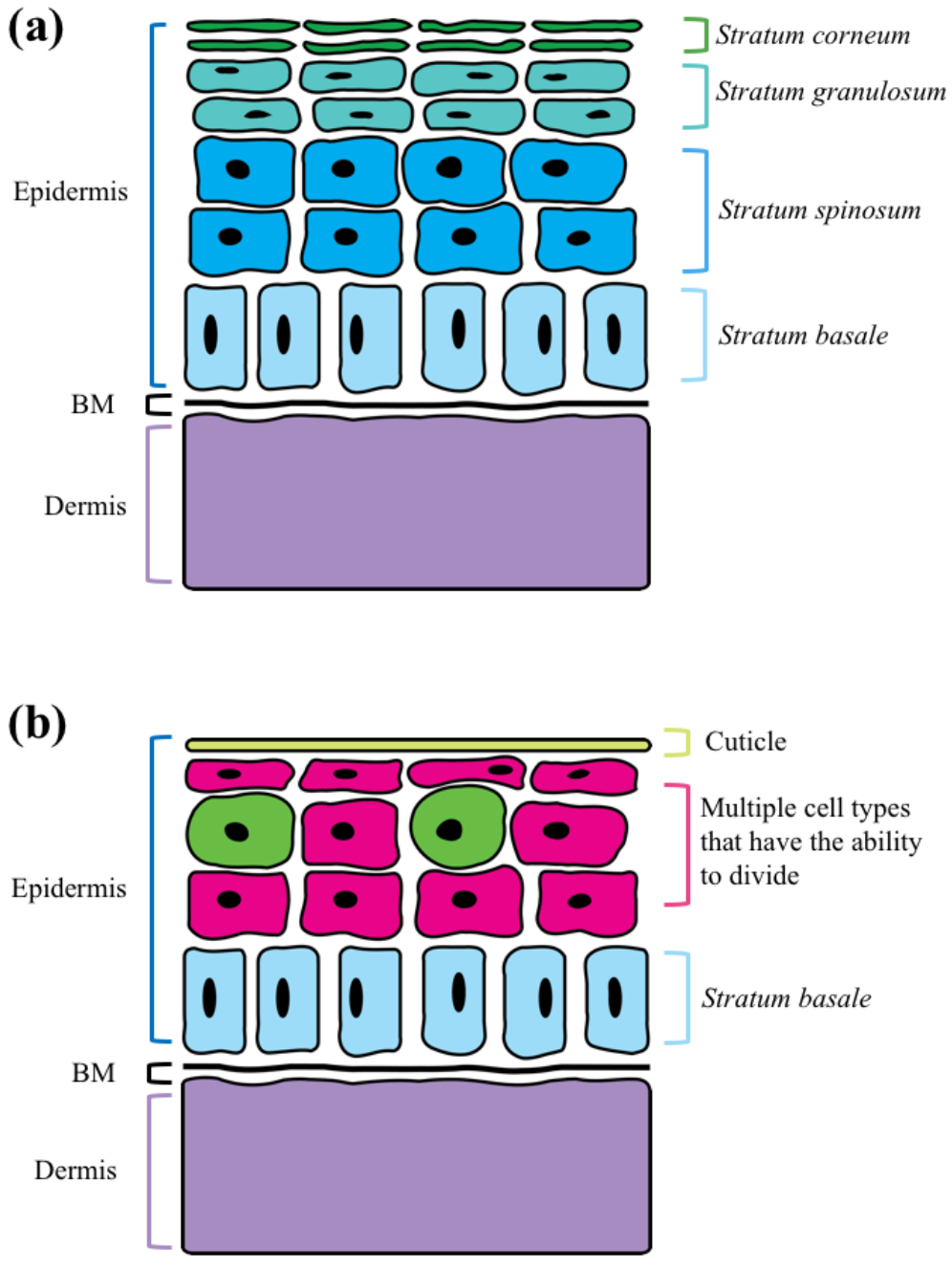

Illustration 1.1 Simplified diagrams of the (a) general skin structure in vertebrates and (b) fish skin structure. BM= basement membrane.

dead and only contain keratin and keratin-associated proteins. This layer is important for terrestrial and semi-aquatic animals because it acts as a barrier to pathogens and to water loss (Colville and Bassert, 2002). Fishes are the only vertebrates that lack the *stratum corneum* layer, which may be due to the fact that they evolved in an aquatic environment where they do not run the risk of desiccation (Rakers et al., 2010). As a result, all cells in fish skin are living and, although the main skin-progenitor cells are located in the *stratum basale*, all cells in the epidermis have the ability to divide (Henrikson and Matoltsy. 1968; Rakers et al., 2010; **Illustration 1.1b**). Because they lack a *stratum corneum*, fishes secrete a mucopolysaccharide cuticle for added protection from the external environment (Hawkes, 1974). Fishes are also the only vertebrates to possess dermal-derived scales, which are secreted by cells in the dermis and are generally covered by epidermis (Bone and Moore, 2008). Therefore, although the general structure of the skin is conserved among vertebrates, fishes possess a slightly different structure.

1.2 The tight junction complex

All vertebrates possess epithelial and endothelial tissue, which maintain distinct body compartments and separate the variable external environment from the relatively constant internal milieu of the organism (Gonzalez-Mariscal et al., 2003). To maintain specific compartments, epithelia and endothelia must (1) be made up of polarized cells—where the top (apical) and bottom (basal) sides of the cell differ—and (2) form relatively impermeable barriers to their surrounding medium (Gonzalez-Mariscal et al., 2003). The tight junction (TJ) complex, present between all epithelial and endothelial cells, is used to accomplish these tasks (Gonzalez-Mariscal et al., 2003). TJ complexes are present between adjacent cells, where they form "kissing" points on the apical side of a cell that seal the intercellular space between them **(**Gonzalez-Mariscal et al., 2003). Most

junctions occur at the boundary where two cells meet (bicellular junctions; bTJ) or at corners where three cells meet (tricellular junctions; tTJ) (**Illustration 1.2)**. TJs are known to play two roles in epithelia and endothelia. One of their functions is to act as a "fence" and maintain cell polarity, where TJs prevent proteins on the apical side of the cell from intermixing with the basolateral proteins (Pisam and Ripoche, 1976). Their second role is to act as a "gate" and regulate the paracellular permeability of a tissue: the movement of solutes between cells of an epithelium or endothelium (Fromter and Diamond, 1972). In this way, TJs form a barrier to the unwanted movement of solutes, ions, water, and pathogens into or out of the internal fluids (Günzel, 2017).

Although the term "tight junction" implies that TJs create an impassable barrier to solute movement, this is not true of most TJs, where their permeability can be regulated selectively (Gonzalez-Mariscal et al., 2003). Indeed**,** in general there is less resistance for solutes to move through TJs between cells than to cross the plasma membranes of a cell (Fromter and Diamond, 1972). Tissue resistance can typically be correlated with the number of TJ strands that are present between cells, which explains why the mammalian proximal kidney tubule, having an average of 1.2 strands between cells, has less electrical resistance than the urinary bladder of a toad with 8 strands (Claude and Goodenough, 1973). However, strand number cannot always predict the "tightness" of an epithelial tissue. Certain tissues, such as the frog urinary bladder and rabbit ileum, can have comparable numbers of TJ strands, but large differences in ion conductance (Martinez-Palomo and Erlij, 1975). Thus, the molecular components that make up a TJ complex must be able to confer selectivity to the paracellular pathway.

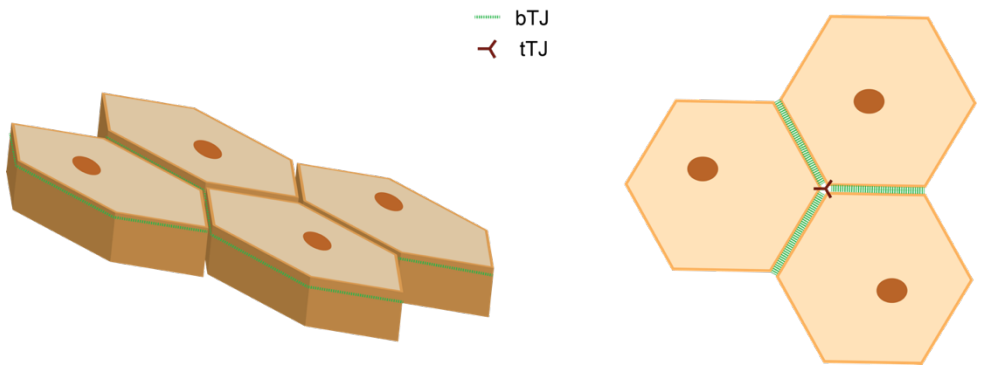

Illustration 1.2 Diagram of bicellular tight junctions (bTJ) and tricellular tight junctions (tTJ) between epithelial cells.

It is now known that several groups of proteins make up the TJ complex and regulate the paracellular permeability between adjacent cells (**Illustration 1.3**). These include cytosolic scaffolding proteins (e.g., ZO-1, cingulin) and transmembrane proteins (e.g., occludin, claudins, tricellulin) (Gonzalez-Mariscal et al., 2003). Transmembrane proteins span the space between adjacent cells, whereas cytosolic proteins anchor the transmembrane TJ proteins to the actin cytoskeleton within the cell. Together, they act in concert to regulate the paracellular permeability of a tissue.

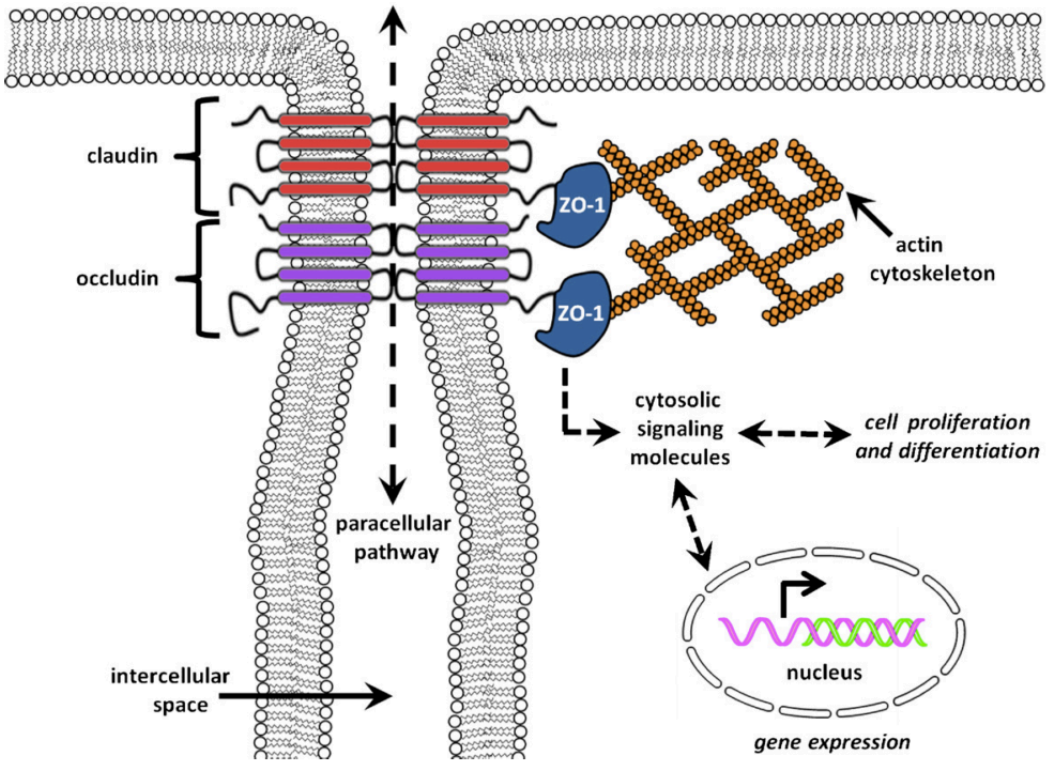

Illustration 1.3 Model of the TJ complex between epithelial cells. Claudin and Occludin proteins are transmembrane proteins that occlude the intercellular space and regulate paracellular permeability. ZO-1 and other scaffolding proteins link the transmembrane proteins to the actin cytoskeleton and act as signal transducers. From Chasiotis et al., 2012a.

1.2.1 Cytosolic scaffolding proteins: ZO-1 and Cingulin

The first TJ protein ever discovered was aptly named Zonula Occludens-1 (ZO-1; Stevenson et al., 1986), however, additional ZO proteins have since been characterized in vertebrates (Bauer et al., 2010). The current understanding of ZO-1 protein function is that it plays two roles in the cell. The first is to provide structural support to transmembrane TJ proteins (e.g. Claudins, Occludin) by linking it to the cytoskeleton. This is accomplished with the presence of domains that specifically interact with transmembrane TJ proteins and a carboxyl terminal that interacts with cytoskeletal actin (Bauer et al., 2010). The other function of ZO-1 is to act as a signal transducer by activating cellular signaling pathways that affect gene expression, differentiation and epithelial proliferation

(Gonzalez-Mariscal et al., 2003). With regards to its function in the TJ complex, it was found to be important for the assembly of TJs in mammalian epithelial cell culture, where ZO-1 silencing led to a drastic slowing of TJ formation (McNeil et al., 2006). Indeed, ZO-1 protein was shown to be crucial for embryonic development mice, where ZO-1 knockouts were lethal (Katsuno et al., 2008). However, in developed TJs, depletion of ZO-1 was found to have no deleterious effects on the continued function of the TJ complex (McNeil et al., 2006). Less is known about the function of ZO-1 in aquatic vertebrates. In goldfish (*Carassius auratus*) and rainbow trout (*Oncorhynchus mykiss*), ZO-1 was found to be broadly expressed in discrete organs (Chasiotis and Kelly, 2012; Kolosov et al., 2014). Additionally, the abundance of *zo-1* transcript altered throughout the development of cultured rainbow trout gill epithelia and responded to environmental changes in goldfish (Chasiotis et al., 2012b). Additionally, mammalian ZO-1 has been found to interact with another cytosolic TJ protein, cingulin, isolated from mammals and the African clawed frog, *Xenopus laevis* (D'Atri et al., 2002; Guillemot and Citi, 2006).

Cingulin (Cgn) is another cytosolic TJ protein that provides structural support to the TJ complex (Gonzalez-Mariscal et al., 2003). Like ZO-1, Cgn interacts directly with the actin cytoskeleton, and is believed to help organize actin filaments during the formation of the TJ complex (Guillemot and Citi, 2006). In addition, Cgn has been found to interact with other cytoskeletal components, such as myosin and microtubules in mammalian cell culture (Cordenonsi et al., 1999a; Yano et al., 2013). In aquatic vertebrates, Cgn exhibited ubiquitous tissue expression and altered in abundance during the development of epithelial barrier properties (Kolosov et al., 2014). Cgn was also found to interact with the transmembrane protein Occludin in *Xenopus,* in addition to its interaction with ZO-1 (Cordenonsi et al., 1999b; D'Atri et al., 2002). Therefore,

both ZO-1 and Cgn are important scaffolding proteins that provide structural support to the TJ complex.

1.2.2 Transmembrane TJ proteins

TJ proteins that are embedded in the plasma membrane can be classified according to the number of transmembrane regions that they possess (Günzel and Fromm, 2012). Proteins possessing one, three or four transmembrane regions have been discovered in epithelial and endothelial TJ complexes, but the four transmembrane proteins have been the subjects of greatest study (Günzel and Fromm, 2012). These tetraspan proteins fall into two protein families: (1) the TJ-associated MARVEL proteins (TAMPs), which include Occludin (Ocln) and Tricellulin (Tric), and (2) the Claudin (Cldn) family (Günzel and Fromm, 2012).

1.2.2.1 The TAMPs Ocln and Tric

The first transmembrane TJ protein discovered was Ocln (Furuse et al., 1993). Ocln appears to have arisen in deuterostomes as an important structural protein (Chapman et al., 2010) and since its discovery it has been found in the epithelia and/or endothelia of almost all vertebrate groups (Feldman et al., 2005). Ocln possesses cytosolic N- and C-terminal domains as well as two loops of similar size that extend from the cell exterior (Furuse et al., 1993; **Illustration 1.4**). Around 130 amino acids in the C-terminal domain are conserved among various vertebrate species (Ando-Akastuka et al., 1996; Chasiotis and Kelly, 2008). The first extracellular loop (ECL), which interacts with other Ocln proteins, has very few charged amino acids (Feldman et al., 2005). The interaction of Ocln ECLs between adjacent cells helps to maintain the "fence" and "gate" functions of the TJ complex (Lacaz-Vieira et al., 1999).

Given its widespread distribution in vertebrates, Ocln is regarded to play an important role in the TJ complex, however, it is not essential for TJ function. A great example of this dichotomy can be seen in Ocln knockout mice, where the mice are viable and exhibit no change in epithelial barrier function, but develop pathologies such as growth retardation, bone thinning and brain calcification (Saitou et al., 2000). Additionally, Ocln does not seem to be responsible for the ion-selectivity of an epithelium because it lacks charged amino acids in its ECL (Yu et al., 2005). Therefore, other transmembrane proteins must be present that provide ion-selectivity to an epithelial tissue: the Claudin superfamily of proteins (see **section 1.2.2.2** below). In fishes, Ocln is well studied and has been correlated to epithelial paracellular permeability (Chasiotis et al., 2010). Ocln has been shown to alter in mRNA abundance with epithelial development, salinity change, and osmoregulatory hormones in a variety of aquatic animals (Chasiotis and Kelly, 2009; Kolosov et al., 2014; Chasiotis et al., 2010). Therefore, Ocln is an important TJ component that does not contribute to the ion-selectivity of a tissue.

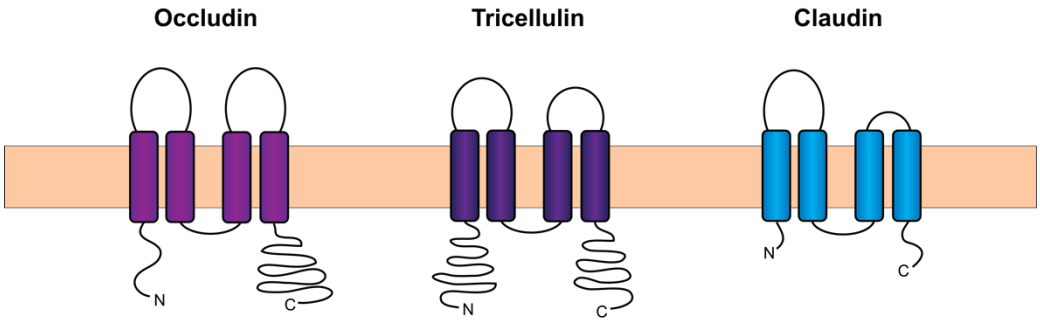

Illustration 1.4 Transmembrane tendency of 3 tetraspanin tight junction

Tric has cytosolic N- and C-terminals, and two ECLs (Ikenouchi et al., 2005; **Illustration 1.4**). Additionally, Tric shares some C-terminal homology with Ocln, and both possess a four transmembrane MARVEL domain, which allows these proteins to traffic to cholesterol-rich

regions of the plasma membrane (Sánchez-Pulido et al., 2002; Ikenouchi et al., 2005). However, Tric is unique because it belongs to the only transmembrane protein family (angulins) that is concentrated at regions of tricellular contact between vertebrate epithelial cells (Ikenouchi et al., 2005; Kolosov and Kelly, 2013). Although sequence similarity between vertebrate groups is not high (e.g. 55% similarity between rainbow trout and mouse Tric; Kolosov and Kelly, 2013), the function of this protein is conserved among vertebrates. Tric seals the hollow "tube" that is formed between three cells and restricts passage to macromolecules and ions, which decreases overall paracellular permeability (Krug et al., 2009; Kolosov and Kelly, 2013). This protein is also important in the organization of bicellular and tricellular TJs, where knockdown of Tric in mouse cell culture affects the development of bTJs (Ikenouchi et al., 2005). Therefore, Tric plays an important role in maintaining the integrity of the vertebrate TJ complex and limiting macromolecule movement.

1.2.2.2 Cldn TJ proteins

Cldns comprise a large superfamily of proteins, from 27 proteins in mammals to 63 in fishes (Chasiotis et al., 2012a; Gunzel and Fromm, 2012). The large difference in the number of Cldns between these groups is the result of a whole genome and tandem gene duplication events that occurred in teleost fishes (Chasiotis et al., 2012a). The majority of our knowledge on Cldns comes from studies into the mammalian or teleostean Cldn proteins.

Cldns possess the same structural characteristics as Ocln and Tric (**Illustration 1.4**), but bear no sequence similarity (Feldman et al., 2005). Additionally, unlike Ocln, the expression of Cldns in cells is sufficient to form TJ strands, and loss of just one Cldn protein may greatly affect the paracellular permeability of a tissue (Furuse et al., 1998; Furuse et al., 2002). For example,

Cldn-1 knockout mice exhibited impairment of the epidermal barrier and died shortly after birth (Furuse et al., 2002). Similarly, knockdown of Cldn-b (Claudin-30 homologue) in larval zebrafish led to an increase in whole-body permeability and sodium efflux (Kwong and Perry, 2013). Therefore, Cldn proteins appear to be important in the formation and maintenance of the TJ barrier in vertebrates.

The function of each Cldn protein is a result of its structural characteristics. Cldns have one ECL that is larger than the other, which contains charged amino acids (Günzel and Fromm, 2012). When the ECLs of Cldn proteins interact, the charged amino acids determine the ion selectivity: they can form ion-selective barriers or pores. This is a complex concept, given that a tissue possessing TJs is "tighter" than one lacking TJs altogether. However, in an established TJ complex, the expression of a pore-forming TJ protein would increase paracellular permeability, whereas a barrier-forming TJ protein would decrease it (Günzel and Fromm, 2012). Using knockdown and overexpression studies, several Cldns have been characterized into these categories. In mammals, Cldn-1 is known to be barrier-forming and Cldn-2 is pore-forming (Günzel and Fromm, 2012) and in fishes, Cldn-30, -31 and -8d are barrier-forming, (Kwong and Perry, 2013; Kolosov et al., 2017; Kolosov and Kelly, 2017).

In addition to their individual barrier- and pore-forming properties, Cldn proteins have a specific set of binding partners within a TJ strand or across cells, which further increases their ability to regulate the paracellular permeability of a tissue (Gonzalez-Mariscal, 2003). For example, in mammals, Cldn-1 is able to interact with Cldn-1 and Cldn-3 but not Cldn-2 (Piontek et al., 2011). Additionally, in rainbow trout, knockdown of Cldn-31 in a cultured gill epithelium affected Cldn-8d levels, indicating that they may be binding partners in the gill (Kolosov et al., 2017). In contrast, knockdown of Cldn-8d did not affect Cldn-31 (Kolosov and Kelly, 2017).

Given that these proteins possess different ion-selective properties, altering Cldn-Cldn interactions may change the ion selectivity of a tissue.

Finally, Cldn proteins also exhibit discrete organ and cell distribution (Günzel and Fromm, 2012; Chasiotis et al., 2012a; Bui and Kelly, 2014; Gauberg et al., 2017), providing each tissue with a unique capacity for regulating paracellular permeability. For example, spatial differences in the expression of barrier- and pore-forming Cldn proteins can explain the difference in permeability of the "leaky" proximal and "tight" distal segments of the nephron in the vertebrate kidney (Angelow et al., 2008). Overall, the large number of Cldns expressed in vertebrates, the unique properties of each Cldn protein, and the discreet organ (and within-tissue) distribution indicates that they are non-redundant in their function and that they play a dominant role in regulating the paracellular permeability and ion selectivity of a tissue.

1.3 TJ proteins in the skin of vertebrates

The majority of what is known about TJs in the skin of vertebrates comes from studies on mammals. TJ proteins can localize to the epidermal cells or to vasculature in the dermis. To date, Ocln, Tric, ZO-1, Cgn and multiple Cldn proteins have been detected and localized in the mammalian epidermis (Kirschner and Brandner, 2012; **Illustration 1.5**). Like in simple epithelia, TJs and TJ proteins in the stratified epidermis act as barriers to solute movement out of the extracellular fluid and into the external environment (Hashimoto, 1971; Furuse et al., 2002; Yamamoto et al., 2008). However, because the epidermis is stratified, the function of TJ proteins in all epidermal layers may not be the same. The outermost living layer of epidermal cells, which in most vertebrates is the *stratum granulosum*, was found to be responsible for providing barrier properties to the skin as it was the only layer to inhibit the passage of various molecular tracers

(Hashimoto, 1971; Martinez-Palomo et al., 1971; Furuse et al., 2002; **Illustration 1.5**). Interestingly, mammalian TJ proteins were found to exhibit different expression patterns within the epidermis and all reported TJ proteins were present in the *stratum granulosum* (Kirschner and Brandner, 2012; **Illustration 1.5**). The presence of all TJ proteins in the *stratum granulosum* may explain why this layer provides the barrier functions to the epidermis. Indeed, the role that TJ proteins play in providing barrier properties to the epidermis can be further observed in human skin diseases, such as psoriasis vulgaris. In this disease, particular TJ proteins that were only expressed in the upper layers of the epidermis began exhibiting broader expression in the deeper layers (Yoshida et al., 2001; Kirschner et al., 2009). This was also correlated to the movement of a molecular tracer out of the epidermis, which was inhibited deeper in the skin (in the *stratum spinosum*) with psoriasis instead of the *stratum granulosum* (Brandner et al., 2015). Therefore, TJ proteins are important for providing barrier properties to the epidermis, specifically the *stratum granulosum*.

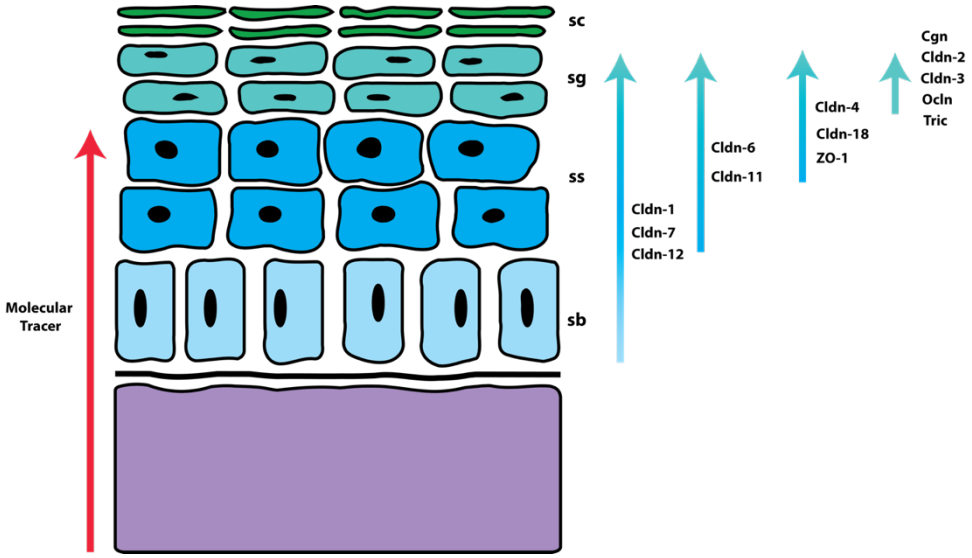

Illustration 1.5 The localization of various TJ proteins in the mammalian epidermis. TJ proteins can localize to different epidermal layers. The movement of a molecular tracer through the epidermis is also visualized, passing through all epidermal layers and stopping at the *stratum granulosum*. sb= *stratum basale*, ss= *stratum spinosum*, sg= *stratum granulosum*, sc= *stratum corneum*. Based on data from Kirschner and Brandner, 2012.

As was mentioned above, the majority of studies conducted on TJ proteins in the skin have been performed on mammals. In this regard, other vertebrate groups have received little attention on this topic. Aquatic and semi-aquatic vertebrates that live in, or are frequently in contact with, an aqueous environment are especially valuable to investigate. Their skin is an important barrier because it must limit the passive movement of ions and solutes into the water, and any disruption of the skin barrier can result in the loss of homeostasis (Kent et al., 1988; Voyles et al., 2009). Additionally, the transcripts encoding at least 25 different *cldn* genes have been detected in the skin of one group of aquatic vertebrates, the teleost fishes (Loh et al., 2004; Gauberg et al., 2017) and a few of these have been found to respond to environmental salinity (Bagherie-Lachidan et al., 2008, 2009) or cortisol, the principal corticosteroid of teleost fishes (Gauberg et al., 2017). In another vertebrate group, the amphibians, skin *ocln* mRNA abundance was found to change with salinity (Chasiotis and Kelly, 2009). Apart from these studies, nothing is known about how TJ proteins regulate the barrier properties of the skin of aquatic and semi-aquatic vertebrates. Therefore, this thesis will provide a first look into the barrier properties of the skin that are attributed by the TJ complex in the teleost fish *Oncorhynchus mykiss* and the amphibian *Litoria caerulea*.

1.4 References

Angelow, S., Ahlstrom, R., Yu, A.S.L., 2008. Biology of claudins. Am. J. Physiol. Renal Physiol. 295, F867–F876.

Ando-Akatsuka, Y., Saitou, M., Hirase, T., Kishi, M., Sakakibara, A., Itoh, M., Yonemura, S., Furuse, M., Tsukita, S., 1996. Interspecies diversity of the Occludin sequence: cDNA cloning of human, mouse, dog, and rat-kangaroo homologues. J. Cell Biol. 133, 43–47.

Bauer, H., Zweimueller-Mayer, J., Steinbacher, P., Lametschwandtner, A., Bauer, H.C., 2010. The dual role of zonula occludens (ZO) proteins. J. Biomed. Biotechnol. 2010.

Bone, Q., Moore, R., 2008. Biology of Fishes. Abingdon, Oxon: Taylor & Francis. pp. 13-32.

Bagherie-Lachidan, M., Wright, S.I., Kelly, S.P., 2008. Claudin-3 tight junction proteins in *Tetraodon nigroviridis* : cloning, tissue-specific expression, and a role in hydromineral balance. Am J Physiol Integr Comp Physiol 294, 1638–1647.

Bagherie-Lachidan, M., Wright, S.I., Kelly, S.P., 2009. Claudin-8 and -27 tight junction proteins in puffer fish *Tetraodon nigroviridis* acclimated to freshwater and seawater. J. Comp. Physiol. B. 179, 419–31.

Brandner, J., Zorn-Kruppa, M., Yoshida, T., Moll, I., Beck, L., De Benedetto, A., 2015. Epidermal tight junctions in health and disease. Tissue Barriers 3, 1–13.

Bui, P., Kelly, S.P., 2014. Claudin-6, -10d and -10e contribute to seawater acclimation in the euryhaline puffer fish *Tetraodon nigroviridis*. J. Exp. Biol. 217, 1758–67.

Chasiotis, H., Kelly, S.P., 2008. Occludin immunolocalization and protein expression in goldfish. J. Exp. Biol. 211, 1524–1534.

Chasiotis, H., Kelly, S.P., 2009. Occludin and hydromineral balance in *Xenopus laevis*. J. Exp. Biol. 212, 287–296.

Chasiotis, H., Wood, C.M., Kelly, S.P., 2010. Cortisol reduces paracellular permeability and increases Occludin abundance in cultured trout gill epithelia. Mol. Cell. Endocrinol. 323, 232–8.

Chasiotis, H., Kelly, S.P., 2012. Effects of elevated circulating cortisol levels on hydromineral status and gill tight junction protein abundance in the stenohaline goldfish. Gen. Comp. Endocrinol. 175, 277–83.

Chasiotis, H., Kolosov, D., Bui, P., Kelly, S.P., 2012a. Tight junctions, tight junction proteins and paracellular permeability across the gill epithelium of fishes: a review. Respir. Physiol. Neurobiol. 184, 269–81.

Chasiotis, H., Kolosov, D., Kelly, S.P., 2012b. Permeability properties of the teleost gill epithelium under ion-poor conditions. Am. J. Physiol. Regul. Integr. Comp. Physiol. 302, R727-39.

Chapman, J. a, Kirkness, E.F., Simakov, O., Hampson, S.E., Mitros, T., Weinmaier, T., Rattei, T., Balasubramanian, P.G., Borman, J., Busam, D., Disbennett, K., Pfannkoch, C., Sumin, N., Sutton, G.G., Viswanathan, L.D., Walenz, B., Goodstein, D.M., Hellsten, U., Kawashima, T., Prochnik, S.E., Putnam, N.H., Shu, S., Blumberg, B., Dana, C.E., Gee, L.,

Kibler, D.F., Law, L., Lindgens, D., Martinez, D.E., Peng, J., Wigge, P. a, Bertulat, B., Guder, C., Nakamura, Y., Ozbek, S., Watanabe, H., Khalturin, K., Hemmrich, G., Franke, A., Augustin, R., Fraune, S., Hayakawa, E., Hayakawa, S., Hirose, M., Hwang, J.S., Ikeo, K., Nishimiya-Fujisawa, C., Ogura, A., Takahashi, T., Steinmetz, P.R.H., Zhang, X., Aufschnaiter, R., Eder, M.-K., Gorny, A.-K., Salvenmoser, W., Heimberg, A.M., Wheeler, B.M., Peterson, K.J., Böttger, A., Tischler, P., Wolf, A., Gojobori, T., Remington, K. a, Strausberg, R.L., Venter, J.C., Technau, U., Hobmayer, B., Bosch, T.C.G., Holstein, T.W., Fujisawa, T., Bode, H.R., David, C.N., Rokhsar, D.S., Steele, R.E., 2010. The dynamic genome of Hydra. Nature 464, 592–6.

Claude P., Goodenough DA., 1973. Fracture faces of zonulae occludentes from "tight" and "leaky" epithelia. J Cell Biol 58, 390-400.

Colville, T.P., Bassert, J.M., 2002. Clinical anatomy and physiology for veterinary Technicians. St. Louis: Mosby. pp. 149-156.

Cordenonsi, M., D'Atri, F., Hammar, E., Parry, D.A.D., Kendrick-Jones, J., Shore, D., Citi, S., 1999a. Cingulin contains globular and coiled-coil domains and interacts with ZO-1, ZO-2, ZO-3, and myosin. J. Cell Biol. 147, 1569–1581.

Cordenonsi, M., Turco, F., Atri, F.D., Hammar, E., Martinucci, G., Meggio, F., Citi, S., 1999b. *Xenopus laevis* Occludin. Identification of in vitro phosphorylation sites by protein kinase CK2 and association with cingulin. Eur. J. Biochem. 264, 374–384.

D'Atri, F., Nadalutti, F., Citi, S., 2002. Evidence for a functional interaction between cingulin and ZO-1 in cultured cells. J. Biol. Chem. 277, 27757–27764.

Elliott, D.G., 2000. Chapter 17 - Integumentary System, in: Ostrander, G.K. (Ed.), The Laboratory Fish, Handbook of Experimental Animals. Academic Press, London, pp. 271–306.

Feldman, G.J., Mullin, J.M., Ryan, M.P., 2005. Occludin: Structure, function and regulation. Adv. Drug Deliv. Rev. 57, 883–917.

Fromter, E., Diamond, J., 1972. Route of passive ion permeation in epithelia. Nat. New Biol. 235, 9–13.

Furuse, M., Hata, M., Furuse, K., Yoshida, Y., Haratake, A., Sugitani, Y., Noda, T., Kubo, A., Tsukita, S., 2002. Claudin-based tight junctions are crucial for the mammalian epidermal barrier: A lesson from Claudin-1-deficient mice. J. Cell Biol. 156, 1099–1111.

Furuse, M., Hirase, T., Itoh, M., Nagafuchi, a., Yonemura, S., Tsukita, S., Tsukita, S., 1993. Occludin: A novel integral membrane protein localizing at tight junctions. J. Cell Biol. 123, 1777–1788.

Furuse M, Sasaki H, Fujimoto K, Tsukita S. 1998. A single gene product, claudin-1 or -2, reconstitutes tight junction strands and recruits occludin in fibroblasts. J Cell Biol 141: 1539-1550.

Gauberg, J., Kolosov, D., Kelly, S.P., 2017. Claudin tight junction proteins in rainbow trout (*Oncorhynchus mykiss*) skin: Spatial response to elevated cortisol levels. Gen. Comp. Endocrinol. 240, 214–226.

Gonzalez-Mariscal, L., Betanzos, A., Nava, P., Jaramillo, B., 2003. Tight junction proteins. Prog. Biophys. Mol. Biol. 81, 1–44.

Guillemot, L., Citi, S., 2006. Cingulin, a cytoskeleton-associated protein of the tight junction, in Tight Junctions. Springer US, Boston, MA, pp. 54–63.

Günzel, D., Fromm, M., 2012. Claudins and other tight junction proteins. Compr. Physiol. 2, 1819–1852.

Günzel, D., 2017. Claudins: vital partners in transcellular and paracellular transport coupling. Pflugers Arch. Eur. J. Physiol. 1–10.

Hashimoto, K. 1971. Intercellular spaces of the human epi- dermis as demonstrated with lanthanum. J. Invest.Dermatol. 57: 17–31.

Hawkes, J.W., 1974. The structure of fish skin. Cell Tissue Res. 149, 147–158.

Henrikson, R., Matoltsy, A.G., 1968. The fine structure of teleost epidermis. 1. Introduction and filament-containing cells. J. Ultrastruct. Res. 21, 194–212.

Ikenouchi, J., Furuse, M., Furuse, K., Sasaki, H., Tsukita, S., Tsukita, S., 2005. Tricellulin constitutes a novel barrier at tricellular contacts of epithelial cells. J. Cell Biol. 171, 939–945.

Katsuno, T., Umeda, K., Matsui, T., Hata, M., Tamura, A., Itoh, M., Takeuchi, K., Fujimori, T., Nabeshima, Y., Noda, T., Tsukita, S., Tsukita, S., 2008. Deficiency of Zonula Occludens-1 causes embryonic lethal phenotype associated with defected yolk sac angiogenesis and apoptosis of embryonic cells. Mol. Biol. Cell 19, 2465–2475.

Kent, M.., Dungan, C.F., Elston, R.A., Holt, R.A., 1988. *Cytophaga* sp. (Cytophagales) infection in seawater pen-reared Atlantic salmon *Salmo salar*. Dis. Aquat. Organ. 4, 173–179.

Kirschner, N., Brandner, J.M., 2012. Barriers and more: Functions of tight junction proteins in the skin. Ann. N. Y. Acad. Sci. 1257, 158–166.

Kirschner, N., Poetzl, C., Driesch, P.V. Den, Wladykowski, E., Moll, I., Behne, M.J., Brandner, J.M., 2009. Alteration of tight junction proteins is an early event in psoriasis putative involvement of proinflammatory cytokines. Am. J. Pathol. 175, 1095–1106.

Kolosov, D., Chasiotis, H., Kelly, S.P., 2014. Tight junction protein gene expression patterns and changes in transcript abundance during development of model fish gill epithelia. J. Exp. Biol. 217, 1667–81.

Kolosov, D., Donini, A., Kelly, S.P., 2017. Claudin-31 contributes to corticosteroid-induced alterations in the barrier properties of the gill epithelium. Mol. Cell. Endocrinol. 439, 457–466.

Kolosov, D., Kelly, S.P., 2013. A role for Tricellulin in the regulation of gill epithelium permeability. Am. J. Physiol. Regul. Integr. Comp. Physiol. 304, R1139-48.

Kolosov, D., Kelly, S.P., 2017. Claudin-8d is a cortisol-responsive barrier protein in the gill epithelium of trout J. Mol. Endocrinol. 59, 1-12.

Krug, S.M., Amasheh, S., Richter, J.F., Milatz, S., Gunzel, D., Westphal, J.K., Huber, O., Shulzke, J.D., Fromm, M., 2009. Tricellulin forms a barrier to macromolecules in tricellular tight junctions without affecting ion permeability. Mol. Biol. Cell 20, 3713–3724.

Kwong, R.W.M., Perry, S.F., 2013. The tight junction protein Claudin-b regulates epithelial permeability and sodium handling in larval zebrafish, *Danio rerio*. Am. J. Physiol. Regul. Integr. Comp. Physiol. 304, R504-13.

Lacaz-Vieira, F., Jaeger, M.M.., Farshori, P., Kachar, B., 1999. Small synthetic peptides homologous to segments of the first external loop of Occludin impair tight junction resealing. J. Membr. Biol. 168, 289–297.

Lillywhite, H.B., 2006. Water relations of tetrapod integument. J. Exp. Biol. 209, 202–26.

Loh, Y.H., Christoffels, A., Brenner, S., Hunziker, W., Venkatesh, B., 2004. Extensive expansion of the claudin gene family in the teleost fish, *Fugu rubripes*. Genome Res. 1248–1257.

Martinez-Palomo, A., Erlij, D., Bracho, H., 1971. Localization of permeability barriers in the frog skin epithelium. J. Cell Biol. 50, 277–287.

Martinez-Palomo A., Meza I., Beaty G., Cereijido M., 1975. Structure of tight junctions in epithelia with different permeability. Proc Natl Acad Sci USA 72, 4487-4491.

McNeil, E., Capaldo, C., Macara, I., 2006. Zonula Occludens-1 function in the assembly of tight junctions in Madin-Darby Canine Kidney epithelial cells. Mol. Biol. Cell 17, 1922–1932.

Piontek, J., Fritzsche, S., Cording, J., Richter, S., Hartwig, J., Walter, M., Yu, D., Turner, J.R., Gehring, C., Rahn, H.P., Wolburg, H., Blasig, I.E., 2011. Elucidating the principles of the molecular organization of heteropolymeric tight junction strands. Cell. Mol. Life Sci. 68, 3903–3918.

Pisam, M., Ripoche, P., 1976. Redistribution of surface macromolecules in dissociated epithelial cells. J. Cell Biol. 71, 907–920.

Rakers, S., Gebert, M., Uppalapati, S., Meyer, W., Maderson, P., Sell, A.F., Kruse, C., Paus, R., 2010. "Fish matters": The relevance of fish skin biology to investigative dermatology. Exp. Dermatol. 19, 313–324.

Saitou, M., Furuse, M., Sasaki, H., Schulzke, J.D., Fromm, M., Takano, H., Noda, T., Tsukita, S., 2000. Complex phenotype of mice lacking Occludin, a component of tight junction strands. Mol. Biol. Cell 11, 4131–4142.

Sánchez-Pulido, L., Martín-Belmonte, F., Valencia, A., Alonso, M.A., 2002. MARVEL: A conserved domain involved in membrane apposition events. Trends Biochem. Sci. 27, 599–601.

Stevenson, B.R., Siliciano, J.D., Mooseker, M.S., Goodenough, D.A., 1986. Identification of ZO-1: a high molecular weight polypeptide associated with tight junction (zonula occludens) in a. J. Cell Biol 103, 755–766.

Yamamoto, T., Saeki, Y., Kurasawa, M., Kuroda, S., Arase, S., Sasaki, H., 2008. Effect of RNA interference of tight junction-related molecules on intercellular barrier function in cultured human keratinocytes. Arch. Dermatological Res. 300, 517–524.

Yoshida, Y., Morita, K., Mizoguchi, A., Ide, C., Miyachi, Y., 2001. Altered expression of Occludin and tight junction formation in psoriasis. Arch. Dermatological Res. 293, 239–244.

Yu, A.S.L., McCarthy, K.M., Francis, S.A., McCormack, J.M., Lai, J., Rogers, R.A., Lynch, R.D., Schneeberger, E.E., 2005. Knockdown of occludin expression leads to diverse phenotypic alterations in epithelial cells. Am. J. Physiol. Cell Physiol. 288, C1231-41.

Voyles, J., Young, S., Berger, L., Campbell, C., Voyles, W.F., Dinudom, A., Cook, D., Webb, R., Alford, R.A., Skerratt, L.F., Speare, R., 2009. Pathogenesis of chytridiomycosis, a cause of catastrophic amphibian declines. Science. 326, 582–585.

Whitear, M., 1970. The skin surface of bony fishes. J. Zool. 160, 437–454.

2. Chapter Two: The barrier properties of rainbow trout, *Oncorhynchus mykiss* skin attributed to Claudin proteins

2.1 Summary

The skin of teleost fishes is in direct contact with the external environment and acts as a barrier to passive ion loss in freshwater (FW). The majority of passive ion loss occurs between epithelial cells via the paracellular pathway, which is regulated by the tight junction (TJ) complex. Claudins (Cldns) are a large superfamily of TJ proteins that play a dominant role in regulating paracellular ion movement. Teleost skin expresses around half of all described teleost Cldn genes, indicating that it may have retained expression to be dynamically regulated and adjust to environmental changes. Additionally, it was recently discovered that fish skin is able to respond to an osmoregulatory hormone in a region-specific manner. However, virtually nothing is known about how the skin responds to environmental salinity change. To gain a broader understanding of how TJs contribute to the barrier properties of fish skin, region-specific permeability of the skin was examined, along with the localization of select TJ proteins in the epidermis. Additionally, alterations in TJ protein abundance following exposure of fish to ion-poor surroundings (ion-poor water, IPW) were examined. Rainbow trout (*Oncorhynchus mykiss*), were exposed to ion-poor water (IPW) for 6 hours, 24 hours, and 14 days and Cldn protein abundance was examined in the dorsal and ventral regions of the skin. Results indicated that the skin exhibited regional differences in paracellular permeability, which could be linked to Cldn abundance, and that Cldn proteins responded to IPW in a time- and region-dependent manner. Additionally, one Cldn protein was found to be cell-specific and paralleled changes in serum Ca^{++} levels with IPW exposure. Therefore, the skin exhibited a dynamic response to a change in environmental salinity.

2.2 Introduction

2.2.1 Maintaining salt and water balance under freshwater conditions

Freshwater (FW) fishes live in an environment in which the external ion concentration is much lower than the ion concentration of their internal fluids. As a result, unwanted ion loss occurs into the surrounding water. To maintain salt and water balance, FW fishes must employ the gills, kidney, gastrointestinal tract and skin to regulate active and passive ion transport (Marshall and Grosell, 2005). The gills and intestine actively uptake environmental and dietary ions, respectively, while the kidney retains ions not excreted in dilute urine, and the skin acts as a barrier to passive ion loss (Marshall and Grosell, 2005).

2.2.2 Coping with alterations in water ion content

The need to ionoregulate is often examined in fishes that can tolerate a variety of salinities, or in fishes that spend time on land (Marshall and Grosell, 2005), because changes in water ion content can produce very drastic alterations in the physiology of fishes (Marshall and Grosell, 2005; Colombo et al., 2006). For example, the active and passive transport of ions across epithelia—and the proteins involved in regulating this movement—are altered in euryhaline fishes that move between seawater (SW) and FW environments (McCormick and Bradshaw, 2006). In addition, multiple studies have exposed fishes to ion-poor water (IPW) to determine how ion-poor surroundings influence the ability of these organisms to regulate salt and water balance. A number of studies have been conducted on rainbow trout, and used IPW as a tool to examine multiple physiological parameters, including the alteration in TJ protein mRNA abundance (see **section 2.2.4**), that occur with this environmental challenge (Perry and Laurent, 1989; Greco et al., 1996; McKinley, 2008; Kolosov and Kelly., 2016; Gauberg et al., 2017). However, no one has ever

examined the effects of IPW on TJ proteins in the skin of fishes, a tissue that is directly exposed to the external environment.

2.2.3 The skin of teleost fishes

The integument of adult teleosts is an intricate organ, composed of several layers (e.g. dermis, epidermis) and cell types (e.g. epithelial cells, mucous cells). The epidermis interfaces directly with the external environment (Van Oosten, 1957; Rakers et al., 2010) and is unique in that it is not keratinized, and hence remains metabolically active to cope with changes in environmental conditions (Rakers et al., 2010). Adult fish skin has been shown to limit ion loss in FW, and when it was disrupted (e.g. by infectious disease), this led to disturbances in systemic salt and water balance (Pickering and Richards, 1980; McCormick et al., 1992; Kent et al., 1998; Nowak, 1999). However, unlike the other teleost osmoregulatory organs, which have a large active component, the skin of adult fishes is classically regarded as simply a static, passive barrier (Marshall and Grosell, 2005). Contrary to the idea that the teleost skin is a static barrier, the permeability of this organ was demonstrated to alter with changes in salinity (Abraham et al., 2001, Huising et al., 2003, Cooper et al., 2013), suggesting that adjustments in the barrier properties play a role in ionoregulatory homeostasis. Given that the epidermis of the majority of adult fishes studied does not play a significant role in the active ion transport via the transcellular pathway, it seems likely that alterations in the barrier properties of skin that occur in response to changes in environmental ion levels will be driven by changes in the paracellular pathway. In turn, this will be controlled by the molecular components of the epidermal TJ complex that occlude the paracellular space and control paracellular solute movement.

2.2.4 Claudins in the skin of teleost fishes

Over 60 *claudin (cldn)* genes have been reported in teleosts, exhibiting differences in tissue expression and abundance (Kolosov et al., 2013) Over 25 of those *cldn* genes have been detected in the skin of various teleosts (Loh et al., 2004; Clelland and Kelly, 2010; Bui and Kelly, 2014; Kolosov et al., 2014; Gauberg et al., 2017). The large variety of Cldn proteins expressed in the skin may indicate that, like the gill (where a multitude of Cldn proteins are expressed to regulate paracellular permeability to ions), the skin may have retained expression of many TJ proteins so it could be dynamically regulated to adjust to the environmental and physiological needs of the fish. This is especially important for fishes that may be exposed to environments that differ in water ion content. More specifically, these fishes would need to alter the permeability properties of exposed epithelial tissues via the Cldn proteins to adjust to the new environment. For example, in previous experiments, cultured goldfish gill epithelia treated with the serum from IPW-exposed fish exhibited changes in *cldn* mRNA abundance with an associated decrease in paracellular permeability (Chasiotis et al., 2012). With regards to the fish skin, two studies demonstrated that certain TJ protein transcripts alter in abundance with changes in salinity (Bagherie-Lachidan et al., 2008; Bagherie-Lachidan et al., 2009). However, apart from these two studies on the skin of teleosts, virtually nothing is known about how Cldns in this tissue respond to changes in salinity, and if this reflects changes in the paracellular permeability of the skin. Additionally, TJ protein transcripts have been found to exhibit differences in abundance in a temporal (Kolosov et al., 2014) and spatial (Gauberg et al., 2017) manner. Therefore, it would be critical to examine the effects of altered salinity over time and in different regions of the skin.

To gain an understanding of the skin barrier properties in teleosts, the paracellular permeability of rainbow trout, *Oncorhynchus mykiss,* skin was measured in the dorsal and ventral

regions. Protein localization of Cldn-8d, -10c, -28b, -31, and -32a and regional abundance of Cldn-8d and -32a were also examined in the skin to determine how these Cldns may have contributed to establishing the permeability properties of the skin. Additionally, to extrapolate on the role that these Cldn proteins may play in regulating the permeability properties of the skin, trout were exposed to IPW for 6 hours, 24 hours, and 14 days. Cldn transcript and protein abundance were examined in the dorsal and ventral regions of the skin with IPW exposure. In this study, it was hypothesized that Cldn protein abundance and skin permeability would differ between dorsal and ventral skin regions. It was also hypothesized that the Cldn proteins would alter with IPW exposure in a time- and region-dependent manner.

2.3 Materials and Methods

2.3.1 Experimental Animals

160 rainbow trout (*Oncorhynchus mykiss*, ~40g) were obtained from a local supplier (Humber Springs Trout Hatchery, Orangeville ON, Canada) and separated into four equal groups of 40 fish/group. Each group of trout was housed in 200-liter opaque polyethylene tanks supplied with flow-through dechlorinated FW (approximate composition in μM: $[Na^+]$: 590, $[Cl^-]$: 930, $[Ca^{++}]$: 760, and $[K^+]$: 43). Fish were held under a constant photoperiod of 12 h light: 12 h dark and fed *ad libitum* once daily with commercial trout pellets (Martin Profishent, Elmira, ON, Canada). Fish were used for experiments after allowing them to settle into lab conditions for at least two weeks. Fish culture and all experimental procedures were conducted according to a protocol approved by the York University Animal Care Committee and conformed to the guidelines of the Canadian Council on Animal Care.

2.3.2 Exposure of fish to IPW

Rainbow trout were introduced to IPW by replacing flow-through FW with flow-through IPW. To expedite water change, but keep animal disturbance to a minimum, tank water was repeatedly drained (by ~ two thirds) and filled over a period of 1 hour. Complete water change took 2 hours. IPW water was composed of 80% reverse osmosis (RO) water (approximate composition in µM: $[Na^+]$: 20, $[Cl^-]$: 40, $[Ca^{++}]$: 2, and $[K^+]$: 0.4) and 20% dechlorinated FW (as described in **section 2.3.1**). Cl^- content of FW and IPW source water were determined prior to the onset of IPW exposure using colorimetric mercuric thiocyanate/ferric perchlorate chloride assay (Zall et al, 1956). During the FW to IPW changeover, water samples were taken every hour and Cl^- content was measured to confirm that changeover resulted in the correct and stable ratio of 80% IPW water and 20% FW. Once the tank water was confirmed to be IPW, this point was considered t=0. Cl^- content in water samples was measured daily for the entirety of the experiment ($[Cl^-]$= 198 ± 6 µM in IPW). Fish were sampled at 3, 6, and 24 h, as well as 7 and 14 day periods. To minimize disturbance, fish were sampled from one tank at 3 and 24 h and from another tank at 6 h, 7 days and 14 days. Fish were also netted in the same manner from FW tanks in parallel with the IPW fish. Ten fish were netted from IPW and FW tanks per time point, anaesthetized with 0.5 g/L of buffered tricaine methanesulfonate TMS-222 (Syndel Laboratories, Vancouver, Canada) and euthanized by spinal transection.

2.3.3 Tissue sampling

Blood was drawn from every fish prior to spinal transection, clotted at 4°C for 30 minutes and spun at 10,000g for 10 mins at 4°C. The serum was aliquoted and stored at -80°C. Following blood collection and spinal transection, fish were placed on ice and skin tissue was collected for

immunohistochemical analysis (see **section 2.3.5** for details) and molecular analysis (see **section 2.3.9** and **2.3.10** for details) from one fish at a time. A dorsoventrally spanning flank of skin was removed from the left and right side of each fish and separated into two equal sections: dorsal and ventral. Tissue designated "dorsal" spanned 1 cm ventrally from the mid-dorsal line. Tissue designated "ventral" extended dorsally 1 cm from the mid-ventral line. Samples of each skin region (~ 80 mg) were placed into 1 mL of TRIzol® Reagent (Invitrogen Canada, Inc., Burlington, ON, Canada), flash frozen in liquid nitrogen and stored at -80°C until further processing (see **section 2.3.8**). For immunohistochemical analysis, dorsal and ventral regions of skin were fixed in Bouin's fixative solution for 4 h at room temperature. Skin tissue samples were then briefly rinsed with and stored in 70% ethanol at 4°C until further processing (see **section 2.3.5** for details). Following the collection of skin tissues for molecular and histological analysis, a full flank of epaxial muscle was collected from every fish (see **section 2.3.7** for details).

2.3.4 Antibodies

The affinity purified polyclonal antibodies used for immunohistochemsitry and Western blot analysis were custom-synthesized (New England Peptide, MA, USA; Genscript, NJ, USA) to specifically target *O. mykiss* antigenic peptides for Cldn-8d (SYFDPAYDEKAAKSC), -10c (CWEGSMSIKLKE), -28b (CPPKDENHNVKYSK), -31 (CFSSDSSPRRGPAAQ), and -32a (CSRAKSGSSGGTAKY). The theoretical sizes of Cldn-8d, -10c, -28b, -31 and, -32a are: 38, 21, 22, 23, 21 kDa, respectively.

2.3.5 Immunohistochemical analysis

Scales (with overlying epidermis) were carefully pulled off individual fish and fixed in 3% paraformaldehyde (PFA) overnight. Samples were washed in phosphate buffered saline + 0.1% Triton X-100 (PBT) three times (5 minutes each) and blocked with antibody dilution buffer (ADB: 10% goat serum, 3% bovine serum albumin (BSA), 0.05% Triton X-100, PBS pH 7.4). Scales were incubated overnight at room temperature with rabbit anti-Cldn-8d, -10c, -28b, -31, -32a antibodies. Antibodies were diluted in ADB to final dilutions of 1:100 (Cldn-8d, -28b, -32a) and 1:200 (Cldn-10c, -31). As negative controls, one sample was also incubated overnight with ADB alone. The next day, samples were again rinsed with PBT three times for 5 minutes and then washed 3 times for 30 minutes. Subsequently, samples were incubated with fluorescein-isothiocyanate (FITC)-labelled goat anti-rabbit antibody (1:500 in ADB; Jackson ImmunoResearch Laboratories, Inc.) overnight at room temperature. Finally, the samples were rinsed and washed three times and mounted on glass slides using Permount Mounting Medium (Fischer Scientific, Pittsburg, Pennsylvania) containing 5 μg ml^{-1} 4',6-diamidino-2-phenylindole (DAPI; Sigma-Aldrich Canada Ltd, Oakville, ON, Canada). Fluorescence images were captured using a Zeiss LSM 700 inverted confocal microscope and merged using ImageJ software.

2.3.6 Chloride and [^{3}H] polyethylene glycol (PEG) permeability assays

Skin was dissected from the dorsal and ventral regions of fishes acclimated to FW. Skin samples spanned 2 cm across the mid-dorsal and mid-ventral regions. Each fish was suspended in mid-air using clamps for the dissection to avoid damaging the epidermis. As a positive control, dorsal skin samples were scraped using a razor blade so that the epidermis had been removed but the dermis remained intact. Each skin sample was immediately mounted onto vertical diffusion chambers

(Franz cells): 5 mL FW was added to the apical chamber while the basolateral chamber contained 1 mL of modified Cortland's saline with the composition (in mM) Na^+: 142, Cl^-: 136, K^+: 2.6, HCO_3^-: 9.7, Ca^{2+}: 1.6, Mg^{2+}: 0.9, PO_4^-: 3.0, SO_4^{2-}: 0.9, and glucose: 5.6 with BSA (Sigma Aldrich, Canada Ltd) 20 mg ml^{-1} as a replacement for plasma protein. Samples were collected from the FW (apical) and saline (basolateral) chambers after 4 hours and run with a chloride assay (Zall et al., 1956) to determine Cl^- content. For permeability experiments with [^{3}H]polyethylene glycol (4000 Da, PEG-4000), 1.5 μCi of PEG-4000 was added to the donor chamber and 50 μl and 500 μL samples were collected from the basolateral and apical chambers, respectively, after 4 hours. [^{3}H] activity in the samples was measured using a scintillation counter (Tricarb 2100 Liquid Scintillation Analyzer, Packard Instruments) and permeability of dorsal and ventral skin samples was calculated using the equation from Kelly and Wood (2001),

$$P\ (cm/s) = \frac{([\Delta PEG*_{Ap}])(Volume_{Ap})}{([PEG*_{Bl}])(Time)(3600)(Area)}$$

where $\Delta PEG*_{Ap}$ is the change in radioactive PEG-4000 concentration on the apical side, $Volume_{Ap}$ is the volume of the apical chamber (1 mL), $PEG*_{Bl}$ is the radioactive PEG-4000 concentration on the basolateral side, 3,600 converts hours to seconds, and Area defines the area of the Franz cell chamber opening (0.64 cm^2).

2.3.7 Muscle moisture and serum ion concentration

Following the collection of skin tissues for molecular and histological analysis, a full flank of epaxial muscle was collected from every fish, placed into a pre-weighed Falcon-tube and dried to a constant weight at 60°C in the oven (the muscle moisture content was calculated as the differential of wet and dry mass of the sample). Serum [Cl^-] was determined according to Zall et

al. (1956) using serum samples diluted 1:1000 in 1% HNO_3. Serum [Na^+] and [Ca^{++}] were measured using reference and ion-selective microelectrodes (ISMe). Electrodes were constructed according to Donini and O'Donnell (2005).

2.3.8 RNA extraction and cDNA synthesis

Total RNA was extracted from skin tissue using TRIzol Reagent (Invitrogen Canada, Inc.) as follows: Skin samples in 1 ml of TRIzol® were defrosted and homogenized for 10 seconds at 30,000 rpm (PRO250 Homogenizer, Pro Scientific, CT, USA). Samples were incubated for 5 minutes at room temperature (RT) to permit dissociation of nucleoprotein complexes. Then, 0.2 ml of chloroform was added to every sample. Samples were vigorously agitated by hand for 15 seconds and incubated at RT for 3 minutes. Following incubation, samples were centrifuged for 15 min at 12,000g in a chilled centrifuge (4°C) and the top aqueous phase from every sample containing RNA was pipetted into a sterile bullet tube. Samples were gently mixed with 0.5 ml of isopropyl alcohol and incubated at RT for 10 minutes to precipitate RNA. Samples were subsequently centrifuged for 10 minutes at 12,000g in a chilled centrifuge to pellet the RNA. Isopropanol was removed from samples by aspiration and pellets were washed with 1 ml of 75% ethanol diluted in diethylpyrocarbonate (DEPC)-treated water to displace isopropanol. Samples were finally centrifuged for 5 minutes at 7,500g in a chilled centrifuge in order to settle pellets detached during the previous wash stage. Ethanol was removed by aspiration and RNA pellets were dissolved in appropriate amount of DEPC-treated water. RNA concentration was determined using a Multiskan Spectrum spectrophotometer (Thermo Electron Corp, Bethesda, ON, Canada) using an absorbance ratio of 260 nm. Integrity of RNA samples was assessed using 260/280 nm absorbance ratio.

Extracted RNA was treated with DNase I (Amplification Grade; Invitrogen Canada, Inc.) for 15 min at RT to remove possible genomic DNA leftover from the RNA extraction process. DNase was then inactivated for 10 min at 65°C and first-strand cDNA was synthesized using SuperScript^{TM} Reverse Transcriptase (0.4µl/sample), 100 mM dNTP mix (1µl/sample), and Oligo(dT)$_{12-18}$ primers (0.8µl/sample) (Invitrogen Canada, Inc.). cDNA was then used for quantitative real-time PCR (qPCR) analysis.

2.3.9 qPCR analysis of *cldn* mRNA abundance

Gene specific primers designed for rainbow trout *cldns*, reported by Kolosov et al. (2014), were used for qPCR. Transcript abundance of *cldns* was examined by qPCR using a Chromo4 Detection System (CFB-3240; Bio-Rad Laboratories) and SYBR Green I Supermix (Bio-Rad Laboratories Canada Ltd.) under the following conditions: 1 initial cycle of denaturation (95 C, 4 min), followed by 40 cycles of denaturation (95^{o} C, 30 sec), annealing (58-61^{o} C, 30 sec) and extension (72^{o} C, 30 sec). A melting curve was constructed after each qPCR run, ensuring that a single product was synthesized during each reaction. For all qPCR analyses, transcript abundance was normalized to elongation factor 1-α (*ef-1α)* transcript abundance after determining by statistical analysis that *ef-1α* did not significantly alter (P>0.10) between dorsal and ventral skin regions, time points, and in response to experimental conditions. Rainbow trout *ef-1α* mRNA was amplified using primers previously reported by Kolosov et al. (2014).

2.3.10 Western blot analysis of Cldn protein abundance

Rainbow trout skin tissues were thawed and sonicated on ice in chilled radioimmunoprecipitation assay (RIPA) lysis buffer (0.6% Tris-HCl, 0.8% NaCl, 1% deoxycholic acid, 1% Triton X-100,

1% SDS, 1mM EDTA, 1mM PMSF, 1mM DTT) containing 1:200 protease inhibitor cocktail (Sigma-Aldrich Canada Ltd). Tissues were sonicated at a 1:3 w:v tissue to sonication buffer ratio using a Misonix Sonicator XL-2000. Homogenates were centrifuged at 13,000 rpm for 20min at 4°C and supernatants were collected after centrifugation. Protein content was quantified using the Bradford reagent (Sigma-Aldrich Canada Ltd) according to the manufacturer's guidelines with bovine serum albumin as a standard. Samples were prepared for SDS-PAGE by boiling at 100°C in Laemelli buffer (Sigma-Aldrich Canada Ltd) with 5% 2-mercaptoethanol (Sigma-Aldrich, Canada Ltd) for 10-15 minutes; 25-100µg of skin tissue homogenates were electrophoretically separated by SDS-PAGE in 12% acrylamide gels at 150V. After electrophoresis, protein was transferred to a polyvinylidene difluoride (PVDF) membrane (Immobilon-P PVDF Membrane, Millipore Sigma, Canada) over a 1 hour period. Following transfer, the membrane was washed in Tris-buffered saline with Tween-20 [TBS-T; TBS (10mM Tris, 150mM NaCl, pH 7.4) with 0.05% Tween-20], and blocked for 1 hour in 5% non-fat dried skimmed milk powder in TBS-T (5% milk TBS-T). The membrane was then incubated overnight at 4°C with rabbit polyclonal anti-Claudin-8d, -10c, -28b, -31, and -32a antibodies (1:1000 to 1:10,000 dilution in 5% milk TBS-T). Following incubation with primary antibody, the membrane was washed with TBS-T (3 times x 5 minutes) and incubated at room temperature with horseradish peroxidase (HRP)-conjugated goat anti-rabbit antibody (1:5000 dilution in 5% milk TBS-T; Bio-Rad Laboratories Ltd, Canada) for 1 hour, and then washed with TBS-T. To visualize protein bands, blots were incubated in Clarity™ Western ECL Blotting Substrate (Bio-Rad Laboratories Ltd, Canada) for 5 minutes at RT and imaged using ChemiDoc™ MP system (Bio-Rad Laboratories Ltd, Canada).

Western blots for Claudins were carried out as outlined above using equal amounts of protein from each tissue sampled. As a loading control, membranes were subsequently stripped

with stripping buffer (100mM glycine, 30 mM KCl, 20mM sodium acetate, pH 2.2), washed with TBS-T, blocked with 5% milk TBS-T and incubated overnight at 4°C with mouse monoclonal anti-actin JLA20 antibody (1:500 in 5% milk TBS- T; Developmental Studies Hybridoma Bank). Membranes were then washed with TBS-T and incubated at RT with HRP-conjugated goat anti-mouse antibody (1:5000 in 5% skimmed milk TBS-T; Bio-Rad Laboratories, Inc.) for 1 hour, washed with TBS-T, and visualized as described above. Claudin and actin protein expression were quantified using ImageJ software. Actin was used for normalization after statistically validating that actin protein abundance did not significantly differ between control and experimental groups.

2.3.11 Statistical analysis

All data are expressed as mean values ±SEM (n), where n represents the number of fish sampled. Significant differences ($P \leq 0.05$) between groups were determined using one-way analysis of variance (ANOVA), two-way ANOVA, the Student's t-test or the paired t-test, as indicated. All statistical analyses were performed using SigmaPlot 12.5 (Systat Software Inc., San Jose, CA).

2.4 Results

2.4.1 Immunolocalization of Cldn proteins in the epidermis and dermis of rainbow trout, *Oncorhynchus mykiss.*

Cldn-8d, -10c, -28b, -31, and -32a protein localization was examined in the dorsal epidermis of rainbow trout (**Figure 2.1**). Peri-junctional staining was observed for Cldn-8d, -28b, and -32a, where the proteins localized to junctions between cells. Cldn-31 exhibited cytosolic staining and Cldn-10c did not localize to the epidermis. Instead, Cldn-10c was present in the dermis, just under the scales (**Figure 2.2**).

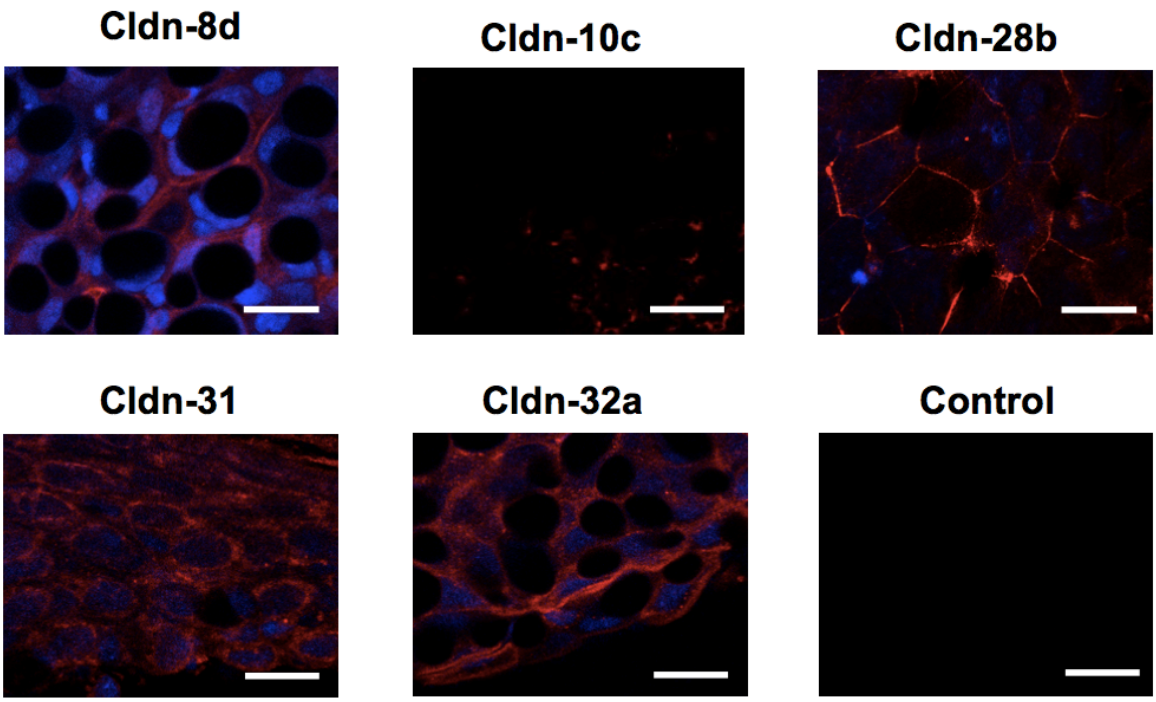

Figure 2.1. Whole mount immunolocalization of Claudin (Cldn)-8d, -10c, -28b, -31, and -32a in the dorsal skin of rainbow trout *(Oncorhynchus mykiss*). Cldn proteins are in red, nuclear staining is in blue. Scale bars= 20 µm.

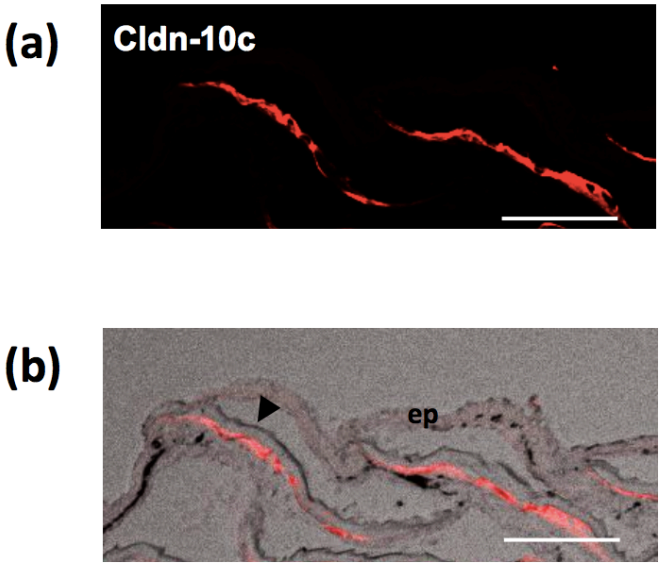

Figure 2.2. Immunolocalization of Cldn-10c in the ventral skin of rainbow trout (*Oncorhynchus mykiss*). Panel (a) depicts Cldn-10c (red) fluorescence and panel (b) shows an overlay of Cldn-10c staining over a brightfield microscopy image of the skin. Arrowhead points to a scale. ep= epidermis. Scale bars= 400 µm

2.4.2 Chloride and PEG permeability of dorsal and ventral regions of rainbow trout skin

Net Cl^- flux (**Figure 2.3a**) and permeability to PEG-4000 (**Figure 2.3b)** were greater in the ventral skin compared to the dorsal skin. Additionally, to test whether the epidermis or the dermis was responsible for providing the most resistance to ion movement, the dorsal skin was descaled and ion flux was measured (**Figure 2.3c**). Net Cl^- flux tripled through descaled skin compared to scaled skin.

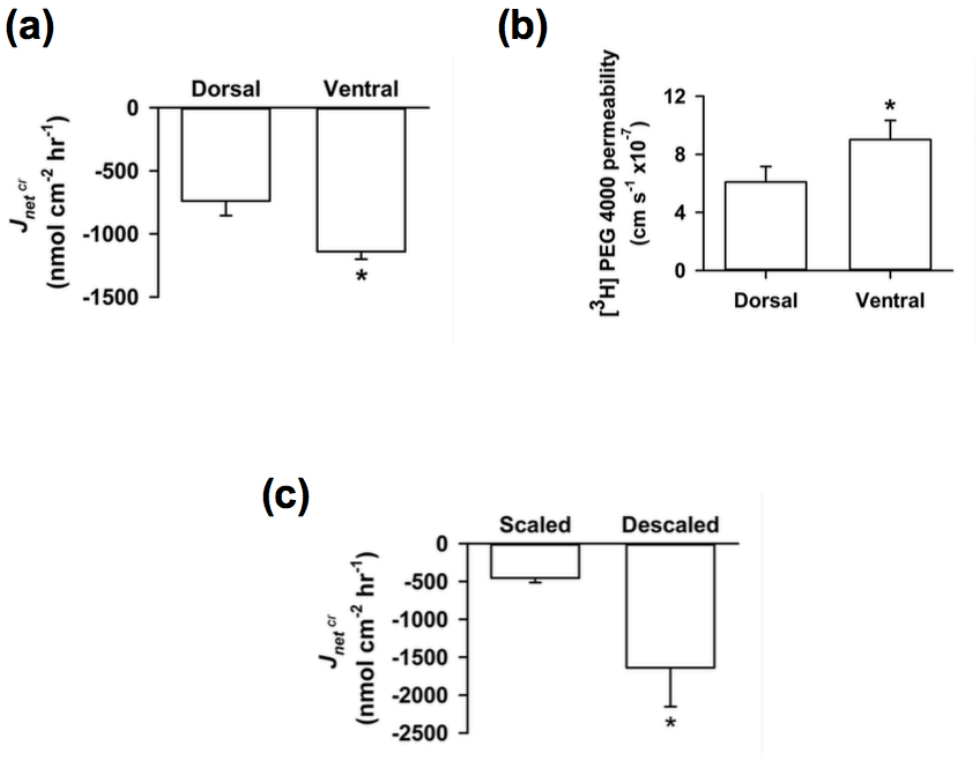

Figure 2.3. Net (a,c) chloride (Cl^-) flux and (b) [^{3}H] PEG-4000 permeability across rainbow trout (*Oncorhynchus mykiss*) skin. Solute flux was measured through (a-b) dorsal and ventral regions of rainbow trout skin under freshwater conditions and (c) when dorsal skin was descaled. All data are mean values ± SEM (n=3). Asterisks indicate significant difference as determined by a paired t-test.

2.4.3 Cldn-8d and -32a abundance in the dorsal and ventral regions of rainbow trout skin

To link regional paracellular permeability to TJ protein abundance, Cldn-8d and Cldn-32a protein abundance was examined in the dorsal and ventral skin of rainbow trout (**Figure 2.4**). Cldn-8d was lower in the ventral than the dorsal skin region, while Cldn-32a was higher in the ventral skin than the dorsal skin.

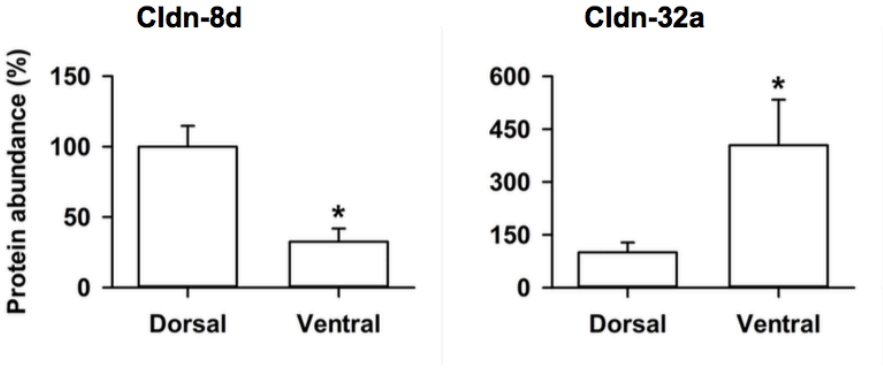

Figure 2.4. Claudin (Cldn) protein abundance in dorsal and ventral regions of rainbow trout (*Oncorhynchus mykiss*) skin under freshwater conditions. Claudin abundance was examined in skin tissue by Western blot. All data are mean values ± SEM (n=5). Asterisks indicate significant difference as determined by a Student's t-test. Actin was used as a reference protein.

2.4.4 Time course effect of IPW on rainbow trout serum ion levels and muscle moisture content

Ion levels and muscle moisture content were examined in the serum of rainbow trout following exposure to IPW for 3, 6, and 24 h, as well as 7 and 14 days (**Figure 2.5)**. In FW control fish, neither serum ion levels nor muscle moisture content was altered throughout the time course. IPW treatment had no effect on serum [Cl^-] or serum [Na^+] compared to FW controls. However, Serum [Ca^{++}] exhibited a transient increase following 6 h of IPW exposure. Muscle moisture content increased at 24 hours and decreased after 7 days of IPW treatment. By 14 days, no significant difference in any parameter examined was detected between FW and IPW fish.

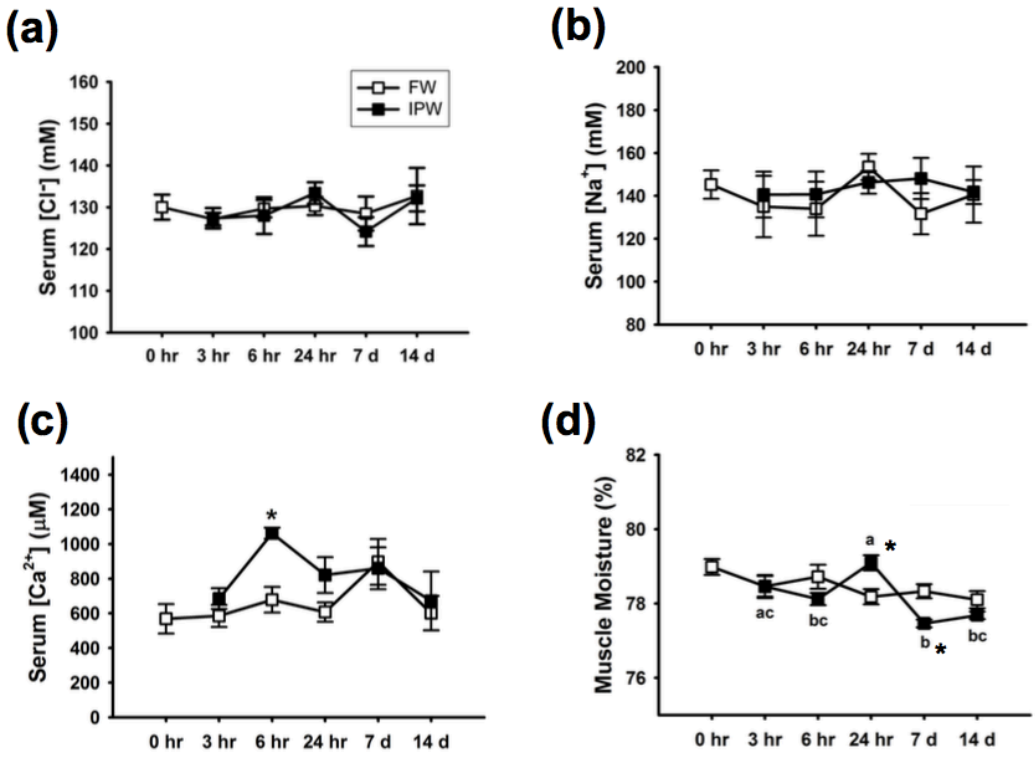

Figure 2.5. Effect of ion-poor water (IPW) treatment on (a) serum chloride (Cl^-) concentration, (b) serum sodium (Na^+) concentration (c) serum calcium (Ca^{++}) concentration, and (d) muscle moisture content at 0 hr, 3 hr, 6hr, 24 hr, 7 days and 14 days in rainbow trout (*Oncorhynchus mykiss).* All data are expressed as mean values ± SEM (n = 8 for (a, c) and n=5 for (b), n=10 for (d)), where n is the number of fish sampled. Different lower-case lettering indicates significant differences as determined by one-way ANOVA. Asterisks indicate significant differences between samples acquired from freshwater (FW) fish versus those from fish exposed to IPW as determined by a two-way ANOVA.

2.4.5 Time course effect of IPW exposure on *cldn* mRNA abundance in dorsal and ventral skin regions of rainbow trout.

The effect of IPW on *cldn* mRNA abundance was found to be region and time specific (**Figure 2.6**). At 6 hours of IPW treatment, only two *cldns* (*cldn-10c* and *-32a*) altered in abundance, however, after 14 days, all *cldns* exhibited a change in abundance in either the dorsal or ventral region.

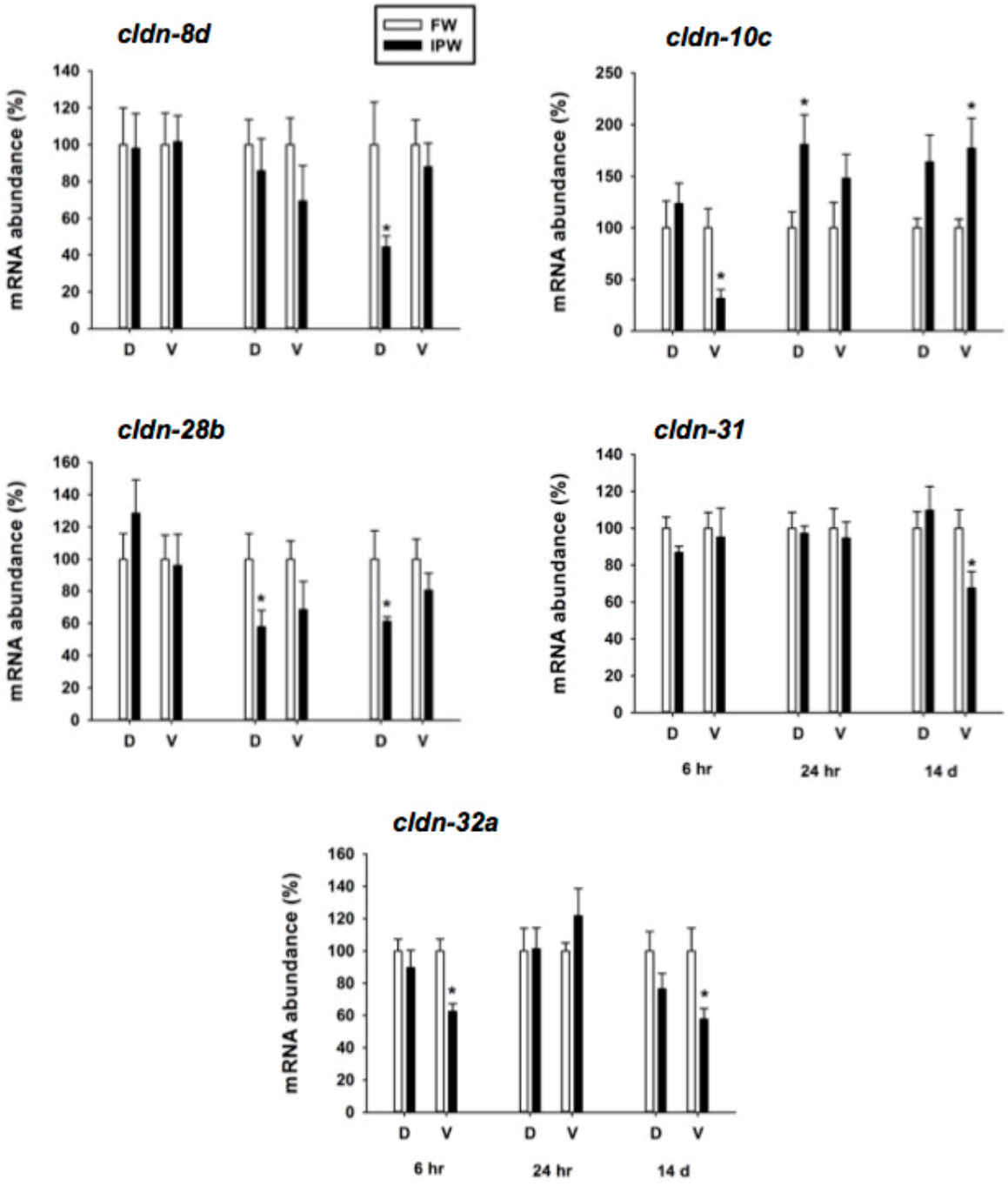

Figure 2.6. Effect of 6 hour, 24 hour and 14 day ion-poor water (IPW) exposure on claudin *(cldn)* mRNA abundance in dorsal (D) and ventral (V) regions of rainbow trout (*Oncorhynchus mykiss*) skin. Claudin mRNA was examined in skin tissue by quantitative PCR. All data are mean values ± SEM (n=8). Asterisks indicate significant differences between freshwater (FW) and IPW-exposed fish as determined by a Student's t-test. Transcript abundance in each skin region of IPW-exposed fish was expressed relative to samples taken from FW animals assigned a value of 100. *ef-1α* was used as a reference gene.

2.4.6 Time course effect of IPW exposure on Cldn protein abundance in dorsal and ventral skin regions in rainbow trout.

Cldn protein abundance was found to alter in a time- and region-specific manner following IPW treatment (**Figure 2.7**). Only Cldn-28b abundance did not change at any of the time points. The majority of Cldn protein levels altered at 6 hours of IPW exposure, whereas after 14 days only Cldn-8d and -10c exhibited changes in protein abundance. Cldn-8d levels increased in the dorsal region, Cldn-10c levels decreased in the ventral region, and Cldn-31 and -32a levels returned to FW levels following 14 days of IPW treatment.

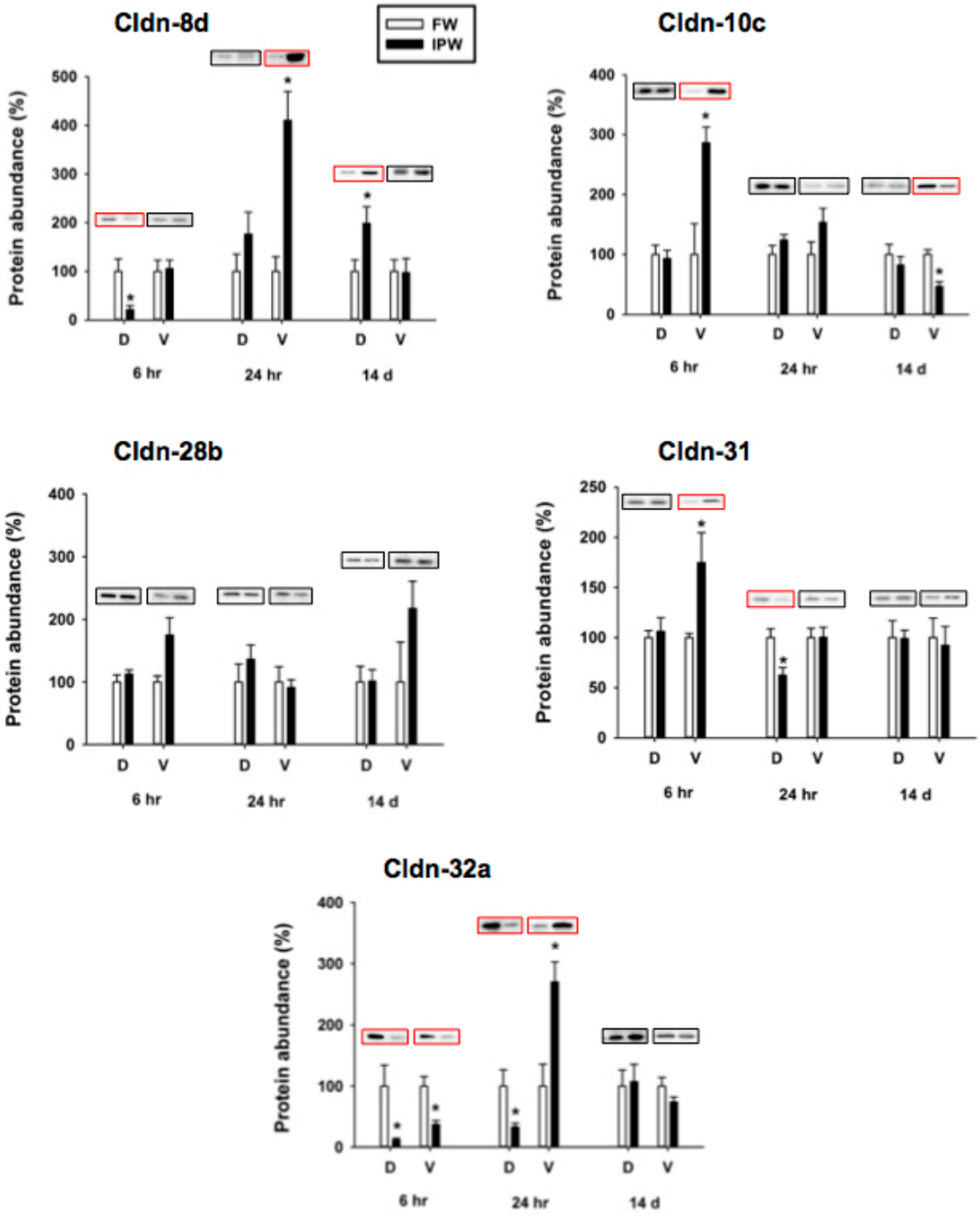

Figure 2.7. Effect of 6 hour, 24 hour and 14 day ion-poor water (IPW) exposure on Claudin (Cldn) protein abundance in dorsal (D) and ventral (V) regions of rainbow trout (*Oncorhynchus mykiss*) skin. Claudin abundance was examined in skin tissue by Western blot. All data are mean values ± SEM (n=5). Asterisks indicate a significant difference between freshwater (FW) and IPW-exposed fish as determined by a Student's t-test. Actin was used as a reference protein. Representative blots are visualized above each set of bars.

2.5 Discussion

2.5.1 Overview

This study examined the localization of Cldn TJ proteins in the skin of rainbow trout as well as region-specific permeability properties of the skin and the effects of IPW treatment on mRNA and protein abundance of select Cldns in the skin. To the best of my knowledge, studies examining the region-specific permeability properties and the effect of IPW on Cldn protein abundance in the skin of fishes are lacking to date. In the current study, it was determined that the skin exhibits differences in regional (i.e. dorsal versus ventral) permeability and Cldn protein abundance. Notably, these data support the idea that the molecular physiology of the TJ complex plays a role in regional differences in the barrier properties of fish skin as proposed by Gauberg et al (2017). Additionally, IPW exposure resulted in region- and time-specific changes in Cldn protein abundance, indicating that the skin may have altered in paracellular permeability to cope with the change in salinity. Finally, Cldn-10c was found to localize to the scales within the dermis, and changes in Cldn-10c abundance paralleled changes in serum [Ca^{++}] with IPW exposure. These results indicate that a putative link may exist between Cldn-10c protein abundance and Ca^{++} mobilization from the scales in trout acclimated to IPW. Therefore, the hypotheses that trout skin exhibits differences in regional permeability and that TJ proteins in the skin can alter in abundance with IPW exposure can be accepted.

2.5.2 All examined Cldn proteins, except Cldn-10c, were present in the epidermis

The expression of TJ proteins in the epidermis was detected under freshwater (FW) conditions. The localization of Cldn-8d, -28b, -31, and -32a in the epidermis (**Figure 2.1**) indicates that, for these Cldns, any changes in protein abundance (see **section 2.5.6**) may be linked to the barrier

function of the epidermis, which directly interfaces with the surrounding environment. Cldn-10c was the only protein that localized to the dermis, underneath the scales (**Figure 2.2**). Cell-specific localization was consistent with reports of Cldn-10c being cell-specific in the gill epithelium of rainbow trout (Kolosov et al., 2014) which may indicate that Cldn-10c has a unique function in the osmoregulatory response, such as mobilizing Ca^{++} from the scales (see **section 2.5.6**). Therefore, the majority of Cldns examined can be linked to the barrier properties of the epidermis.

2.5.3 Permeability differed between dorsal and ventral skin regions

The epidermis is the main barrier to ion loss into FW and in the current study "descaling," or removal, of the epidermis resulted in a much greater efflux of Cl^- into the external environment (**Figure 2.3c**). In FW, trout skin possessed inherent regional differences in its permeability to Cl^-, which is an ion naturally present in trout serum, and [^{3}H]PEG-4000, which is a paracellular permeability marker (**Figure 2.3a-b**). The dorsal region was less permeable to both solutes than the ventral region. In fishes, muscle tissue was found to have higher perfusion rates than adipose tissue (Hinton and Giulio, 2008). Thus, because the dorsal skin is in direct contact with underlying vascularized muscle tissue (**Illustration 2.1a**), it may have to remain tighter to prevent the loss of solutes across a larger electrochemical gradient. Given that the skin was sampled from the dorsal and ventral regions as depicted in **Illustration 2.1b** for the permeability studies, the observed differences in paracellular permeability may indeed be a reflection of the perfusion of the underlying structures.

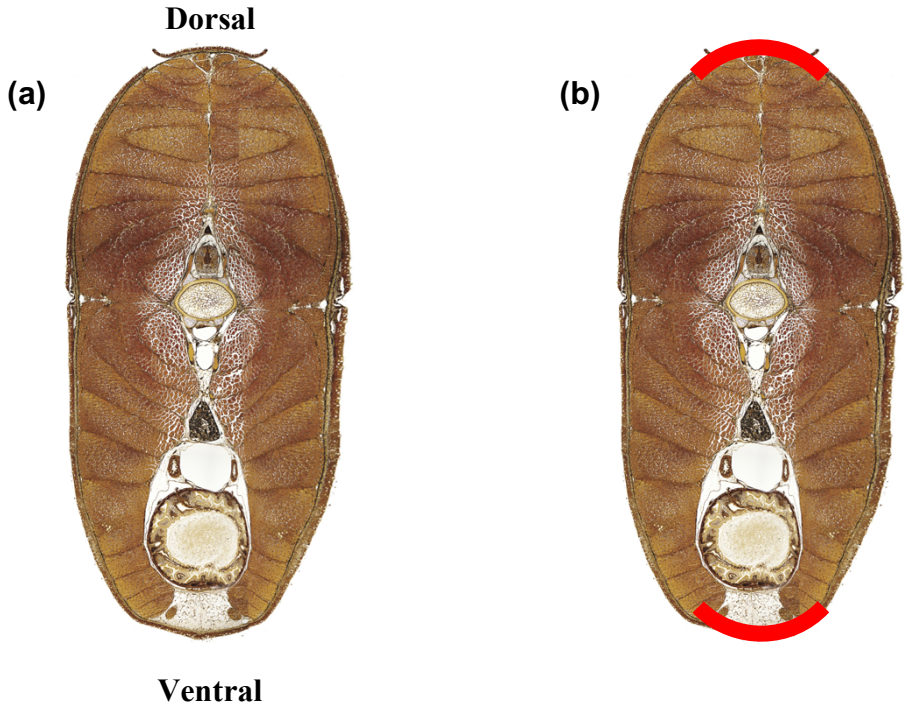

Illustration 2.1. A cross section through the body of rainbow trout, *Oncorhynchus mykiss*. Panel (a) shows the structures underlying the dorsal and ventral skin. Muscle is in direct contact with the dorsal skin, whereas the ventral skin overlies white adipose tissue. Panel (b) demonstrates (in red) where skin samples were dissected to run the permeability assays. Original image by Guillaume Salze. Modified and substantially altered here.

2.5.4 Cldn abundance in the skin was consistent with differences in permeability

The abundance of Cldn-8d and -32a was consistent with the observed differences in permeability of the dorsal and ventral regions of the skin obtained in this study. Cldn-8d is a barrier-forming protein in the gill of rainbow trout (Kolosov and Kelly, 2017) and is more abundant in the dorsal skin than the ventral skin (**Figure 2.4**). Conversely, the abundance of *cldn-32a* has been inversely linked with the barrier properties of the gill epithelium (i.e. cldn-32a abundance increases as gill epithelium permeability decreases; Kolosov et al., 2014). Therefore, elevated Cldn-32a abundance in ventral versus dorsal skin would be consistent with increased permeability of the ventral region. Given the properties of these Cldn proteins, it may be speculated that their differences in

abundance were contributing to the regional paracellular permeability properties of the skin (see **section 2.5.3**).

2.5.5 IPW exposure transiently altered serum Ca^{++} levels and muscle moisture content

Serum [Na^+] and [Cl^-] did not alter over the 14-day period of IPW exposure (**Figure 2.5**). Na^+ and Cl^- are the most abundant ions in rainbow trout serum (Al-Jandal and Wilson, 2011), thus, the undisturbed systemic [Na^+] and [Cl^-] indicate that rainbow trout were able to maintain ion balance with both acute and chronic IPW treatment. Conversely, muscle moisture content changed significantly with 24 hours and 7 days of IPW exposure (**Figure 2.5d**), indicating that trout were able to maintain ion balance better than water balance. However, after 14 days of IPW exposure, muscle moisture content returned to FW levels. Exposure to IPW also resulted in a time-dependent change in Ca^{++} levels (**Figure 2.5c**). Oddly, the levels of serum Ca^{++} increased, despite the fact that under IPW conditions, the chemical gradient that promotes passive loss of ions into the surrounding water is increased. The increase in systemic Ca^{++} levels may have been due to mobilization of Ca^{++} from scales to maintain sufficient levels of this ion in the blood (see **section 2.5.6.4**). Despite any changes in [Ca^{++}] or water balance that may have occurred with IPW exposure, they returned to control levels following 14 days of IPW exposure. Therefore, at 14 days the fish were completely acclimated to IPW conditions.

2.5.6 IPW exposure regionally altered the mRNA and protein abundance of skin Cldns

Cldn-8d, -10c, -28b, -31, and -32a were chosen to be examined in this study because the majority have been found to respond to IPW at the mRNA level in rainbow trout gills (Kolosov and Kelly, 2016). Additionally, in rainbow trout skin, transcript levels of all of these Cldns, with the exception

of Cldn-32a, were found to alter with systemic administration of the osmoregulatory hormone cortisol (Gauberg et al., 2017). With IPW exposure, abundance of all Cldns examined in this study altered at either the mRNA or protein level (**Figures 2.6-2.7**). The change in mRNA and protein abundance was region-specific and time-dependent in all cases.

Some proteins altered in abundance during the acute stages of IPW exposure (Cldn-31, -32a), whereas others exhibited changes even after 14 days (Cldn-8d, -10c) (**Figure 2.7**). This may indicate that the Cldn-31 and -32a were important for the acute response to IPW challenge, whereas changes in Cldn-8d and -10c were required for IPW acclimation. The time-dependent changes are discussed in detail below.

2.5.6.1 IPW exposure for 6 h decreased abundance of select epidermis-associated Cldns

At 6 h of IPW exposure, protein abundance of Cldn-8d decreased in the dorsal region and Cldn-32a decreased in both dorsal and ventral regions (**Figure 2.7**). Cldn-31 was the only epidermis-associated protein to increase in abundance after 6 h of IPW exposure. Given that Cldn-8d is a barrier-forming protein (Kolosov and Kelly, 2017), it is surprising that it would decrease in abundance with IPW exposure. However, the rainbow trout gill is known to significantly restructure in epithelial morphology with IPW exposure and acclimation (Perry and Laurent, 1989; Kolosov and Kelly, 2016). The epidermis of the common carp (*Cyprinus carpio*) was also found to undergo cellular restructuring when exposed to a different salinity (Huising et al., 2003). Therefore, Cldn-8d may have been degraded due to cellular restructuring in the dorsal skin during the initial stages of IPW acclimation.

Similarly, Cldn-32a may have also been degraded in the dorsal and ventral regions with cellular restructuring (**Figure 2.6** and **2.7**). Cldn-32a abundance has been inversely associated with

the barrier properties of the trout gill epithelium (Kolosov et al., 2014). Therefore, decreased Cldn-32a abundance may have resulted in the 'tightening' of the dorsal and ventral epidermis. However, because the decrease in Cldn-32a protein abundance in the ventral region corresponded with decreased mRNA levels, the change in the ventral region was likely a part of a deliberate response to IPW rather than an effect of simple protein degradation.

The idea of ventral skin becoming 'tighter' under IPW conditions is further supported by the fact that the abundance of Cldn-31, a barrier-forming protein in the cultured trout gill epithelium (Kolosov et al., 2017), increased in the ventral skin. Therefore, upon immediate exposure to IPW (6 h) a potential restructuring may have decreased Cldn-8d and -32a in the dorsal skin, while the changes in Cldn-32a and -31 abundance in the ventral skin were aimed at 'tightening' this skin region to match the FW dorsal barrier levels prior to further restructuring.

2.5.6.2 IPW exposure for 24 h may have resulted in region-specific changes in skin permeability

Following 24 hours of IPW exposure, Cldn-8d protein abundance increased significantly in the ventral region, and returned to FW levels in the dorsal region. Conversely, Cldn-31 levels ceased being upregulated in the ventral region and began being downregulated in the dorsal region. In rainbow trout gill cell culture, Cldn-8d and -31 protein abundance were found to be linked, where a knockdown of Cldn-31 abolished the typical increase in Cldn-8d abundance in response to an osmoregulatory hormone, cortisol (Kolosov et al., 2017). Thus, in the skin, changes in the abundance of Cldn-8d and -31 may also be linked.

In addition to the changes in Cldn-8d and -31 abundance, Cldn-32a also altered with 24 hours of IPW exposure, remaining low in the dorsal region but being upregulated in the ventral

region. If Cldn-32a abundance is inversely related to epithelial tightness in the skin of rainbow trout as it is in the gill epithelium, the decrease in Cldn-32a abundance in the dorsal skin (in association with Cldn-8d no longer being downregulated) may indicate that the dorsal skin is less permeable with 24 hours of IPW exposure compared to FW. On the other hand, in the ventral region, an increase in Cldn-32a is coincident with the upregulation of Cldn-8d. In mammalian kidney, Cldn-8 has been found to interact with pore-forming Cldn-4 in order to establish anion selectivity in this tissue (Hou et al., 2010). Thus, a similar phenomenon may be occurring in the ventral skin of rainbow trout with 24 hours of IPW exposure, where Cldn-8d may be interacting with Cldn-32a (a teleostean Cldn-4 homologue; Loh et al., 2004).

Given that the mRNA of Cldn-8d, -31 and -32a proteins did not alter in the dorsal and ventral regions, despite the changes in protein abundance, it is likely that the changes in protein abundance were occurring as a result of post-translational modifications to the proteins. A variety of Cldn proteins, including Cldn-8, have been reported to undergo post-translational modifications in mammals (Findley and Koval, 2009; Gong et al., 2015). Therefore, it is possible that the regulation of Cldn proteins in the skin occurred mainly at the protein level.

Overall, during the acute stages of IPW exposure, there appears to be a balanced interplay between Cldn-8d, -31 and -32a proteins, where their abundance changed drastically over the 24-hour period, but was not dependent on mRNA levels. Overall, data suggests that the dorsal region may be less permeable after 24 hours of IPW exposure.

2.5.6.3 IPW exposure for 14 days resulted in a coordinated regulation of epidermal Cldns

After 14 days, Cldn-8d was the only epidermal-associated protein that was upregulated in the skin. This may have resulted in an overall reduction of dorsal skin paracellular permeability after 14

days of IPW acclimation. This would increase the difference in paracellular permeability between dorsal and ventral skin regions observed under FW conditions (see **section 2.5.4; Figure 2.3a-b**), which would further prevent the passive loss of ions from the underlying muscle (**Figure S2.1**). Although none of the other epidermal Cldns exhibited differences in protein abundance compared to their FW controls, they all showed regional differences in mRNA levels. This suggests that the observed mRNA changes were aimed at maintaining unaltered protein levels necessary for acclimation to the IPW environment. Therefore, elevated levels of Cldn-8d were important for IPW acclimation, and the levels of other Cldns were tightly regulated.

2.5.6.4 Cldn-10c may be linked to Ca^{++} mobilization from the scales

Cldn-10c protein abundance was found to increase in the ventral skin following 6 hours of IPW exposure and decrease back to control levels after 24 hours (**Figure 2.7**). This paralleled the increase in $[Ca^{++}]$ in the serum at 6 hours, and decline at 24 hours (see **section 2.5.5; Figure 2.5c**). Importantly, Cldn-10c was the only Cldn to localize beneath the scales in the dermis instead of a typical epidermal cell-cell contact localization (**Figure 2.2**). Cldn-10 isoforms have been found to be pore-forming in vertebrates (Gunzel and Fromm, 2012; Bui and Kelly, 2014), therefore, it is possible that Cldn-10c in the skin of rainbow trout may also be a pore-forming Cldn. Additionally, based on its immunolocalization under the scales, there is a potential that Cldn-10c is located adjacent to hyposquamal scleroblasts (Metz et al., 2012). Hyposquamal scleroblasts are cells that secrete the basal plate matrix (a calcified, collagen-containing layer of the scale) (Ohira *et al.,* 2007). If Cldn-10c localizes to the scleroblasts, it may play a role in Ca^{++} mobilization in rainbow trout scales. In previous studies, scale Ca^{++} content of fish held in water containing low $[Ca^{++}]$ (i.e. IPW) was found to decrease in order to maintain serum mineral balance (Flik *et al.,* 1986; Rodgers,

1984). Therefore, there is reason to suggest that Cldn-10c may be regulating serum [Ca^{++}] by mobilizing Ca^{++} deposited in the scales.

2.6 Conclusions and future perspectives

Overall, the inherent permeability of rainbow trout skin in FW differs between the dorsal and ventral regions, and this may be linked to the spatial abundance of Cldn proteins. Additionally, Cldn abundance altered, at the transcript or protein level, in a time-dependent and region-specific manner during IPW acclimation. Cldn-8d, -31 and -32a to be involved in alterations to skin barrier properties with acute IPW exposure, while regional upregulation of Cldn-8d is important for long-term IPW acclimation. Finally, Cldn-10c appears to be cell-specific and may contribute to the regulation of serum Ca^{++} levels. Therefore, the skin of rainbow trout is not a static, passive organ, but is rather tightly regulated in a region-specific manner in response to IPW exposure.

Future studies should examine the paracellular permeability of the skin with IPW exposure at different time points, to determine whether the changes in Cldn protein abundance correlate with paracellular permeability. Additionally, it would be interesting to examine the effect of seawater (SW) on regional Cldn abundance in the skin of rainbow trout. Given that SW presents different physiological challenges and results in a different restructuring of osmoregulatory organs compared to FW (McCormick, 2011), it would be interesting to contrast the Cldn proteins that are affected with this salinity challenge with those involved in IPW acclimation. It would also be interesting to examine the effect of salinity change on fishes that are able to actively transport ions with their skin, such as the mangrove rivulus (*Kryptolebias marmoratus*; LeBlanc et al., 2010). It would be useful to know whether Cldns play an equal or greater role in active skin tissue, and whether regional paracellular permeability differs in these fishes under control conditions as well.

Additionally, examining the effect of salinity change on Cldn abundance in the skin of fishes with a more pronounced dorso-ventral axis (e.g., mudskipper) would allow for better understanding of the function of individual Cldns in regulating the skin barrier function. Finally, to understand the involvement of Cldn-10c in Ca^{++} regulation, a study could be conducted that examines the effect of low and high water [Ca^{++}] (without perturbing environmental levels of other ions) on serum [Ca^{++}] and Cldn-10c abundance. A time-course study could also be performed, examining the abundance of Cldn-10c in scale pockets after scales have been pulled out of the skin. A scleroblast marker, such as Zns5 (Simões et al., 2014), could be used to visualize potential co-localization of Cldn-10c and scleroblasts.

2.7 References

Abraham, M., Iger, Y., Zhang, L., 2001. Fine structure of the skin cells of a stenohaline freshwater fish *Cyprinus carpio* exposed to diluted seawater. Tissue Cell 33, 46–54.

Al-Jandal, N.J., Wilson, R.W., 2011. A comparison of osmoregulatory responses in plasma and tissues of rainbow trout (*Oncorhynchus mykiss*) following acute salinity challenges. Comp. Biochem. Physiol. - A Mol. Integr. Physiol. 159, 175–181.

Bagherie-lachidan, M., Wright, S.I., Kelly, S.P., 2008. Claudin-3 tight junction proteins in *Tetraodon nigroviridis*: cloning, tissue-specific expression, and a role in hydromineral balance. Am J Physiol Integr Comp Physiol 294, 1638–1647.

Bagherie-Lachidan, M., Wright, S.I., Kelly, S.P., 2009. Claudin-8 and -27 tight junction proteins in puffer fish *Tetraodon nigroviridis* acclimated to freshwater and seawater. J. Comp. Physiol. B. 179, 419–31.

Bui, P., Kelly, S.P., 2014. Claudin-6, -10d and -10e contribute to seawater acclimation in the euryhaline puffer fish *Tetraodon nigroviridis*. J. Exp. Biol. 217, 1758–67.

Chasiotis, H., Kolosov, D., Kelly, S.P., 2012. Permeability properties of the teleost gill epithelium under ion-poor conditions. Am. J. Physiol. Regul. Integr. Comp. Physiol. 302, R727-39.

Cooper, C.A., Wilson, J.M., Wright, P.A., 2013. Marine, freshwater and aerially acclimated mangrove rivulus (*Kryptolebias marmoratus*) use different strategies for cutaneous ammonia excretion. AJP Regul. Integr. Comp. Physiol. 304, R599–R612.

Clelland, E.S., Kelly, S.P., 2010. Tight junction proteins in zebrafish ovarian follicles: Stage specific mRNA abundance and response to 17B-estradiol, human chorionic gonadotropin, and maturation inducing hormone. Gen. Comp. Endocrinol. 168, 388–400.

Colombo, L., Dalla Vale, L., Fiore, C., Armanini, D., Belvedere, P., 2006. Aldosterone and the conquest of land. J. Endocrino. Invest 29, 373–379.

Donini, A., O'Donnell, M.J., 2005. Analysis of Na^+, Cl^-, K^+, H^+ and NH_4^+ concentration gradients adjacent to the surface of anal papillae of the mosquito *Aedes aegypti*: application of self-referencing ion-selective microelectrodes. J. Exp. Biol. 208, 603-610.

Findley, M.K., Koval, M., 2009. Regulation and roles for claudin-family tight junction proteins. IUBMB Life 61, 431–437.

Flik, B.Y.G., Fenwickf, J.C., Kolarj, Z., Bonga, S.E.W., Kolar, Z., Mayer-Gostan, N., Bonga, S.E.W., 1986. Effects of low ambient calcium levels on whole-body calcium flux rates and internal calcium pools in the freshwater cichlid teleost, *Oreochromis mossambicus*. J. Exp. Biol. 120, 249–264.

Gauberg, J., Kolosov, D., Kelly, S.P., 2017. Claudin tight junction proteins in rainbow trout (*Oncorhynchus mykiss*) skin: Spatial response to elevated cortisol levels. Gen. Comp. Endocrinol. 240, 214–226.

Gong, Y., Wang, J., Yang, J., Gonzales, E., Perez, R., Hou, J., 2015. KLHL3 regulates paracellular chloride transport in the kidney by ubiquitination of Claudin-8. Proc. Natl. Acad. Sci. 112, 4340–4345.

Greco, A.M., Fenwick, J.C., Perry, S.F., 1996. The effects of soft-water acclimation on gill structure in the rainbow trout *Oncorhynchus mykiss*. Cell Tiss Res 285, 75–82.

Günzel, D., Fromm, M., 2012. Claudins and other tight junction proteins. Compr. Physiol. 2, 1819–1852.

Hinton, D. E., & Giulio, R. T. D. (2008). The Toxicology of Fishes. Taylor & Francis. pp. 78.

Hou, J., Renigunta, A., Yang, J., Waldegger, S., 2010. Claudin-4 forms paracellular chloride channel in the kidney and requires Claudin-8 for tight junction localization. Proc. Natl. Acad. Sci. U. S. A. 107, 18010–18015.

Huising, M.O., Guichelaar, T., Hoek, C., Verburg-van Kemenade, B.M.L., Flik, G., Savelkoul, H.F.J., Rombout, J.H.W.M., 2003. Increased efficacy of immersion vaccination in fish with hyperosmotic pretreatment. Vaccine 21, 4178–4193.

Kelly, S.P., Wood, C.M., 2001. Effect of cortisol on the physiology of cultured pavement cell epithelia from freshwater trout gills. Am. J. Physiol. Regul. Integr. Comp. Physiol. 281, 811–820.

Kent, M.., Dungan, C.F., Elston, R.A., Holt, R.A., 1988. *Cytophaga* sp. (Cytophagales) infection in seawater pen-reared Atlantic salmon *Salmo salar*. Dis. Aquat. Organ. 4, 173–179.

Kolosov, D., Bui, P., Chasiotis, H., Kelly, S.P., 2013. Claudins in teleost fishes. Tissue Barriers 1, 1–15.

Kolosov, D., Chasiotis, H., Kelly, S.P., 2014. Tight junction protein gene expression patterns and changes in transcript abundance during development of model fish gill epithelia. J. Exp. Biol. 217, 1667–81.

Kolosov, D., Kelly, S.P., 2016. Dietary salt loading and ion-poor water exposure provide insight into the molecular physiology of the rainbow trout gill epithelium tight junction complex. J. Comp. Physiol. B. 186, 739-757.

Kolosov, D., Donini, A., Kelly, S.P., 2017. Claudin-31 contributes to corticosteroid-induced alterations in the barrier properties of the gill epithelium. Mol. Cell. Endocrinol. 439, 457–466.

Kolosov, D., Kelly, S.P., 2017. Claudin-8d is a cortisol-responsive barrier protein in the gill epithelium of trout J. Mol. Endocrinol. 59, 1-12.

Kwong, R.W.M., Perry, S.F., 2013. Cortisol regulates epithelial permeability and sodium losses in zebrafish exposed to acidic water. J. Endocrinol. 217, 253–264.

LeBlanc, D.M., Wood, C.M., Fudge, D.S., Wright, P.A., 2010. A fish out of water: gill and skin remodeling promotes osmo- and ionoregulation in the Mangrove killifish *Kryptolebias marmoratus*. Physiol. Biochem. Zool. 83, 932–949.

Loh, Y.H., Christoffels, A., Brenner, S., Hunziker, W., Venkatesh, B., 2004. Extensive expansion of the claudin gene family in the teleost fish, *Fugu rubripes*. Genome Res. 1248–1257.

Madsen, S.S., Engelund, M.B., Cutler, C.P., 2015. Water transport and functional dynamics of Aquaporins in osmoregulatory organs of fishes. Biol. Bull. 229, 70–92.

Marshall, W.S., Grosell, M., 2005. Ion osmoregulation, and acid–base balance. Physiol. Fishes 177–230.

McCormick, S.D., 2011. Hormonal control of metabolism and ionic regulation, in Encyclopedia of Fish Physiology: From Genome to Environment. Elsevier Inc. pp 1466-1473.

McCormick, S.D., Bradshaw, D., 2006. Hormonal control of salt and water balance in vertebrates. Gen. Comp. Endocrinol. 147, 3–8.

McCormick, S.D., Hasegawa, S., Hirano, T., 1992. Calcium uptake in the skin of a freshwater teleost. Proc. Natl. Acad. Sci. U. S. A. 89, 3635–3638.

McKinley, R.S., 2008. Effects of soft-water acclimation on the physiology, swimming performance, and cardiac parameters of the rainbow trout, *Oncorhynchus mykiss*. Fish Physiol. Biochem. 34, 313–322.

Metz, J.R., de Vrieze, E., Lock, E.J., Schulten, I.E., Flik, G., 2012. Elasmoid scales of fishes as model in biomedical bone research. J. Appl. Ichthyol. 28, 382–387.

Nowak, B.F., 1999. Significance of environmental factors in aetiology of skin diseases of teleost fish. Bull. Eur. Assoc. Fish Pathol. 19, 290–292.

Ohira, Y., Shimizu, M., Ura, K., Takagi, Y., 2007. Scale regeneration and calcification in goldfish *Carassius auratus*: quantitative and morphological processes. Fish. Sci. 73, 46–54.

Perry, B.Y.S.F., Laurent, P., 1989. Adaptational responses of rainbow trout to lowered external NaCl concentration: contribution of the branchial chloride cell. 168, 147–168.

Pickering, A.D., Richards, R.H., 1980. Factors influencing the structure, function and biota of the salmonid epidermis. Proc. R. Soc. Edinbg.

Rakers, S., Gebert, M., Uppalapati, S., Meyer, W., Maderson, P., Sell, A.F., Kruse, C., Paus, R., 2010. “Fish matters”: The relevance of fish skin biology to investigative dermatology. Exp. Dermatol. 19, 313–324.

Simões, M.G., Bensimon-Brito, A., Fonseca, M., Farinho, A., Valério, F., Sousa, S., Kumar, A., Jacinto, A., 2014. Denervation impairs regeneration of amputated zebrafish fins. BMC Dev. Biol. 14, 780.

Van Oosten, J. (1957). The skin and scales, in The Physiology of Fishes Vol. 1. (Ed. Brown, M.E.) New York: Academic Press. pp. 207-244.

Zall, D.M., Fisher, D., Garner, M.Q., 1956. Photometric determination of chlorides in water. Anal. Chem. 28, 1665–1668.

3. Chapter Three: Effects of photoperiod on TJ protein mRNA abundance in the skin of rainbow trout, *Oncorhynchus mykiss*

3.1 Summary

Circadian rhythms arise when cyclical environmental changes (e.g. light-dark cycles) enforce endogenous rhythms on animal physiology. Animals have evolved the ability to entrain their physiology to the external environment in order to anticipate and adapt to changes in environmental cues. In fishes, many peripheral tissues, including the skin, have been found to express circadian genes, however, only a handful of studies have examined mRNA rhythmicity in the teleost skin to date. In this regard, no circadian studies have been conducted on factors involved in regulating the barrier properties of teleost fish skin such as barrier proteins (i.e. tight junction (TJ) proteins), matrix metalloproteinases, or receptors of hormones documented to modulate TJ permeability. This study examined skin transcript abundance of clock genes, TJ proteins, matrix metalloproteinases and corticosteroid receptors over a 12 h light: 12 h dark (12-hour LD) period in rainbow trout, *Oncorhynchus mykiss*. Data indicated that trout skin expressed clock genes, some of which exhibited circadian-like rhythms. TJ protein transcripts oscillated in a gene- and region-specific manner. Corticosteroid receptor transcripts and matrix metalloproteinase transcripts also exhibited circadian-like rhythms in a region- and gene-dependent manner. Data provide new insight into teleost fish skin barrier properties and underscore the complexity of barrier function.

3.2 Introduction

3.2.1 Circadian rhythms and clock genes

Circadian rhythms arise when cyclical environmental changes (e.g. LD cycles) enforce endogenous rhythms on animal physiology. Animals have evolved the ability to entrain their

physiology to the external environment in order to anticipate and adapt to changes in environmental cues, such as temperature and food availability (Gerhart-Hines and Lazar, 2015). Circadian periods can be slightly shorter or longer than 24 hours and can be adjusted, or entrained, if the external cues change (Gerhart-Hines and Lazar, 2015). The strongest environmental cue that can entrain circadian rhythms is light, most likely because the day/night cycles are the most predictable natural rhythms present in the environment (Gerhart-Hines and Lazar, 2015).

Vertebrates possess a molecular "clock" mechanism, composed of proteins that form a transcriptional-translational feedback loop, which is responsive to light and establishes light-sensitive circadian rhythms in an organism (Gerhart-Hines and Lazar, 2015). The mechanism consists of two transcription factors, CLOCK and BMAL1, which dimerize and bind to promoter sequences, called E-boxes, of repressive proteins like Cryptochrome (CRY) and Period (PER) to initiate their transcription (**Illustration 3.1;** Gerhart-Hines and Lazar, 2015). CRY and PER then dimerize and suppress the CLOCK-BMAL1 dependent transcription of their own genes (Gerhart-Hines and Lazar, 2015). This cycle lasts approximately 24 hours and can be reset with a change in the light/dark cycle. This is a simplified mechanism because in reality the circadian transcription factors are able to regulate the oscillation of a wide variety of genes that are tissue- and cell-specific (Mohawk et al., 2012). For example, clock genes present in the brain and termed "central" pacemakers are able to regulate the rhythms of genes in the brain and in peripheral tissues (Mohawk et al., 2012). Additionally, clock genes present in peripheral tissues are also able to act as pacemakers for that tissue, providing additional layers of regulation to peripheral tissue gene expression (Gerhart-Hines and Lazar, 2015).

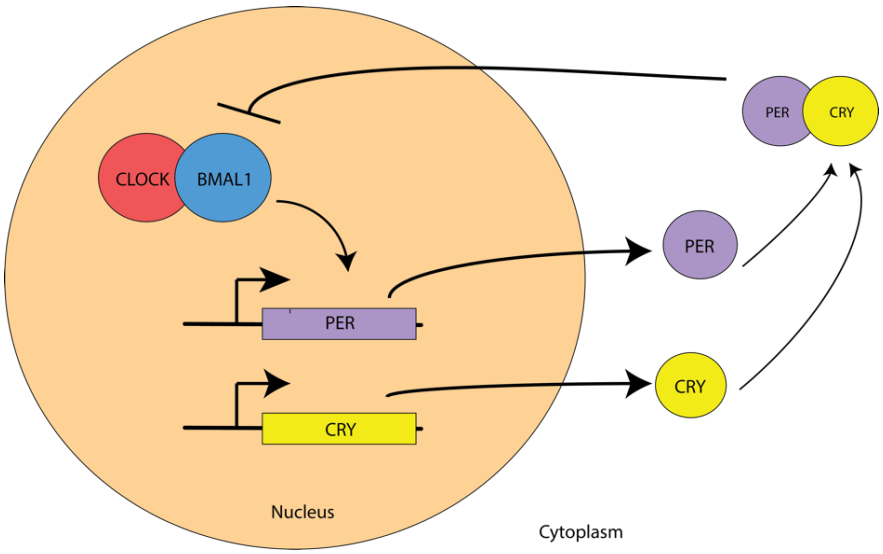

Illustration 3.1 Schematic of the activation of various clock genes in vertebrate cells. The CLOCK-BMAL1 protein complex activates the transcription of various *per* and *cry* genes. Once transcribed and translated, PER and CRY genes form a complex that inhibits the action of CLOCK-BMAL1.

3.2.2 Clock genes in teleosts

Several studies have been conducted on circadian rhythms in teleosts, with an emphasis on the zebrafish model (Idda et al., 2012a). Teleosts have multiple clock genes isoforms due to whole genome and tandem gene duplication events that occurred during teleost evolution (Idda et al., 2012a). For example, it has been reported that zebrafish possess three CLOCK and three BMAL genes, four PER genes and six CRY genes (Kobayashi et al., 2000; Wang 2008a,b,c). Clock isoforms do not appear to be redundant in function because they exhibit different period lengths, light-responsiveness, and tissue-specificity in various teleosts (Kobayashi et al., 2000; Velarde et al., 2009; Lazado et al., 2014).

In mammals, a central clock mechanism that is present in the brain appears to control the oscillations of peripheral (i.e. extracerebral) clock genes, however in teleosts, peripheral clock

genes appear to be independent (Idda et al., 2012a). For example, when the pineal gland, which produces the "sleep" hormone melatonin, was removed in rainbow trout, *Oncorhynchus mykiss*, their melatonin rhythms were not affected. This suggests that rainbow trout lack a central circadian oscillator and that peripheral organs must be maintaining their circadian rhythms (Sánchez-Vázquez et al., 2000). In addition to this, organ culture of peripheral zebrafish tissues (i.e. heart and kidney) demonstrated that clock genes in these organs could respond directly to light in a circadian manner (Whitmore et al., 2000). Therefore, fishes possess many peripheral clock genes that can be entrained to the light-dark cycle, including those found in the skin.

3.2.3 Circadian rhythms in the skin of fishes

The skin is exposed to changes in environmental conditions (e.g. ultraviolet radiation) throughout the day (Plikus et al., 2015). It is therefore natural to expect this organ to possess circadian machinery to anticipate these changes. Indeed, various fish species were found to express clock genes in the skin, and in zebrafish, their mRNA abundance altered with photoperiod (Velarde et al., 2009; Idda et al., 2012b; Lazado et al., 2014). Additionally, because the skin is a multi-layered and heterogeneous organ, its circadian clock can affect the expression/abundance of distinct genes from each cell type and result in different physiological functions (Plikus et al., 2015). For example, the basal epidermal layer of the zebrafish skin, which houses the skin progenitor cells, exhibited changes in cell proliferation activity with photoperiod (Idda et al., 2012b). Additionally, in two tetra species, *Paracheirodon innesi* and *P. axelrodi*, the ventral region of the skin, but not the dorsal, exhibited circadian changes in pigmentation with photoperiod (Hayashi et al., 1993). Thus, it is clear that fish skin can respond to photoperiod and the resulting circadian rhythms can

be cell- and/or region-specific. It is, however, not clear how these rhythms are entrained and controlled.

3.2.4 Cortisol: circadian rhythms and the effect on TJ proteins

Cortisol has been known to exhibit circadian oscillations in various vertebrate clades, including fishes (Chan and Callard, 1972; Kühn *et al.,* 1976; Laidley and Leatherland, 1988; Hoon et al., 2008). While cortisol is well known to be a stress hormone in tetrapods, in fishes cortisol acts as a stress and osmoregulatory hormone (McCormick, 2011). Cortisol, acting through corticosteroid receptors, has been shown to influence serum ion levels, paracellular permeability and the molecular components of the TJ complex in the gill epithelium of fishes (Kelly and Wood, 2001; Chasiotis and Kelly, 2011; Bui et al., 2010; Chasiotis et al., 2010; Kelly and Chasiotis, 2011; Gauberg et al., 2017). Most recently, in rainbow trout, cortisol loading was found to alter the mRNA abundance of various Cldn transcripts in the skin and exhibit a concurrent change in serum ion levels (Gauberg et al., 2017). Therefore, because cortisol levels exhibit circadian rhythms in fishes, and since cortisol can affect TJ protein mRNA abundance in the skin, then it is possible that TJ protein levels oscillate as well. However, no one has ever examined the abundance of TJ protein transcripts over a 12 hour LD period in fishes and linked this to the oscillation of cortisol or corticosteroid receptors.

3.2.5 Matrix metalloproteinases: Function, effect on TJ proteins and circadian rhythms

Matrix metalloproteinases (MMPs) are a large family of proteins, with 24 proteinases characterized in mammals and 26 MMP orthologues identified in zebrafish (Pedersen et al., 2015). The MMPs were originally believed to have one role, the breakdown of the extracellular matrix, but since then have been implicated in diverse physiological processes such as wound repair,

immunity, and cell transformation (Page-McCaw et al., 2007). One of the more recently discovered functions of MMPs is the regulation of epithelial/endothelial paracellular permeability and TJ protein abundance (Chen et al., 2009; Nighot et al., 2015; Wiechmann et al., 2014). Many studies have implicated MMP-2 and MMP-9 in the regulation of TJ proteins by playing a role in their degradation (Chen et al., 2009; Wiechmann et al., 2014). One study found that by using an MMP-9 inhibitor, the degradation of TJ proteins in the blood-brain barrier of mice was significantly reduced (Bauer et al., 2010). Given the above evidence, there is a high likelihood that MMPs, specifically MMP-2 and MMP-9, may contribute to the regulation of TJ protein abundance in the fish skin. However, no studies to date have examined the effect of MMPs on TJ proteins in the fish skin, and fishes in general.

Several studies have found MMP-2 and MMP-9 proteins to exhibit diurnal variations in mammalian and amphibian tissues (Anea et al., 2010; Markoulli et al., 2012; Wiechmann et al., 2014). Additionally, one of these studies was performed on the corneal epithelium, the properties of which (non-keratinizing, stratified squamous epithelium; Wiechmann et al., 2014) are similar to the fish epidermis. The day/night expression of MMPs has not been investigated in teleosts, however, it is very likely that a diurnal rhythm of MMP-2 and MMP-9 transcription exists in fish skin and that it can affect TJ protein mRNA abundance in a cyclical manner.

3.2.6 Circadian oscillation of TJ proteins

Recent studies have discovered that TJ proteins in mammals and amphibians exhibit circadian oscillations over a 24-hour period (Yamato et al., 2010; Kyoko et al., 2014; Wiechmann et al., 2014). One study found that Ocln and Cldn-1 exhibited oscillations in the mouse colon, and this was linked to daily changes in the paracellular permeability of this tissue (Kyoko et al., 2014).

Additionally, this group discovered that the cycling of these TJ proteins depended on the presence of Per2 protein, indicating that TJ protein abundance may be tightly linked to the peripheral clock in the mouse colon (Kyoko et al., 2014). Therefore, in mammals, TJ proteins have been found to oscillate over a 12-hour LD cycle.

Despite what is known in mammals, no studies have been conducted that investigate the potential circadian nature of TJ proteins in fishes. Recall that fish skin can respond to light (see **section 3.2.2**) and that several different mechanisms (e.g. cortisol, MMP) that exhibit circadian rhythms in fishes and other vertebrates have been implicated in the control of TJ protein abundance (see **sections 3.2.3 and 3.2.4**). Therefore, there is a high likelihood that TJ protein transcript abundance will respond to LD cycles.

The hypothesis for the present study is that TJ protein mRNA abundance will alter in the skin of teleosts over a 12-hour LD cycle. The objectives are to determine whether TJ proteins oscillate in fish skin and to investigate the regulatory mechanism behind their oscillations. To gain an understanding of the potential circadian regulation of TJ proteins in fish skin, rainbow trout, *Oncorhynchus mykiss,* will be examined to (1) determine whether clock genes are expressed and whether their protein transcripts oscillate in the skin, (2) examine whether TJ protein transcripts oscillate in the skin, and (3) determine whether regulatory factors, which could alter TJ protein transcript abundance, oscillate in the skin.

3.3 Materials and Methods

3.3.1 Experimental Animals

140 rainbow trout (*Oncorhynchus mykiss*, ~50g) were obtained from a local supplier (Humber Springs Trout Hatchery, Orangeville ON, Canada) and separated into seven equal groups of 20

fish/group. Each group of trout was housed in 200-liter opaque polyethylene tanks supplied with flow-through dechlorinated freshwater (FW, ~composition in μM: [Na^+]: 590, [Cl^-]: 930, [Ca^{++}]: 760, and [K^+]: 43). Fish were held under a constant photoperiod of 12 h light :12 h dark and fed *ad libitum* once daily with commercial trout pellets (Martin Profishent, Elmira, ON, Canada). The feeding schedule was randomized to prevent the fish from anticipating a feeding time. Trout were used for experiments following two weeks in lab conditions and feeding stopped 24 hours before the onset of the experiment. Prior to sampling, trout were exposed to 14 days of a 12-hour LD photoperiod, with lights turning on at 08:00 and turning off at 20:00. Fish culture and all experimental procedures were conducted according to a protocol approved by the York University Animal Care Committee and conformed to the guidelines of the Canadian Council on Animal Care.

3.3.2 Fish sampling procedure

Fish were net-captured every 4 hours over a 24 hour period starting at 13:00. They were netted from separate tanks to avoid netting-induced stress. During the dark phase, a red light was used during sampling to avoid the resetting of circadian clocks, while at the same time providing enough visibility to capture the fish. Trout were anaesthetized with buffered tricaine methanesulfonate TMS-222 (0.5 g/L; Syndel Laboratories, Vancouver, Canada) and euthanized by spinal transection following the cessation of movement.

3.3.3 Tissue sampling

See **section 2.3.3** in Chapter 2 for details. For one gene expression experiment (see **section 3.4.5**), an additional skin sample that spanned 0.5 cm on either side of the lateral line was excised in addition to the dorsal and ventral samples.

3.3.4 Muscle Moisture and Serum Ion Concentration

See **section 2.3.7** in Chapter 2 for details.

3.3.5 RNA extraction and cDNA synthesis

See **section 2.3.8** in Chapter 2 for details.

3.3.6 Analysis of clock and MMP protein mRNA abundance by PCR and gel electrophoresis

Gene-specific primers designed for rainbow trout clock genes, cortisol receptor and clearing enzyme genes, and matrix metalloproteinase genes (see **Table 3.1**) were used in both PCR and qPCR (see **section 3.3.7**). For PCR, the following reaction conditions were utilized: 1 initial cycle of denaturation (95^{o} C, 4 min), then 40 cycles of denaturation (95^{o} C, 30 sec), annealing (58-61^{o}C, 30 sec) and extension (72^{o}C, 30 sec), followed by a final single extension cycle (72^{o}C, 5 min). PCR generated amplicons were visualized by 1.5% agarose gel electrophoresis (120V separation for 1 hour).

Table 3.1. Primer sets and corresponding amplicon sizes, annealing temperatures and GenBank accession numbers for clock genes, cortisol receptor and clearing enzyme genes, and matrix metalloproteinase genes in rainbow trout, *Oncorhynchus mykiss*.

Category	Protein	Gene	Primer sequence (5'-3')	Ta	Amplicon size (bp)	Accession number
Clock	Cryptochrome 3	*cry3*	F: GCTGATAACCACGACGAACA R: ATAAAGAGAGCGGGGGACTG	60	313	N/A
	Period 2	*per2*	F: CCAATAACAGTCAGCCATCC R: TCACACTCCTTACCCCCAC	58	364	N/A
Cortisol receptors and clearing enzyme	Glucocorticoid receptor 1	*gr1*	F:GGACTGAAACACAGCAAGGAC R: GCAATACTCGCCTCCAACAG	59	335	NM_001124730
	Glucocorticoid receptor 2	*gr2*	F: AGAACACGTCTGCCATGC R: CTGGAGAAAGCGGAGGTAG	57	346	NM_001124482
	Mineralocorticoid receptor	*mr*	F: TGTGTCTGGGTAATGGTAGC R: CGTTGTTGTTGTTCTCTTGG	56	369	AY495584
	11β-hydroxysteroid dehydrogenase type 2 isoform	*11β-hsd*	F: GGCTGTGGTTCTTCTGTGTG R: GATGAGGGGAGCAGGTCTTC	59	257	NM_001124218.1
Matrix metalloproteinases	Matrix metalloproteinase-2	*mmp2*	F: ACCTGTGGTGTTTGATGCTG R:AGCCTTTCTCTATCTGGTCTGC	59	242	N/A
	Matrix metalloproteinase-9	*mmp9*	F: AGAGAGGGAAAGGCAAGGTG R:GTTGGAGTTCATTCGCCAGTAG	60	203	N/A

3.3.7 Analysis of clock, TJ, corticosteroid hormone receptor, and MMP protein mRNA by quantitative real-time PCR (qPCR).

See **section 2.3.9** in Chapter 2 for details. For all qPCR analyses, transcript abundance was normalized to *ef-1α* transcript abundance after determining by statistical analysis that *ef-1α* did not significantly alter (P_{dorsal}=0.990; $P_{ventral}$=0.968) between time points. Rainbow trout *ef-1α* mRNA was amplified using primers previously reported by Kolosov et al. (2014).

3.3.8 Statistical analyses

All data were expressed as mean values ±SEM (n), where n represents the number of fish sampled. Significant differences ($P \leq 0.05$) between groups were determined using one-way analysis of variance (ANOVA) or the Student's t-test as indicated. All statistical analyses were performed using SigmaPlot 12.5 (Systat Software Inc., San Jose, CA, USA). To evaluate the rhythmicity of the changes in mRNA abundance, cosinor analyses were performed. A periodic sinusoidal function was fitted to the values of mRNA abundance using the formula:

f(t)= M+Acos[(2π(t-φ)/τ] where f(t)=the gene expression level at a particular time point; M=mesor; the mean value of all the points; A=amplitude of oscillation; t=time in hours; φ= acrophase; time of first peak; and τ=period, usually 24 hours (**Illustration 3.2**). Cosinor significance was calculated according to Hernández-Pérez et al. (2015). The noise/signal of the amplitude was calculated using the ratio standard error of the amplitude over amplitude: SE(A)/A. A gene was considered to display a circadian rhythm if it passed both SE(A)/A≤0.3 and ANOVA p≤0.05.

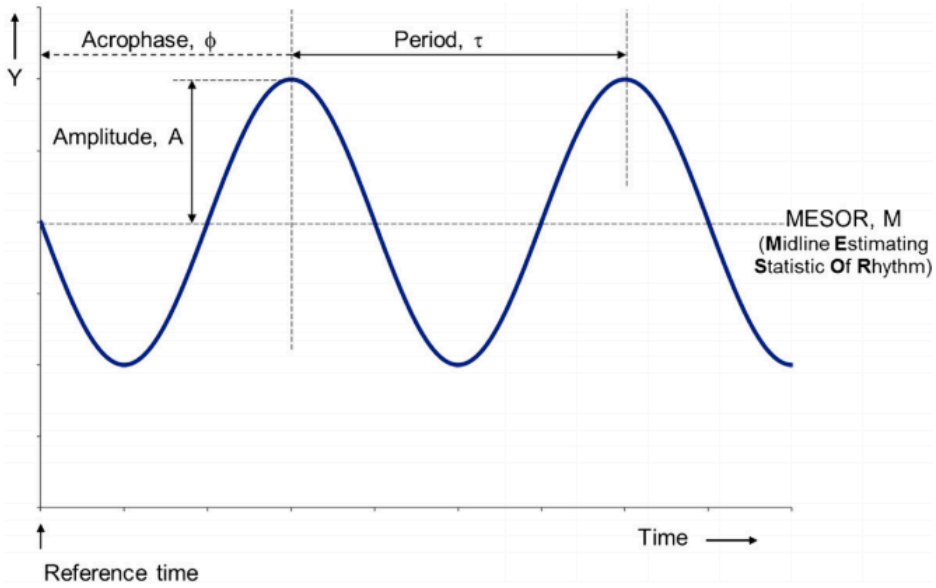

Illustration 3.2 Sinusoidal rhythm characteristics. From Cornelissen, 2014.

3.4 Results

3.4.1 Effect of a 12-hour LD cycle on serum ion concentration and muscle moisture content in rainbow trout.

Following two weeks of acclimation to a 12 h light: 12 h dark photoperiod, rainbow trout serum ion levels and muscle moisture content was examined (**Figure 3.1**). The 12 hour-LD photoperiod had no effect on serum chloride and sodium levels or on muscle moisture content.

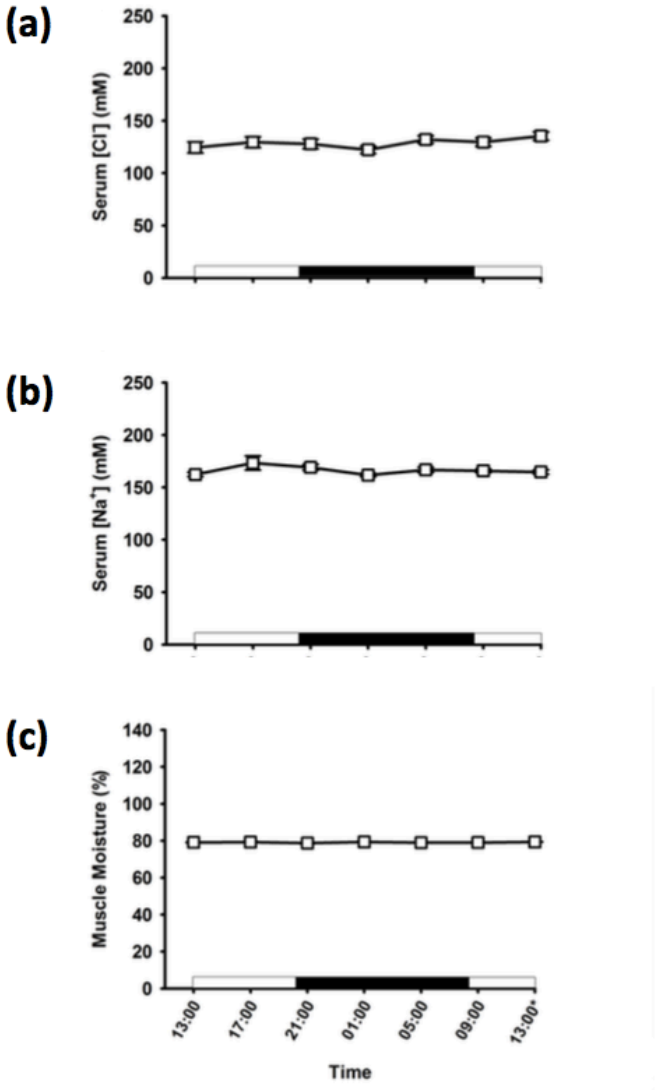

Figure 3.1. (a) Serum chloride (Cl^-) concentration, (b) serum sodium (Na^+) concentration, and (c) muscle moisture content in rainbow trout (*Oncorhynchus mykiss)* during a 12 h light: 12 h dark cycle. All data are expressed as mean values ± SEM (n = 10), where n is the number of fish sampled.

3.4.2 Effect of 12 hour LD cycle on clock gene transcription in the dorsal and ventral skin of rainbow trout.

All examined clock genes were present in the skin of rainbow trout (**Figure 3.2**) and the effect of the LD cycle was gene dependent (**Figure 3.3)**. Transcript levels of *per2* responded to light: they were lowest in the dark phase, and peaked at the onset of the light phase in both the dorsal and ventral regions. There was a significant difference in mRNA abundance over time in the dorsal and ventral regions, as determined by a one-way ANOVA, and both regions passed cosinor analysis (**Table 3.2**). The levels of *cry3* were unaffected by photoperiod.

Figure 3.2. Expression of *period2* (*per2*), *cryptochrome3* (*cry3*) and elongation factor 1α (*ef-1α)* in the ventral skin of rainbow trout (O*ncorhynchus mykiss*). Transcripts were examined in the skin with PCR and visualized with 1.5% agarose gel electrophoresis. Negative control was run under the same conditions but contained only sterile water (not shown).

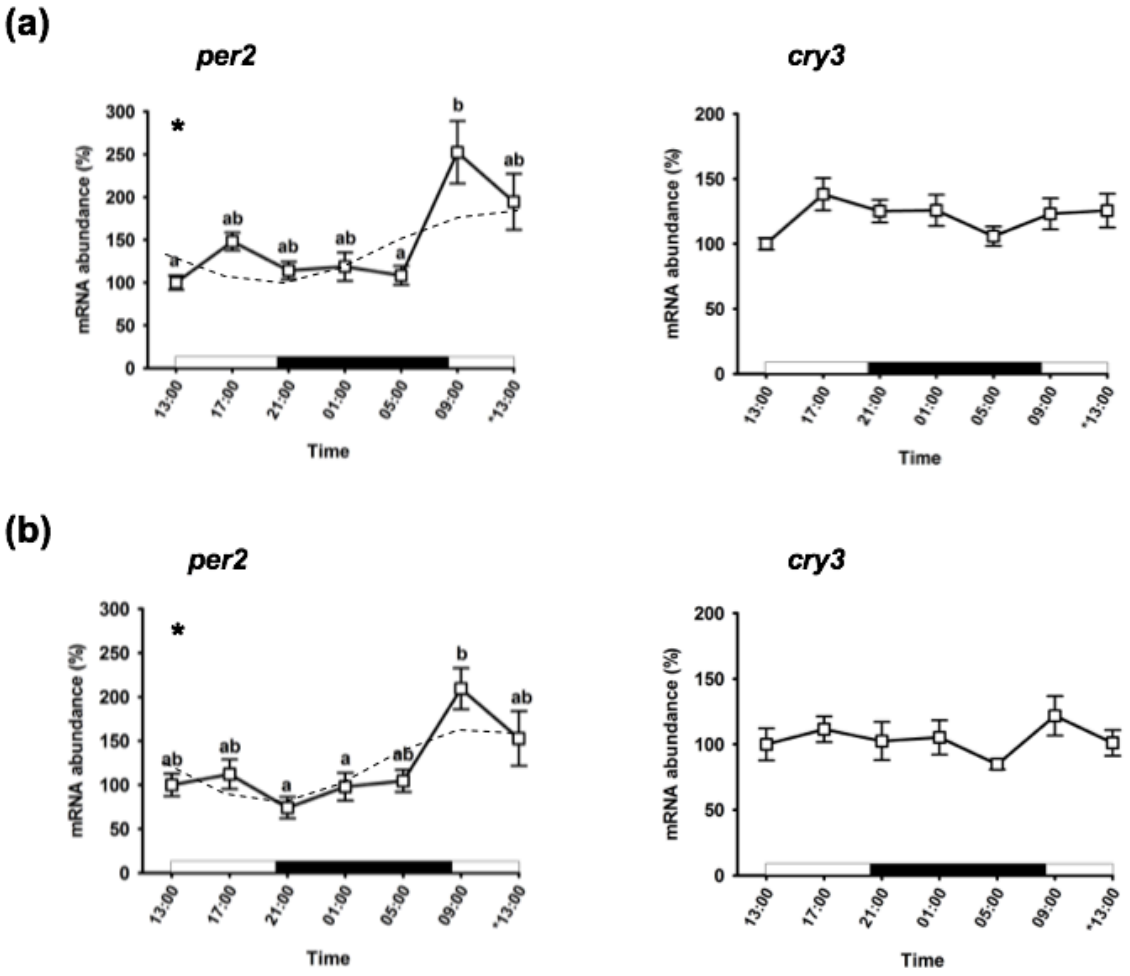

Figure 3.3. Effect of a 12-hour LD photoperiod on clock gene mRNA abundance in the (a) dorsal and (b) ventral regions of rainbow trout (*Oncorhynchus mykiss*) skin. All data are mean values ± SEM (n=8). Lower case lettering indicate significant differences between time points as determined by a one-way ANOVA. Transcript abundance was expressed relative to the first sample point (13:00) taken from FW animals assigned a value of 100. *ef-1α* was used as a reference gene. Asterisks in the top-left corner indicate that the data passed cosinor analysis [SE(A)/A<0.3].

Table 3.2. Cosinor analysis parameters and SE(A)/A values for clock genes in *Oncorhynchus mykiss* skin. Bolded values have SE(A)/A<0.3.

Gene	Region	Mesor	Acrophase	Amplitude	SE(A)/A
cry3	Dorsal	-	-	-	-
	Ventral	-	-	-	-
per2	**Dorsal**	**148.0**	**20**	**76.2**	**0.279**
	Ventral	**122.7**	**20**	**25.5**	**0.272**

3.4.3 Effect of 12-hour LD cycle on *cldn*, *ocln*, and *tric* mRNA abundance in dorsal and ventral skin of rainbow trout

The effect of photoperiod on TJ protein mRNA abundance was gene- and region-specific (**Figure 3.4a**). Five TJ protein transcripts (i.e. *cldn-8d, -10c, -28b, -31,* and *ocln*) altered in abundance in the dorsal skin region throughout the 12-hour LD cycle. All five transcripts exhibited different trends over the 24 hour period. These were as follows: (1) *ocln* levels were high late in the evening and low in the middle of the dark phase; (2) *cldn-8d* mRNA levels in the dorsal skin increased throughout the night, dropped at 09:00, and then increased again 4 hours later; (3) *cldn-10c* abundance was variable but consistently decreased at 01:00 and increased 4 hours later; (4) *cldn-28b* levels mimicked those of *cldn-8d*, however, there was no significant decrease at 09:00; (5) the abundance of *cldn-31* incrementally increased and fell, with a peak at 01:00. Most TJ protein transcripts that altered in the dorsal skin exhibited circadian-like rhythms, with the exception of *cldn-8d* and *ocln* (**Table 3.3**).

Transcripts encoding *cldn-10c, -28b,* and *ocln* also altered in abundance the ventral region over the light-dark cycle (**Figure 3.4b**). Specifically, *cldn-28b* and *ocln* exhibited similar trends in the ventral region to those observed in the dorsal skin region, with transcript levels peaking at 05:00. However, the change in magnitude of *cldn-28b* abundance was 3-fold higher than *ocln*. *Cldn-10c* appeared to have a period of less than 24 hours in the ventral region, with two maxima at 17:00 and 09:00, and a minimum at 01:00. Additionally, the changes in abundance for *cldn-28b* and *ocln* showed significant SE(A)/A values with cosinor analysis in the ventral skin (**Table 3.3**).

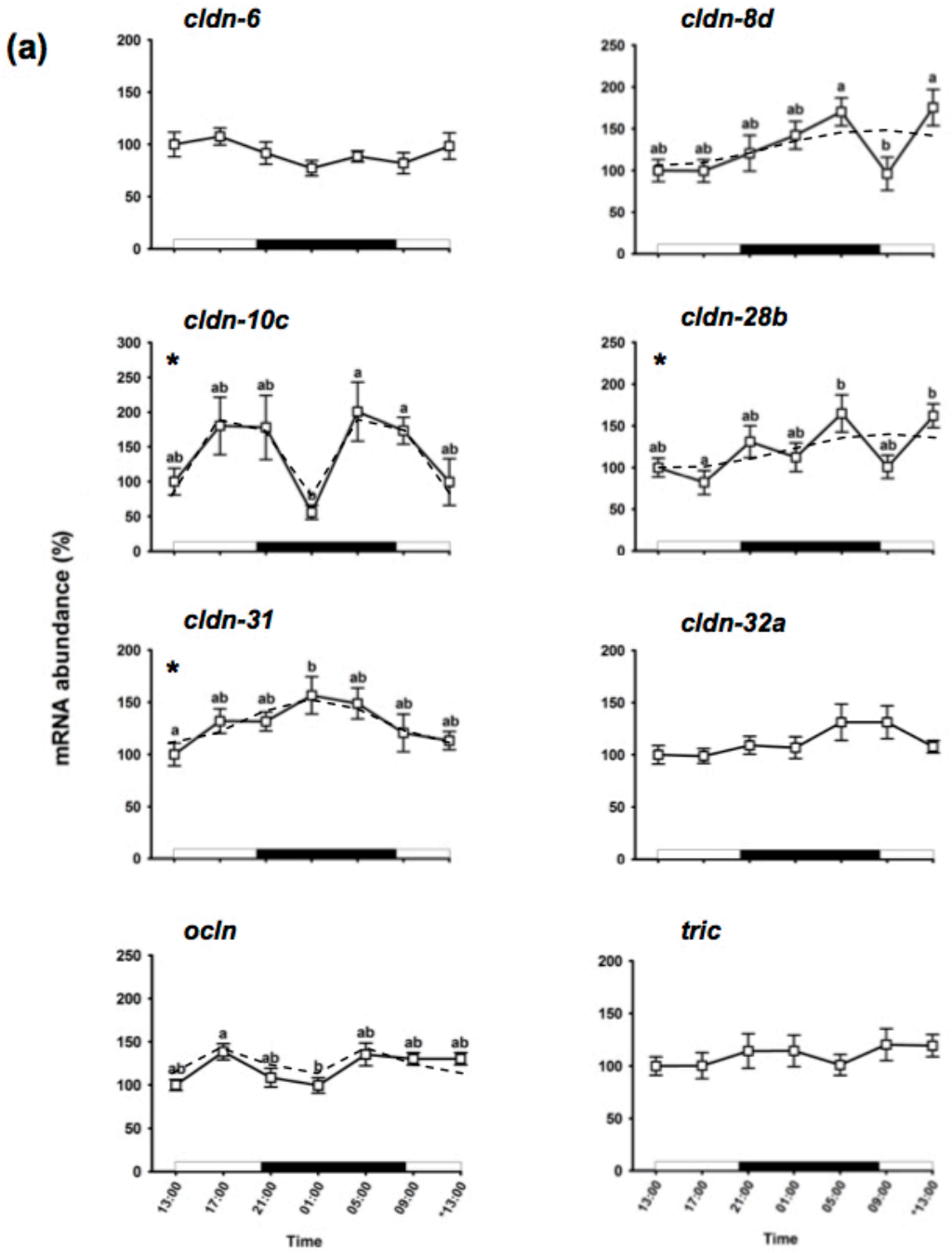

Figure 3.4. Effect of a 12-hour LD photoperiod on claudin *(cldn*), occludin (*ocln*), and tricellulin (*tric*) mRNA abundance in the (a) dorsal and (b) ventral region of rainbow trout (*Oncorhynchus mykiss*) skin. All data are mean values ± SEM (n=8). Lower case lettering indicate significant differences between time points as determined by a one-way ANOVA. Transcript abundance was expressed relative to the first sample point (13:00) assigned a value of 100. *ef-1α* was used as a reference gene. Asterisks in the top-left corner indicate that the data passed cosinor analysis [SE(A)/A<0.3].

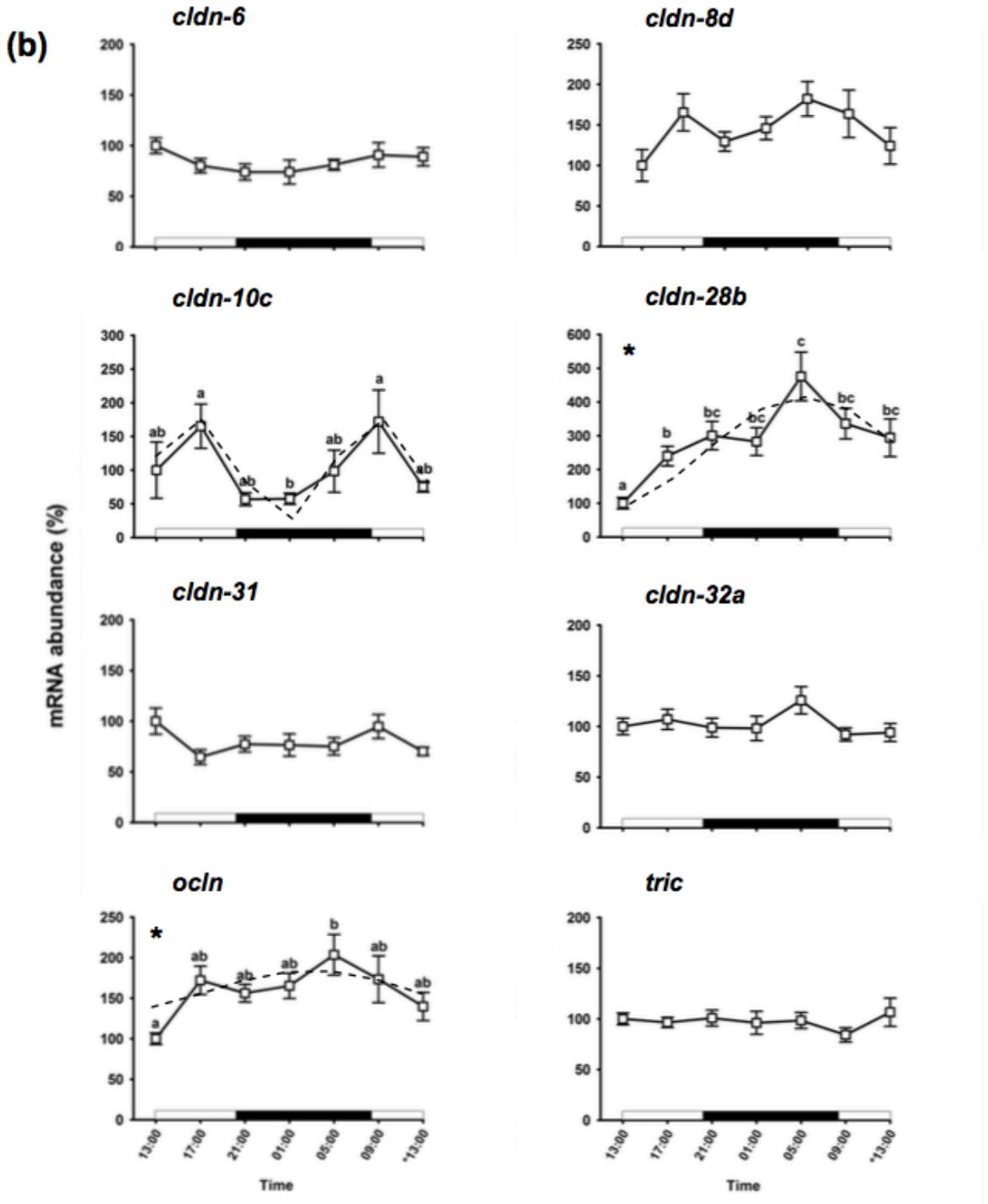

Figure 3.4. See previous page for caption

Table 3.3. Cosinor analysis parameters and SE(A)/A values for TJ genes in *Oncorhynchus mykiss* skin. Bolded values have SE(A)/A<0.3

Gene	Region	Mesor	Acrophase	Amplitude	SE(A)/A
cldn-6	Dorsal	-	-	-	-
	Ventral	-	-	-	-
cldn-8d	Dorsal	129.2	16	37.1	0.346
	Ventral	-	-	-	-
cldn-10c	**Dorsal**	**141.1**	**4**	**20.8**	**0.287**
	Ventral	103.6	4	57.7	0.313
cldn-28b	**Dorsal**	**121.9**	**16**	**41.5**	**0.292**
	Ventral	**289.9**	**16**	**187.9**	**0.226**
cldn-31	**Dorsal**	**129.0**	**12**	**28.3**	**0.263**
	Ventral	-	-	-	-
cldn-32a	Dorsal	-	-	-	-
	Ventral	-	-	-	-
ocln	Dorsal	120.4	4	19.4	0.332
	Ventral	**158.7**	**16**	**51.8**	**0.236**
tric	Dorsal	-	-	-	-
	Ventral	-	-	-	-

3.4.4 Effect of 12-hour LD cycle on glucocorticoid receptor 1 (*gr1*) and 2 (*gr2*), mineralocorticoid receptor (*mr*), and 11ß-hydroxysteroid dehydrogenase (11*β* -hsd) mRNA levels in the skin of rainbow trout

Transcripts encoding the two glucocorticoid receptors of rainbow trout (i.e. *gr1* and *gr2*) transcripts exhibited the same trends (**Fig 3.5**). More specifically, in the dorsal region, their levels peaked at 09:00 and decreased by perceived mid-day (**Figure 3.5a**). In the ventral region, *gr1* and *gr2* abundance was unaltered (**Figure 3.5b**). In contrast, *mr* abundance oscillated in both the dorsal and ventral skin regions, increasing from perceived mid-afternoon and peaking at 01:00 in both

regions (**Figure 3.5a-b**). Cosinor analysis showed that the change in *mr, gr1* and *gr2* abundance was circadian-like in the skin (**Table 3.4**). Abundance of cortisol clearing enzyme transcript *11ß-hsd* did not alter in abundance over the 24 hour period.

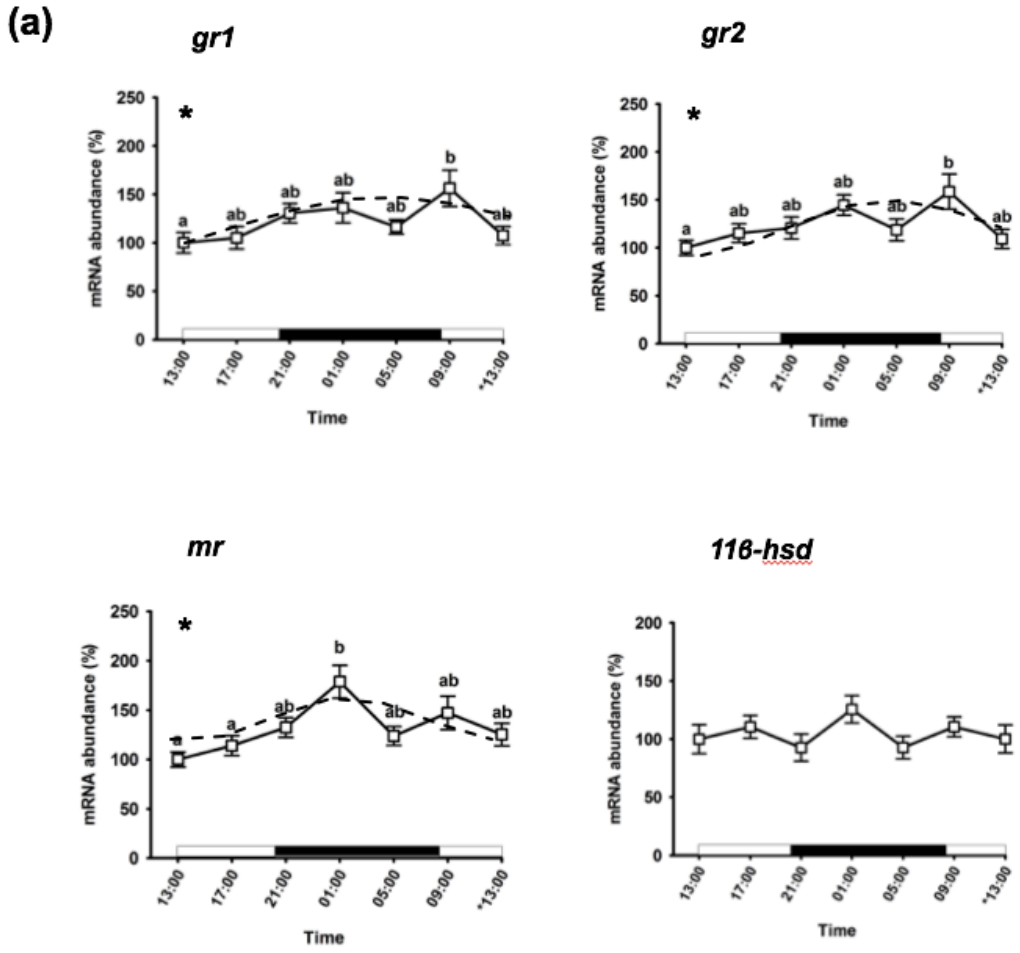

Figure 3.5. Effect of a 12-hour LD photoperiod on glucocorticoid 1 (*gr1*), glucocorticoid 2 (*gr2*), and mineralocorticoid (*mr*) receptor, as well as 11β-hydroxysteroid dehydrogenase (*11ß-hsd*) mRNA abundance in the (a) dorsal and (b) ventral regions of rainbow trout (*Oncorhynchus mykiss*) skin. All data are mean values ± SEM (n=8). Lower case lettering indicate significant differences between time points as determined by a one-way ANOVA. Transcript abundance was expressed relative to the first sample point (13:00) taken from FW animals assigned a value of 100. *ef-1α* was used as a reference gene.

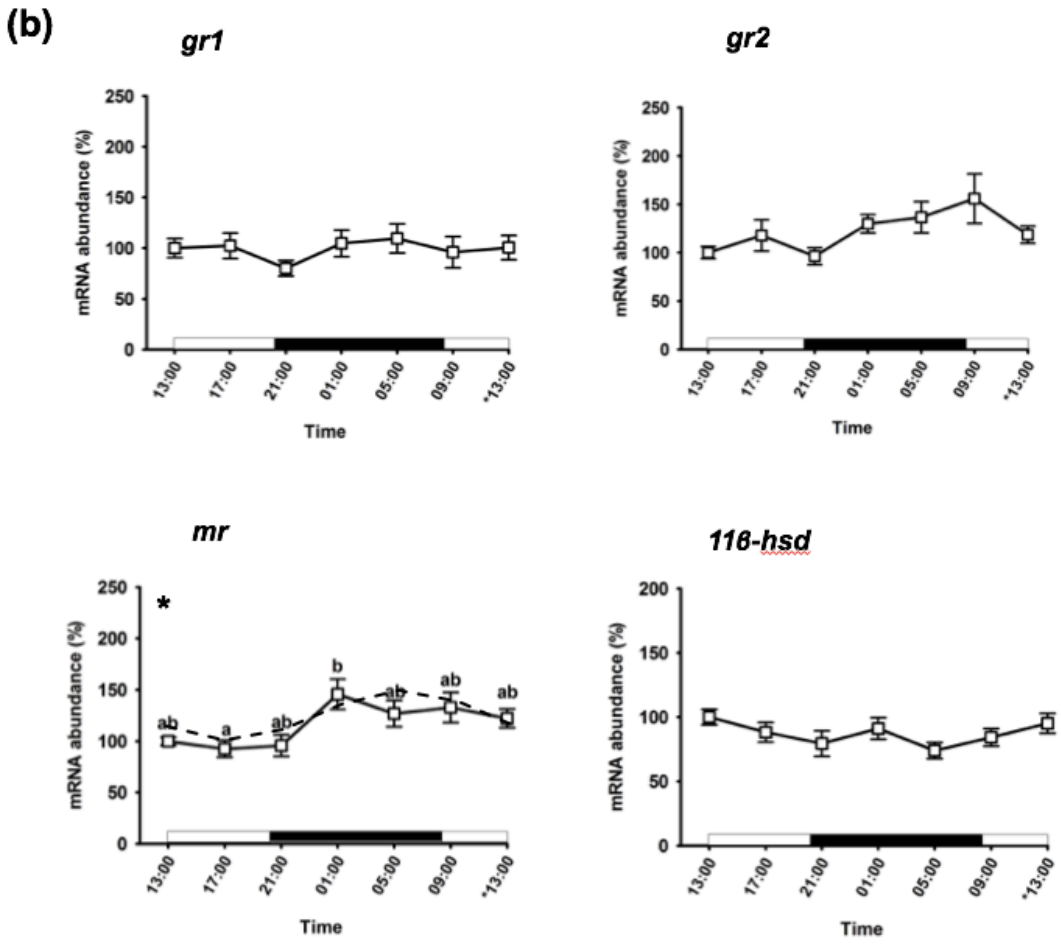

Figure 3.5. See previous page for caption

Table 3.4. Cosinor analysis parameters and SE(A)/A values for corticosteroid receptor and cortisol-clearing enzyme genes in *Oncorhynchus mykiss* skin. Bolded values have SE(A)/A<0.3.

Gene	Region	Mesor	Acrophase	Amplitude	SE(A)/A
gr1	**Dorsal**	**121.8**	**20**	**28.2**	**0.272**
	Ventral	-	-	-	-
gr2	**Dorsal**	**124.9**	**20**	**29.3**	**0.263**
	Ventral	-	-	-	-
mr	**Dorsal**	**131.6**	**12**	**39.4**	**0.244**
	Ventral	**116.6**	**12**	**26.6**	**0.293**
11β-hsd	Dorsal	-	-	-	-
	Ventral	-	-	-	-

3.4.5 Effect of 12-hour LD cycle on matrix metalloproteinase (*mmp*) mRNA levels in the skin of rainbow trout

Transcripts encoding *mmp-2* and *mmp-9* were present in all regions of trout skin examined in this study (**Figure 3.6**). The levels of *mmp-2* were not affected by photoperiod in the dorsal and ventral skin (**Figure 3.7a-b**). In the dorsal region, *mmp-9* abundance increased from 13:00 to 17:00, decreased over the next 8 hours, and began to increase and stabilize at the end of perceived night (**Figure 3.7a)**. In the ventral region, *mmp-9* cycled over the 24 hour period, with lowest levels at 09:00 (**Figure 3.7b**). Both the dorsal and ventral skin *mmp-9* oscillations exhibited significant SE(A)/A values with cosinor analysis (**Table 3.5**).

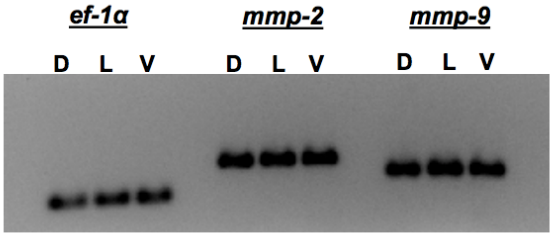

Figure 3.6. Expression of elongation factor 1α (*ef-1α*), matrix metalloproteinase 2 (*mmp-2*), and matrix metalloproteinase 9 (*mmp*-9) mRNA in the dorsal (D), lateral (L), and ventral (V) regions of rainbow trout (O*ncorhynchus mykiss*) skin. Transcripts were examined in the skin with PCR and visualised with 1.5% agarose gel electorophoresis. Negative control was run under the same conditions but contained only sterile water (not shown).

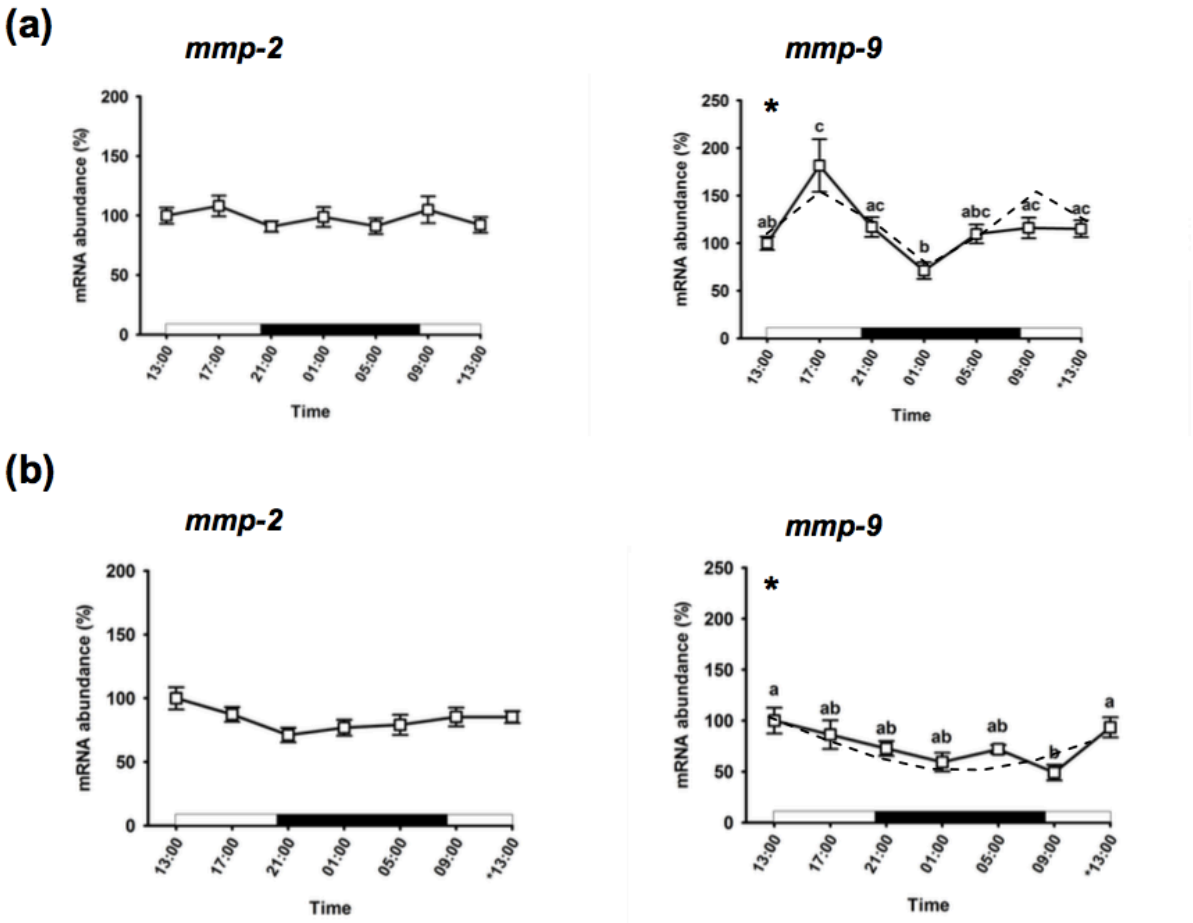

Figure 3.7. Effect of a 12-hour LD photoperiod on matrix metalloproteinase (*mmp*) mRNA abundance in the (a) dorsal and (b) ventral regions of rainbow trout (*Oncorhynchus mykiss*) skin. All data are mean values ± SEM (n=8). Lower case lettering indicate significant differences between time points as determined by a one-way ANOVA. Transcript abundance was expressed relative to the first sample point (13:00) taken from FW animals assigned a value of 100. *ef-1α* was used as a reference gene.

Table 3.5. Cosinor analysis parameters and P values for matrix metalloproteinase genes in *Oncorhynchus mykiss* skin. Bolded values have SE(A)/A<0.3.

Gene	Region	Mesor	Acrophase	Amplitude	SE(A)/A
mmp-2	Dorsal	-	-	-	-
	Ventral	-	-	-	-
mmp-9	**Dorsal**	**148.1**	**20**	**55.3**	**0.277**
	Ventral	**122.7**	**0**	**25.5**	**0.272**

3.5 Discussion

3.5.1 Overview

This study examined the change in mRNA abundance of TJ proteins in the dorsal and ventral skin of rainbow trout in response to a 12-hour LD cycle. This study is the first to report changes in mRNA abundance of TJ, clock, corticosteroid receptor, and matrix metalloprotease genes over a LD cycle in the skin of fishes. It was found that *per2* exhibited circadian-like rhythms in the dorsal and ventral-regions of the skin. Transcripts encoding TJ proteins such as *cldn-8d, -10c, -28b, -31* and *ocln* oscillated in either the dorsal or ventral regions of the skin. Additionally, *gr1* and *gr2* exhibited circadian-like changes in the dorsal skin region and *mr* changed in the dorsal and ventral regions. Finally, *mmp-9* but not *mmp-2* altered in a circadian-like manner in both regions. The hypothesis that TJ gene transcripts oscillate over a 24-hour period can be accepted.

3.5.2 Serum ions and muscle moisture content did not alter with a 12-hour LD period

Serum Cl^- and Na^+ concentration did not exhibit circadian rhythms, which is consistent with previous reports of Cl^- and Na^+ levels over a 24-hour period (Laidley and Leatherland, 1988; Pavlidis et al., 1999). Cl^- and Na^+ are the most abundant ions in the serum of rainbow trout, (Al-Jandal and Wilson, 2011), therefore it is possible that small changes in abundance would be difficult to detect. Other, less abundant, ions have been shown to oscillate in fishes over a 24-hour period (Kühn et al., 1986, Laidley and Leatherland, 1988), such as Mg^{++} and K^+ in rainbow trout. Therefore, the large relative concentration of serum Cl^- and Na^+ may act as a "buffer," which does not allow these ions to fluctuate. Muscle moisture content also remained constant, which may be linked to the predominant ions remaining steady over the 12-hour LD cycle. These data indicate that salt and water balance were maintained throughout the 24 hour period. Therefore, the

circadian-like changes in skin TJ protein transcript abundance (see **section 3.5.4**) may have been occurring to maintain salt and water balance in rainbow trout.

3.5.3 *per2* but not *cry3* oscillated in the skin of rainbow trout

Two clock genes that encode primary pacemakers in vertebrates, *per2* and *cry3,* were examined in the skin (**Figure 3.2**). Transcript abundance of *per2* was found to change over time in a circadian fashion as determined by cosinor analysis (**Figure 3.3, Table 3.2**). Interestingly, Per2 has been found to be directly light-responsive in zebrafish (Ziv et al., 2005). Additionally, transcript abundance of *per2* has been found to oscillate in the brain, skeletal muscle, and retina of various teleosts, and has been found to peak in these tissues just after the onset of the light phase (Velarde et al., 2009; Vera et al., 2013; Kim et al., 2015). A similar rhythm (i.e. *per2* peaking after the light phase) was observed in the present study, in both dorsal and ventral skin regions. Therefore, the function and regulation of *per2* may be conserved among different teleost species and tissues. Unlike *per2,* the abundance of *cry3* did not change in the skin of rainbow trout over a 24-hour period (**Figure 3.2**). However, in *Oncorhynchus kisutch*, *cry3* abundance in the pituitary gland exhibited robust oscillations over several days (Kim et al. 2015). Transcript abundance of *cry3* also changed over a 24-hour period in the retina and skeletal muscle of two other teleost species (Velarde et al., 2009; Lazado et al., 2014). This may indicate that, although rainbow trout skin expressed *cry3,* its transcription may not be regulated in the same manner as *cry3* in other species or tissues. In zebrafish, Cry3 was not found to suppress CLOCK-BMAL1 activity (Kobayashi et al., 2000; recall **Figure S3.1**), and in Atlantic cod it was found to exhibit discreet tissue expression (Lazado et al., 2014), therefore it could have a unique role in teleosts that does not involve

CLOCK-BMAL1 regulation. Therefore, it is evident that the mRNA abundance of clock genes in the skin of rainbow trout is differentially regulated.

3.5.4 TJ protein mRNA oscillated in the skin of rainbow trout in a region-specific manner over a 12-hour LD period

Many TJ protein gene transcripts (e.g. *cldn-8d, -10c, -28b, -31,* and *ocln*) exhibited oscillations over the 12-hour LD period, with the majority of the changes occurring in the dorsal skin region (**Figure 3.4**). Cldn-10c is believed to be a "leaky" TJ protein in rainbow trout (Kolosov et al., 2014), whereas Cldn-8d, -28b, -31 and Ocln are either known to be barrier forming (Chasiotis et al 2012; Kolosov et al 2017; Kolosov and Kelly, 2017) or have been linked to barrier formation (Kelly and Chasiotis, 2011; Sandbichler et al., 2011). During the dark phase, In the dorsal skin region *cldn-10c* abundance drops, *cldn-31* abundance is high and *cldn-8d* and -*28b* abundance is on the rise (**Figure 3.4a**). *Ocln* is the only barrier-forming transcript that decreases in abundance at night. In the ventral skin region, *cldn-10c* declines at night, and *cldn-28b* and *ocln* are upregulated (**Figure 3.4b**). Therefore, it appears that the paracellular permeability of the dorsal and ventral skin regions decreases during the mid-dark phase. In the dorsal region, the changes in *cldn-8d* and *ocln* abundance do not appear to be circadian-like (**Table 3.3)**, therefore, they may be regulated in a non-circadian manner to "fine tune" the paracellular permeability of the skin in this region. Overall, it would be interesting to examine the paracellular permeability of the skin at the mid-dark and mid-light phase to determine if a change in the aforementioned *cldn* abundance is correlated to paracellular permeability. Additionally, as discussed in **Chapter 2**, Cldn-10c localized to the dermis in rainbow trout, so its abundance may be linked to serum [Ca^{++}] (see **section 2.5.6.4**). Thus, serum [Ca^{++}] may oscillate with photoperiod as well.

Interestingly, none of the genes examined in this study exhibited a difference in mRNA abundance in the ventral region without a concurrent change in the dorsal region. These data indicate that *cldns* possess different regulatory networks that respond to the 12-hour LD cycle, where some respond only in the dorsal region, and others in both skin regions. Additionally, given that *cldn-10c* and *ocln* rhythms appear to be circadian-like in one skin region but not the other, the region-specific regulation of these *cldns* may differ. Therefore, a complex regulatory network seems to be at play. Interestingly, corticosteroid receptors exhibited different patterns of oscillation in the dorsal and ventral regions (see **section 3.5.5**), thus there is evidence that the dorsal and ventral regions are regulated differently.

Although it is evident from this study that TJ protein mRNA abundance can alter in a circadian-like fashion in the skin of rainbow trout, the reason behind these rhythms, and the difference between dorsal and ventral regions, is still unclear. One explanation behind the rhythmic cycling of TJ protein transcripts is UV radiation. Trout, which swim in photic zones, are exposed to UV light during the day on the dorsal side. Research on the effect of UV radiation on fishes has found that it can affect skin thickness and cell composition (Bullock and Roberts, 1992; Kazerouni and Khodabandeh, 2010) and that these effects are most prominent on the dorsal skin (Kaweewat and Hofer, 1997). One study on rainbow trout and other salmonids found that UV-B irradiation resulted in a fungal infection on the dorsal side of each species, resulting in the mortality of all species except rainbow trout (Little and Fabacher, 1994). Therefore, anticipation of the daily UV cycles could be the cause of the diurnal rhythm of TJ protein transcripts, and the difference between the dorsal and ventral skin response.

Alternatively, the change in TJ protein mRNA abundance could be linked to changes in internal factors (e.g. corticosteroids and matrix metalloproteinases) rather than external ones (See **sections 3.5.5** and **3.5.6**).

3.5.5 *gr1, gr2* and *mr* mRNA oscillated in a region-specific manner in the skin of rainbow trout over a 12-hour LD period

The difference in the regional TJ protein transcript response to photoperiod may be a consequence of daily changes in hormone levels. Alterations in circulating levels of cortisol have been reported in rainbow trout and other teleosts (Kühn *et al.,* 1976; Laidley and Leatherland, 1988). Seeing as many of the *cldn* transcripts in this study have been shown to respond to cortisol in the skin of rainbow trout (Gauberg et al., 2017), and Ocln has been found to be cortisol-responsive in the cultured trout gill (Chasiotis et al., 2010), the daily cortisol cycle may be influencing the region-specific transcription of *cldn-8d, -10c, -28b* and *ocln* in the present study via the corticosteroid receptors. Indeed, transcript abundance of *gr1*, and *gr2* oscillated only in the dorsal region, whereas *mr* exhibited circadian-like rhythms in both the dorsal and ventral skin (**Figure 3.5, Table 3.4**). In gill cell culture, it was found that *cldn-28b* increased in transcript abundance by corticosteroid stimulation via the MR only, and *ocln* was responsive to corticosteroids through both the MR and GR (Kelly and Chasiotis, 2011). On the other hand, *cldn-8d* and *-31* responded preferentially to corticosteroid action relayed through the GR compared to the MR (Kelly and Chasiotis, 2011). Therefore, the oscillations of *mr* in the dorsal and ventral skin regions may explain why *cldn-28b* and *ocln* oscillated in both regions. However, *cldn-8d* and *-31* abundance only changed in the dorsal region because *gr1* and *gr2* only oscillated in the dorsal region. Transcript encoding *cldn-10c* also showed circadian oscillations in both skin regions but it is

unknown which corticosteroid receptor is linked to *cldn-10c* transcription. However, it could be predicted that *cldn-10c* mRNA abundance relies on the activation of the MR, similar to *cldn-28b* and *ocln.* The transcript levels of the cortisol clearing enzyme, *11ß -hsd,* did not alter in response to the LD cycle. This suggests that there was no excess in serum cortisol that had to be cleared away over the 24-hour period. Therefore, the circadian fluctuation of corticosteroid receptors may be responsible for the changes in TJ mRNA abundance over the 12-hour LD cycle.

3.5.6 Only *mmp-9* transcripts exhibited circadian-like rhythms in the skin of rainbow trout over a 12-hour LD period

Another potential explanation behind the region-specific changes in TJ gene mRNA abundance with photoperiod is the oscillation of MMPs in the skin. In the present study, *mmp-2* and *mmp-9* were present in all regions of the skin (**Figure 3.6**) and *mmp-9* exhibited circadian-like changes in mRNA abundance with photoperiod (**Figure 3.7, Table 3.5**). Additionally, *mmp-9* oscillations differed between dorsal and ventral skin regions. The difference between *mmp-2* and *mmp-9* response to the 12 hour LD cycle is most likely due to a difference in their regulatory networks (Baker et al., 2002). Interestingly, in a previous study on rat eyes, MMP-9 protein levels were found to be more sensitive to light exposure than MMP-2 (Papp et al., 2007). Therefore, it is likely that in the present study the mRNA abundance of *mmp-9* differed from *mmp-2* because of this difference in light sensitivity. This could also explain the difference in *mmp-9* oscillations in the dorsal and ventral regions, given that the dorsal skin surface is exposed to more light throughout the 24-hour period.

Occludin is known to be a target of MMP-2 and -9 for degradation in vertebrates (Chen et al., 2009; Wiechmann et al., 2014; Nighot et al., 2015). In the present study, when comparing the

traces of *mmp-9* and *ocln*, it is evident that they either parallel (dorsal regions) or mirror (ventral region) each other (**Figure 3.4** and **Figure 3.7**). Therefore, MMP-9 may be altering Ocln protein levels, and the skin attempts to compensate for this by regulating *ocln* mRNA levels. Transcript abundance of *cldn-28b* and *-10c* may also be affected by MMP-9. While no studies have considered the effect of MMPs on Cldn-28b, one study on human hepatoma cell culture demonstrated that the abundance of another Cldn protein, CLDN-10, was linked to MMP abundance (Ip et al., 2007). Therefore, the changes observed in TJ transcript abundance with photoperiod can be due, in part, to the cyclical transcription of *mmp-9* genes in the skin.

3.6 Conclusions and future perspectives

The skin of rainbow trout can be regulated in a circadian-like fashion, as determined by the cycling of *per2.* Various TJ protein transcripts exhibited oscillations in a region-specific manner, with most exhibiting changes in the dorsal region. Additionally, the changes in TJ protein mRNA abundance may have been due to an external factor, such as anticipation of UV radiation, or due to internal regulators such as glucocorticoids or MMPs, which also exhibited circadian-like rhythms.

Future studies should focus on examining the persistence of these TJ rhythms in the absence of light. For a diel rhythm to truly be circadian, it must persist for several 24-hour cycles with no LD cues. Therefore, a future study can be performed where trout are entrained to a 12-hour LD cycle, and then are exposed to at least 24 hours of darkness, with no light stimulus, to see if the TJ protein mRNA rhythms persists. Additionally, to determine if UV is the anticipatory factor for circadian rhythms in the skin, trout can be exposed to UV light at a certain point in the light cycle and TJ protein mRNA abundance can be examined. If the transcript rhythms differ with

UV exposure compared to a control LD cycle without UV, especially in the dorsal skin, it would indicate that UV anticipation is an important factor in setting circadian rhythms in the skin. Finally, to determine whether cortisol is an important contributor to setting circadian rhythms in the skin, two or more groups of trout can be loaded with cortisol (e.g. by feeding) at different times of the day. If the groups exhibit different rhythms of TJ protein and corticosteroid receptor transcript abundance that correspond to the time of cortisol loading, then it can be confirmed that cortisol plays a role in "setting" the biological clock.

3.7 References

Al-Jandal, N.J., Wilson, R.W., 2011. A comparison of osmoregulatory responses in plasma and tissues of rainbow trout (*Oncorhynchus mykiss*) following acute salinity challenges. Comp. Biochem. Physiol. - A Mol. Integr. Physiol. 159, 175–181.

Anea, C.B., Irfan Ali, M., Osmond, J.M., Sullivan, J.C., Stepp, D.W., Merloiu, A.M., Rudic, R.D., 2010. Matrix metalloproteinase 2 and 9 dysfunction underlie vascular stiffness in circadian clock mutant mice. Arterioscler. Thromb. Vasc. Biol. 30, 2535–2543.

Baker, A.H., Edwards, D.R., Murphy, G., 2002. Metalloproteinase inhibitors: biological actions and therapeutic opportunities. J. Cell Sci. 115, 3719–3727.

Bauer, A.T., Bürgers, H.F., Rabie, T., Marti, H.H., 2010. Matrix metalloproteinase-9 mediates hypoxia-induced vascular leakage in the brain via tight junction rearrangement. J. Cereb. Blood Flow Metab. 30, 837–848.

Bui, P., Bagherie-Lachidan, M., Kelly, S.P., 2010. Cortisol differentially alters claudin isoforms in cultured puffer fish gill epithelia. Mol. Cell. Endocrinol. 317, 120–6.

Bullock, a M., Roberts, R.J., 1992. The influence of ultraviolet-B radiation on the mechanism of wound repair in the skin of the Atlantic salmon, *Salmo salar* L. J. Fish Dis. 15, 143–152.

Chan, S.W.C., Callard, I.P., 1972. Circadian rhythm in the secretion of corticosterone by the desert iguana, *Dipsosaurus dorsalis*. Gen. Comp. Endocrinol. 18, 565–568.

Chasiotis, H., Kelly, S.P., 2011. Effect of cortisol on permeability and tight junction protein transcript abundance in primary cultured gill epithelia from stenohaline goldfish and euryhaline trout. Gen. Comp. Endocrinol. 172, 494–504.

Chasiotis, H., Kolosov, D., Bui, P., Kelly, S.P., 2012. Tight junctions, tight junction proteins and paracellular permeability across the gill epithelium of fishes: A review. Respir. Physiol. Neurobiol. 184, 269–281.

Chasiotis, H., Wood, C.M., Kelly, S.P., 2010. Cortisol reduces paracellular permeability and increases Occludin abundance in cultured trout gill epithelia. Mol. Cell. Endocrinol. 323, 232–8.

Chen, F., Ohashi, N., Li, W., Eckman, C., Nguyen, J.H., 2009. Disruptions of Occludin and Claudin-5 in brain endothelial cells in vitro and in brains of mice with acute liver failure. Hepatology 50, 1914–1923.

Garg, S. K., and Sundararaj, B. I., 1986. Role of pineal in the regulation of some aspects of circadian rhythmicity in the catfish, *Heteropneustes fossilis* (Bloch). Chronobiologia 13, 1–11.

Gauberg, J., Kolosov, D., Kelly, S.P., 2017. Claudin tight junction proteins in rainbow trout (*Oncorhynchus mykiss*) skin: Spatial response to elevated cortisol levels. Gen. Comp. Endocrinol. 240, 214–226.

Gerhart-Hines, Z., Lazar, M.A., 2015. Circadian metabolism in the light of evolution. Endocr. Rev. 36, 289–304.

Hayashi, H., Sugimoto, M., Oshima, N., Fuji, R., 1993. Circadian motile activity of erythrophores in the red abdominal skin of tetra fishes and its possible significance in chromatic adaptation. Pigment Cell Res. 6, 29–36.

Hernández-Pérez, J., Míguez, J.M., Librán-Pérez, M., Otero-Rodiño, C., Naderi, F., Soengas, J.L., López-Patiño, M.A., 2015. Daily rhythms in activity and mRNA abundance of enzymes involved in glucose and lipid metabolism in liver of rainbow trout, *Oncorhynchus mykiss*. Influence of light and food availability. Chronobiol. Int. 32, 1391–1408.

Hoon, G., Chung, S., Kyoung, H., Kim, H., Baik, S., Lee, H., Lee, H., Choi, S., Sun, W., Kim, H., Cho, S., Ho, K., Kim, K., 2008. Adrenal peripheral clock controls the autonomous circadian rhythm of glucocorticoid by causing rhythmic steroid production. PNAS 105.

Idda, M.., Bertolucci, C., Vallone, D., Gothilf, Y., Sanchez-Vazquez, F.J., Foulkes, N., 2012a. Circadian clocks: Lessons from fish. Prog. Brain Res. 199, 41–57.

Idda, M.L., Kage, E., Lopez-olmeda, J.F., Mracek, P., Foulkes, N.S., Vallone, D., 2012b. Circadian timing of injury-induced cell proliferation in zebrafish. PLoS One 7, 1–13.

Ip, Y.C., Cheung, S.T., Lee, Y.T., Ho, J.C., Fan, S.T., 2007. Inhibition of hepatocellular carcinoma invasion by suppression of claudin-10 in HLE cells. Mol. Cancer Ther. 6, 2858–2867.

Kavaliers, M., 1980. Circadian locomotor activity rhythms of the burbot, *Lota lota*: Seasonal differences in period length and the effect of pinealectomy. J. Comp. Physiol. 136, 215–218.

Kaweewat, K., Hofer, R., 1997. Effect of UV-B radiation on goblet cells in the skin of different fish species. J. Photochem. Photobiol. B Biol. 41, 222–226. doi:10.1016/S1011-1344(97)00104-8

Kazerouni, E.G., Khodabandeh, S., 2010. Effects of ultraviolet radiation on skin structure and ultrastructure in Caspian Sea Salmon, *Salmo trutta caspius*, during alevin stage. Toxicol. Environ. Chem. 92, 903–914.

Kelly, S.P., Chasiotis, H., 2011. Glucocorticoid and mineralocorticoid receptors regulate paracellular permeability in a primary cultured gill epithelium. J. Exp. Biol. 214, 2308–18.

Kelly, S.P., Wood, C.M., 2001. Effect of cortisol on the physiology of cultured pavement cell epithelia from freshwater trout gills. Am. J. Physiol. Regul. Integr. Comp. Physiol. 281, 811–820.

Kim, J.-H., White, S.L., Devlin, R.H., 2015. Interaction of growth hormone overexpression and nutritional status on pituitary gland clock gene expression in coho salmon, *Oncorhynchus kisutch*. Chronobiol. Int. 32, 113–127.

Kobayashi, Y., Ishikawa, T., Hirayama, J., Daiyasu, H., Kanai, S., Toh, H., Fukuda, I., Tsujimura, T., Terada, N., Kamei, Y., Yuba, S., Iwai, S., Todo, T., 2000. Molecular analysis of zebrafish photolyase/cryptochrome family: two types of cryptochromes present in zebrafish. Genes to Cells 5, 725–738.

Kühn, E.R., Corneillie, S., Ollevier, F., 1986. Circadian variations in plasma osmolality, electrolytes, and cortisol in carp (*Cyprinus carpio*). Gen. Comp. Endocrinol. 61, 459–468.

Kolosov, D., Chasiotis, H., Kelly, S.P., 2014. Tight junction protein gene expression patterns and changes in transcript abundance during development of model fish gill epithelia. J. Exp. Biol. 217, 1667–81.

Kolosov, D., Donini, A., Kelly, S.P., 2017. Claudin-31 contributes to corticosteroid-induced alterations in the barrier properties of the gill epithelium. Mol. Cell. Endocrinol. 439, 457–466.

Kolosov, D., Kelly, S.P., 2017. Claudin-8d is a cortisol-responsive barrier protein in the gill epithelium of trout J. Mol. Endocrinol. 59, 1-12.

Kyoko, O.O., Kono, H., Ishimaru, K., Miyake, K., Kubota, T., Ogawa, H., Okumura, K., Shibata, S., Nakao, A., 2014. Expressions of tight junction proteins Occludin and Claudin-1

are under the circadian control in the mouse large intestine: implications in intestinal permeability and susceptibility to colitis. PLoS One 9, 2–10.

Laidley, C.W., Leatherland, J.F., 1988. Circadian studies of plasma cortisol, thyroid hormone, protein, glucose and ion concentration, liver glycogen concentration and liver and spleen weight in rainbow trout, *Salmo gairdneri* Richardson. Comp. Biochem. Physiol. A. Comp. Physiol. 89, 495–502.

Lazado, C.C., Kumaratunga, H.P.S., Nagasawa, K., Babiak, I., Giannetto, A., Fernandes, J.M.O., 2014. Daily rhythmicity of clock gene transcripts in Atlantic cod fast skeletal muscle. PLoS One 9, 1–12.

Lazado, C.C., Lund, I., Bovbjerg, P., Quang, H., 2015. Humoral and mucosal defense molecules rhythmically oscillate during a light-dark cycle in permit, *Trachinotus falcatus*. Fish Shellfish Immunol. 47, 902–912.

Little, E.E., Fabacher D.L., 1994. Comparative sensitivity of rainbow trout and two threatened salmonids, Apache trout and Lahontan cutthroat trout, to ultraviolet-B radiation. Arch. Hydrobiology. 43, 217-226.

Markoulli, M., Papas, E., Cole, N., Holden, B.A., 2012. The diurnal variation of matrix Metalloproteinase-9 and its associated factors in human tears. Invest. Ophthalmol. Vis. Sci. 53, 1479–84.

Marshall, W.S., Grosell, M., 2005. Ion osmoregulation, and acid – base balance. Physiol. Fishes 177–230.

McCormick, S.D., 2011. Hormonal control of metabolism and ionic regulation, in Encyclopedia of Fish Physiology: From Genome to Environment. Elsevier Inc. pp. 1466-1473.

Mizobe, Y., Oikawa, D., Tsuyama, S., Akimoto, Y., Hamasu, K., Onitsuka, E., Sato, M., Takahata, Y., Morimatsu, F., Furuse, M., 2008. mRNA Expression of Lysyl Oxidase and Matrix metalloproteinase-12 in mouse skin. Biosci. Biotechnol. Biochem. 72, 3067–3070.

Mohawk, J.A., Green, C.B., Takahashi, J.S., 2012. Central and peripheral circadian clocks in mammals. Annu. Rev. Neurosci. 35, 445–462.

Nevid, N.J., Meier, A.H., 1993. A day-night rhythm of immune activity during scale allograft rejection in the gulf killifish, *Fundulus grandis*. Dev. Comp. Immunol. 17, 221–228.

Nighot, P.K., Al-Sadi, R., Rawat, M., Guo, S., Watterson, D.M., Ma, T.Y., 2015. Matrix Metalloproteinase 9-induced increase in intestinal epithelial tight junction permeability contributes to the severity of experimental DSS colitis. Am. J. Physiol. Gastrointest. Liver Physiol. 309, G988–G997.

Page-McCaw, A., Ewald, A.J., Werb, Z., 2007. Matrix metalloproteinases and the regulation of tissue remodelling. Nat. Rev. Mol. Cell Biol. 8, 221–33.

Papp, A.M., Nyilas, R., Szepesi, Z., Lorincz, M.L., Takács, E., Ábrahám, I., Szilágyi, N., Tóth, J., Medveczky, P., Szilágyi, L., Juhász, G., Juhász, G., 2007. Visible light induces matrix metalloproteinase-9 expression in rat eye. J. Neurochem. 103, 2224–2233.

Pavlidis, M., Greenwood, L., Paalavuo, M., Mölsä, H., 1999. The effect of photoperiod on diel rhythms in serum melatonin, cortisol, glucose, and electrolytes in the common dentex, *Dentex dentex*. Gen. Comp. Endocrinol. 113, 240–250.

Pedersen, M.E., Vuong, T.T., Ronning, S.B., Kolset, S.O., 2015. Matrix metalloproteinases in fish biology and matrix turnover. Matrix Biol. 44–46, 86–93.

Plikus, M. V, Van Spyk, E.N., Pham, K., Geyfman, M., Kumar, V., Takahashi, J.S., Andersen, B., 2015. The circadian clock in skin: Implications for adult stem cells, tissue regeneration, cancer, aging, and immunity. J. Biol. Rhythms 30, 163–182.

Sánchez-Vázquez, F.J., Iigo, M., Antonio, J., Tabata, M., 2000. Pinealectomy does not affect the entrainment to light nor the generation of the circadian demand-feeding rhythms of rainbow trout. Physiol. Behav. 69, 455–461.

Sandbichler, A.M., Egg, M., Schwerte, T., Pelster, B., 2011. Claudin 28b and F-actin are involved in rainbow trout gill pavement cell tight junction remodeling under osmotic stress. J. Exp. Biol. 214, 1473–1487.

Velarde, E., Haque, R., Iuvone, P.M., Azpeleta, C., Alonso-Gómez, a L., Delgado, M.J., 2009. Circadian clock genes of goldfish, *Carassius auratus*: cDNA cloning and rhythmic expression of period and cryptochrome transcripts in retina, liver, and gut. J. Biol. Rhythms 24, 104–13.

Vera, L.M., Negrini, P., Zagatti, C., Frigato, E., Sánchez-Vázquez, F.J., Bertolucci, C., 2013. Light and feeding entrainment of the molecular circadian clock in a marine teleost (*Sparus aurata*). Chronobiol. Int. 30, 649–61.

Wang, H., 2008a. Comparative analysis of teleost fish genomes reveals preservation of different ancient clock duplicates in different fishes. Mar. Genomics 1, 69–78.

Wang, H., 2008b. Comparative genomic analysis of teleost fish bmal genes. Genetica 136.

Wang, H., 2008c. Comparative analysis of period genes in teleost fish genomes. J. Mol. Evol. 67, 29–40.

Wiechmann, A.F., Ceresa, B.P., Howard, E.W., 2014. Diurnal variation of tight junction integrity associates inversely with matrix metalloproteinase expression in *Xenopus laevis* corneal epithelium: Implications for circadian regulation of homeostatic surface cell desquamation. PLoS One 9, 1–12.

Whitmore, D., Foulkes, N.., Sassone-Corsi, P., 2000. Light acts directly on organs and cells in culture to set the vertebrate circadian clock. Nature 404, 87–91.

Yamato, M., Ito, T., Iwatani, H., Yamato, M., Imai, E., Rakugi, H., 2010. E-cadherin and Claudin-4 expression has circadian rhythm in adult rat kidney. J. Nephrol. 23, 102–110.

Ziv, L., Levkovitz, S., Toyama, R., Falcon, J., Gothilf, Y., 2005. Functional development of the zebrafish pineal gland: Light-induced expression of Period2 is required for onset of the circadian clock. J. Neuroendocrinol. 17, 314–320.

4. Chapter Four: Effects of *Batrachochytrium dendrobatidis* infection on TJ proteins in the skin of Australian green tree frog, *Litoria caerulea*

4.1 Summary

An emerging infectious disease, Chytridiomycosis, caused by the fungus *Batrachochytrium dendrobatidis* (*Bd*), is threatening amphibian populations worldwide. *Bd* is known to infect the skin and disrupt cutaneous osmoregulation. However, the mechanism behind how this occurs is poorly understood. Recently it has been demonstrated that *Bd* is able to disrupt the junctional components between amphibian skin cells. However, the tight junction (TJ) complex, a key junctional component that regulates the barrier properties of the skin, has not been investigated. Several studies have reported that the TJ complex is essential for proper skin function in amphibians (as it is in other vertebrates), and in amphibians skin TJs play a critical role in mitigating passive ion loss. In other studies, using mammalian models, fungi and fungal toxins have been shown to disrupt TJs in the skin. But a link between fungal infection and the contribution of TJs to the loss of skin integrity in amphibians has yet to be examined. Therefore, this study examined TJ protein genes present in the skin of the green tree frog, *Litoria caerulea,* and examined the effect of *Bd* infection on skin paracellular permeability and TJ protein abundance. Data indicate that *Bd* infection increased the paracellular permeability of the skin linearly with fungal infection load. *Bd* infection increased the mRNA abundance of all TJ proteins examined in this study, however, its effects on protein abundance were not uniform, and instead were consistent with a loss of skin barrier function. Therefore, data support the idea that *Bd* infection is able to alter the paracellular permeability of amphibian skin in part by disrupting TJ proteins and the integrity of the skin TJ complex.

4.2 Introduction

4.2.1 Amphibian skin

Semi-aquatic adult amphibians are frequently exposed to both air and FW. Under FW conditions, amphibians lose ions to the surrounding water and their skin is the main organ responsible for limiting this ion loss (Boutilier et al., 1992). Amphibian skin is largely non-keratinizing and composed mainly of live cells, with only a very thin superficial keratinized cell layer present at the surface which moults at regular intervals (Chuong et al., 2002). This outer layer of amphibian skin, known as the *stratum corneum*, is a negligible barrier compared to the underlying *stratum granulosum*, which accounts for the majority of the selective barrier properties in this organ (Martinez-Palomo et al., 1971; see **Illustration 1.1** in **Chapter 1**). In this regard, amphibian skin can be considered to be a "selectively permeable living barrier" that plays a role in gas exchange as well as salt and water balance (Boutilier et al, 1992). With regard to the latter, the ventral skin surface is most often in contact with an aqueous environment and is an important site for osmoregulation in amphibians (Parsons and Mobin, 1991; Campbell et al., 2012). Overall, the permeability properties of amphibian skin are dictated by (1) the transcellular pathway which actively transports ions across epithelial cells and (2) the paracellular pathway, and more specifically, cell-to-cell TJs which occlude the paracellular space and regulate the loss of solutes into FW (Martinez-Palomo et al., 1971; Ehrenfeld and Klein, 1997).

4.2.2 TJ proteins in the skin of amphibians

It has long been acknowledged that TJs play a substantial role in the barrier function of amphibian skin and can regulate passive ion movement across this tissue (Jorgensen, 1949; Mandel and Curran, 1972; Bruus et al., 1976). Additionally, TJs and at least one TJ protein (i.e. Ocln) have

been shown to be dynamically regulated by changes in environmental conditions in frogs (Castillo et al., 1991; Tokuda et al., 2010; Chasiotis and Kelly, 2009).

Impressively, over 30 TJ protein genes have been reported in amphibians (Cordenonsi et al., 1997; Cardellini et al., 1996; Fesenko et al., 2000; Klein et al., 2002; Chasiotis and Kelly, 2009; Chang et al., 2010; Saharinen et al., 2010; Yamagishi et al., 2010; Baltzegar et al., 2013; Sun et al., 2015). The majority of these TJ protein genes have only been examined in the aquatic anurans *Xenopus laevis* and *Xenopus tropicalis,* thus almost nothing is known about the TJ proteins in terrestrial and semi-aquatic amphibians (Günzel and Yu, 2013). Not surprisingly, even less is known about the function of individual TJ proteins, specifically their role in maintaining ion homeostasis and proper skin function. Given all of the knowledge obtained from studies of TJ proteins in other vertebrates (e.g., mammals, teleost fishes - for reviews see Chasiotis et al., 2012; Günzel and Yu, 2013), it is surprising that no investigations have been initiated into the study of TJ proteins in amphibians, specifically within the major barrier tissue of these animals: the skin.

4.2.3 Infection of amphibian skin by *Batrachochytrium dendrobatidis*

Amphibians are recognised as the most threatened class of vertebrates on the planet, with nearly one third of all species being globally threatened (Stuart et al., 2004). A substantial contributor to this decline is Chytridiomycosis, a cutaneous infection caused by the fungus *Batrachochytrium dendrobatidis* (*Bd;* Stuart et al., 2004). This fungus has shown to infect over 500 amphibian species world-wide and has resulted in one of the greatest losses of biodiversity ever recorded (Fisher et al., 2009; Kilpatrick et al., 2010). Although only the superficial layers of the skin are affected by *Bd*, that alone is able to disrupt the normal functioning of the skin and can lead to death of the infected animal (Voyles et al., 2009). The mechanism used by this fungus to infect amphibian skin

is still poorly understood (Rosenblum et al., 2008; Fisher et al., 2009). What is known is that the fungus begins its life cycle as a free-living zoospore which encysts onto the surface of the skin (Van Rooij et al., 2015; **Illustration 4.1**). This fungus resides in the water and thus infects the ventral skin surface much more than the dorsal skin surface (Berger et al., 2005). The zoospore develops a germ tube that forces it into the deeper layers of the skin, allowing infection of epidermal cells in the *stratum granulosum* (Van Rooij et al., 2015). As the epidermal cells are pushed upwards and begin to keratinize, *Bd* matures into zoosporangia that contain many zoospores (Van Rooij et al., 2015). When the epidermal cells reach the outermost layer, *Bd* develops a "discharge tube" from which its zoospores are released to re-infect the same animal, or infect a new one (Van Rooij et al., 2015).

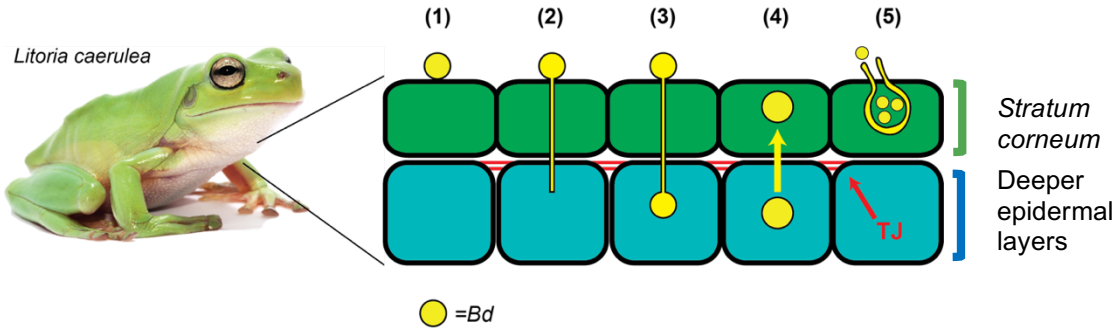

Illustration 4.1 Schematic of the *Bd* life cycle on amphibian skin. The stages of *Bd* infection are as follows: (1) the fungus encysts on to the outer layer of the skin (the *stratum corneum*), (2) the zoospore sends a germ tube into the deeper layers of the skin, (3) *Bd* injects itself into a living epidermal cell, (4) the zoospore develops into a zoosporangia as the skin cells are pushed upwards and mature, and (5) zoosporangia develop a discharge tube from which new zoospores are released.

Following infection, *Bd* has been reported to affect active transport in the ventral skin and disrupt cutaneous osmoregulation, causing an imbalance in serum ion levels (Voyles et al., 2007; Voyles et al., 2009). Although the effects of *Bd* have been examined on active ion transport, the effects of *Bd* on TJs, which regulate passive ion movement, have not been investigated. However,

a dysregulation of TJ function could also affect ion movement across epithelia (Kolosov and Kelly, 2017; Kolosov et al., 2017), thus TJs should not be discounted. Importantly, it has been demonstrated that *Bd* disrupts junctional components between cells of amphibian skin, resulting in skin lesions (Brutyn et al., 2012). These junctional components (i.e. desmosomes) are responsible for cell-cell adhesion, but, unlike TJs, desmosomes do not regulate the permeability properties of the skin. Several fungi and fungal toxins have been shown to directly target and disrupt various junctional components, including TJs, in the skin of other vertebrates (Bouhet and Oswald, 2005; Zhang et al., 2015). Indeed, *Bd* was found to express protease genes, which may be linked to its pathogenicity (Rosenblum et al., 2008), and the application of zoospore supernatant alone was able to disrupt the skin of *Xenopus laevis* (Brutyn et al., 2012). Therefore, although *Bd* supernatant has been shown to disrupt skin junctional components, the effects of *Bd* on the TJ complex, which controls the barrier properties of the skin, have yet to be investigated.

Given that *Bd* has been found to affect cutaneous osmoregulation and to disrupt junctional components in the skin, it is hypothesized that *Bd* will alter the abundance of TJ proteins in the skin of amphibians. To consider this idea further, the green tree frog, *Litoria caerulea,* was chosen as a model amphibian species for the disease Chytridiomycosis as it is highly susceptible to *Bd* infection and has often been used to study this disease in the past (Pessier et al., 1999; Berger et al., 2005; Voyles et al., 2009; Ohmer et al., 2014). The overall aim of this study is to examine the expression of TJ genes and associated proteins in the skin of *L. caerulea*. Specifically, the effect of *Bd* on the TJs in the ventral skin of *L. caerulea* are examined to establish whether a loss of skin barrier properties is associated with a disruption to the TJ complex.

4.3 Materials and Methods

4.3.1 Experimental animals

This study was conducted using the Australian green tree frogs (*Litoria caerulea*). 20 Adult *L. caerulea* (15-70 g) were collected from wet roads in non-protected areas near Fernvale, southeast Queensland in January 2015 by members of the Franklin lab. Sterile gloves were worn when frogs were handled and gloves were changed between animals to prevent the spread of pathogens. Isolated individual frogs were placed into separate moistened plastic bags and transported to The University of Queensland. Frogs were housed separately in ventilated clear plastic containers (26.2x23.7x12 cm). Containers were supplied with paper towels saturated with water that was chemically aged (dilution 1:4000; VitaPet, NSW, Australia) to remove chlorine gas and contained a half PVC pipe for shelter. Frogs were fed five large crickets/week and the enclosures were cleaned, on a weekly basis. Lighting was maintained at a 12 h L:12 h D photoperiod and room temperature was kept constant at 20.5 ± 0.5°C.

Given that natural *L. caerulea* populations can acquire *Bd* infections, frogs were tested for *Bd* using quantitative real-time PCR (qPCR) prior to beginning the experiments (see **section 4.3.4**). Only confirmed uninfected frogs were used for experiments. All experiments were carried out with the prior approval of The University of Queensland Animal Welfare Committee (SBS/316/14/URG).

4.3.2 Preparation of fungal inoculum and experimental exposure

Batrachochytrium dendrobatidis strain EPS4, isolated by E.P. Symonds (School of Veterinary Sciences, The University of Queensland) from a *Mixophyes fleayi* tadpole collected from Gap Creek, Main Range National Park, Queensland, Australia (March 2012), was used for

experimental infection. *Bd* cultures were maintained at 4°C until four days before exposure date. The strain was then passaged onto 25 new 1% agar, 0.5% tryptone, 0.5% tryptone-soy plates, and maintained at 20°C for 4-5 days. Immediately prior to infection, zoospores maintained at 20°C were harvested by flooding plates with sterile distilled water for 30 min. The zoospore suspension was collected, and zoospore concentration was calculated using a haemocytometer following Boyle et al. (2004). Frogs were randomly assigned to be either part of the infected (n = 10) or control (n = 10) groups. Frogs assigned to the infected group were transferred into 300 mL plastic containers (12.5x 8.3x 5 cm) containing 100 mL of aged tap water. Frogs were then inoculated with a dose of ~500 000 *Bd* zoospores for 5 h. Control frogs were exposed to identical conditions in the absence of zoospores. After exposure, frogs were returned to their enclosures.

4.3.3 Monitoring sloughing

Because *L. caerulea* moults its skin on a regular basis, a closed-circuit infrared continuous video monitoring system (Generic 16 channel H.264 digital video recorder, model MDR688ZB (AU)-E, 600TVL Weatherproof infrared cameras, model CI20B-65H) was used to record when frogs sloughed their skin. Slough monitoring began two weeks before fungal exposure to determine a baseline rate for each individual. It was determined that sloughing events were predictable after watching many hours of video footage. Frogs often sloughed at the same time of day, on a consistent cycle. The time in hours between sloughing events was termed the intermoult interval (IMI). Frogs were considered to be in the "intermoult" stage of the cycle from 24 hours after a sloughing event until 24 hours prior to the next sloughing event.

4.3.4 Measuring infection load

Infection load was tested (collected animals) or monitored (inoculated and control animals, two weeks after exposure and every two weeks after that) by swabbing frogs during the IMI. The swabbing protocol involved firmly running a sterile fine-tipped cotton swab (MW100-100; Medical Wire & Equipment, Wiltshire, England) three times over the frog's ventral surface, sides, thighs, feet, webbing and toes. To isolate fungal DNA, liquid from swabs was pipetted into sterile Eppendorf tubes containing 30 to 40 mg of Zirconium/silica beads (Daintree Scientific, Australia) measuring 0.5 mm diameter. 50µl of PrepMan Ultra (Applied Biosystems, Foster City, CA, USA) was then added to each tube. Swabs were homogenized for 45 seconds in a TissueLyser II (Qiagen Pty Ltd, Australia), followed by 1-minute centrifugation at 13,000g. The homogenized sample was placed in a heat block for 10 minutes at 100°C, cooled to RT and spun at 12,000g for 2 minutes. Finally, the supernatant was transferred into a sterile Eppendorf tube. Real-time Taqman PCR assays were conducted on a Mini Opticon real-time PCR detection system (MJ Mini Cycler, Bio-Rad Laboratories, Inc.). Primers were designed against *Bd* rRNA (F: CCTTGATATAATACAGTGTGCCATATGTC, R: AGCCAAGAGATCCGTTGTCAAA), and a minor groove binder (MGB) probe (6FAM-CGAGTCGAACAAAAT-MGBNFQ) was also designed. 25 µl reactions containing 12.5 µl of 2x Taqman Master Mix (Applied Biosystems), 900 nM PCR primers, 250 nM MGB probe, and 5 µl of DNA (diluted 10:1 in water) were prepared in triplicate. Reactions containing DNA from known 100, 10, 1 and 0.1 *Bd* zoospore equivalents (ZE) were prepared, as well as controls with no DNA template. The amplification conditions were as follows: 2 min at 50°C, 10 min at 95°C, followed by 15 s at 95°C and 1 min at 60°C for 50 cycles. A standard curve was constructed from the reactions containing 100, 10, 1 and 0.1 *Bd* zoospores

and the concentration of the test (swabbed) samples were expressed as the number of ZEs. The ZE was calculated by the mean value of the triplicate assay, and log + 1 transformed [Log(ZE+1)].

Frogs were monitored daily for clinical signs of chytridiomycosis, including lethargy, loss of appetite, abnormal posture, pieces of sloughed skin not fully removed or visible within the enclosure, loss of righting reflex, discoloured or reddened skin, and weight loss. Only frogs that exhibited these signs of clinical infection were swabbed and consequently sacrificed for molecular and immunohistochemical analyses (see **section 4.3.8**).

4.3.5 Tissue sampling

Ventral skin samples (<1 cm^2) from the lower abdominal region were collected from IMI animals. Skin samples for RNA extraction (see **section 4.3.10**) were stored in RNA-later (Ambion Inc., TX, USA) first at 4°C overnight and then at −20°C until use. Skin samples for Western blotting (see **section 4.3.9**) were frozen at −80°C until use. Skin samples for immunohistochemistry were fixed in 10% neutral buffered formalin at 4°C overnight, following which formalin was replaced with 70% ethanol and samples were stored until use.

4.3.6 Permeability assays

Skin was dissected from ventral side of control and infected *L. caerulea*. Each skin sample was immediately mounted onto Franz cells: 1 mL FW was added to the apical chamber while the basolateral chamber contained 5 mL of Ringer's solution with the composition (in mM) NaCl: 112, KCl: 2.5, D-glucose: 10, Na_2HPO_4: 2, $CaCl_2$: 1, $MgCl_2$: 1, HEPES sodium salt: 5, HEPES: 5 with pH 7.3-7.4 and osmolality of 230 ± 20 mOsm L^{-1}. For permeability experiments, 0.5 mg of 4 kDa FITC-dextran was added to the basolateral chamber. Once set up, 250 µl of apical and 500

µL basolateral solutions were sampled and placed into a dark container. The Franz cells were covered and kept in darkness. As a positive control, 5 µM of the calcium chelator ethylenediamine-N,N,N′,N′-tetraacetic acid (EDTA) was added to the apical FW solution and Franz cells were fluxed for 24 hours as normal. A standard curve was prepared immediately after mounting the skin onto the Franz cells and placed into a dark container. 750 µL samples were collected from the apical and basolateral chambers after 24 hours and 50 µL were run on a microplate alongside the standard curve under a fluorescent plate reader (DTX880 Multimode Detector, Beckman Coulter Pty Ltd, Australia). The permeability of the skin samples was calculated using a modified equation from Kelly and Wood, 2001,

$$P\ (cm/s) = \frac{(\Delta FL_{Ap})(Volume_{Ap})}{(FL_{Bl})(Time)(3600)(Area)}$$

where ΔFL_{Ap} is the change in fluorescence on the apical side, $Volume_{Ap}$ is the volume of the apical chamber (1 mL), FL_{Bl} is the fluorescence on the basolateral side, 3,600 converts hours to seconds, and Area defines the area of the Franz cell chamber opening (0.2 cm^2).

4.3.7 Antibodies

The affinity purified polyclonal antibodies used for western blot and immunohistochemsitry analysis were either custom-synthesized (New England Peptide, MA, USA) to specifically target *O. mykiss* Cldn-10c (CWEGSMSIKLKE) or commercial antibodies targeting human Cldn-1 (C-terminal), Ocln (C-terminal), Tric (C-terminal) and ZO-1 (N-terminal) (Zymed Technologies Canada, EMD Millipore Canada) The estimated sizes of -10c, Cldn-1, Ocln, and Tric are: 21 kDa, 22 kDa, 60 kDa, 52 kDa respectively.

4.3.8 Immunohistochemical analysis

Fixed skin samples were dehydrated and embedded in paraffin wax using the Leica automated vacuum tissue processor (Leica microsystems, Nussloch, Germany) and embedded in paraffin in embedding rings the following day. Sections (6 μm) of control and infected ventral skin were cut on a rotary microtome (RM2245, Leica Microsystems, Nussloch, Germany) and mounted on glass slides. Sagittal sections of the skin were obtained to use with the Tric antibody to visualize Tric punctate staining that would not be visible in transverse sections. Transverse sections were made for the use with all other antibodies. For staining with antibodies, sections on slides were first dewaxed in xylene, followed by rehydration using a graded ethanol series (100% – 30%), and finally distilled water. Sections were then heated in sodium citrate buffer (10 mM, pH 6.0) for 4 minutes in a microwave. The buffer was allowed to cool for 20 minutes, reheated for 2 minutes and then cooled for a further 15 minutes. Subsequently, slides were bathed for 10 minutes in different PBS solutions: 1% Tween-20 (PBS-T), then 0.05% Triton X-100 in PBS (PBS-TX), and finally 10% antibody dilution buffer (ADB; 2% goat serum, 1% BSA, 0.1% cold fish skin gelatin, 0.1% Triton X-100, 0.05% Tween-20, 0.01 PBS) in PBS (PBS-ADB). Sections were incubated with rabbit polyclonal anti-TJ protein antibodies (1:100 dilution for Cldn-1, Ocln, Tric, and ZO-1, and 1:300 dilution for Cldn-10c in ADB). As negative controls, two sets of slides were also incubated overnight with ADB alone. After overnight incubation, slides were rinsed for 10 minutes in PBS-PF, PBS-TX, and PBS-ADB solutions and incubated with Texas red (TR)-labelled goat anti-rabbit antibody (1:500 in ADB; SC2780, Santa-Cruz Biotechnology) for 1 hour at RT. Slides were then successively washed with PBS, PBS-TX and PBS-PF (10 min each) and rinsed 3 times with distilled water (1min each). Slides were mounted with coverslips using Flouroshield™ DAPI

Mounting Medium (Sigma Aldrich, Australia) and left to dry for 1 hour. Fluorescence images were captured using a Leica DMi8 Inverted Confocal microscope and merged using ImageJ software.

4.3.9 Western blot analysis

L. caerulea skin was thawed and homogenized using the TissueLyser II (Qiagen Pty Ltd, Australia) in chilled radioimmunoprecipitation assay lysis buffer (RIPA; 0.6% Tris-HCl, 0.8% NaCl, 1% deoxycholic acid, 1% Triton X-100, 1% SDS, 1mM EDTA, 1mM PMSF, 1mM DTT) containing 1:200 protease inhibitor cocktail (Sigma-Aldrich Canada Ltd). Tissues were sonicated at a 1:3 w:v tissue to buffer ratio. Homogenates were centrifuged at 13,000 rpm for 20 min at 4°C and supernatants were collected after centrifugation. Protein content was quantified using the Bradford reagent (Sigma-Aldrich Canada Ltd) according to the manufacturer's guidelines with bovine serum albumin (Pierce™ Bovine Serum Albumin Standard Ampules, Thermo Fisher Scientific, Australia) as a standard. Samples were prepared for SDS-PAGE by heating at 70°C in NuPAGE™ LDS sample buffer (Thermo Fisher Scientific, Australia) with NuPAGE™ Reducing agent (Thermo Fisher, Australia) for 10 minutes. 5-25 µg of skin protein were electrophoretically separated in NuPAGE™ 10% Bis-Tris Protein gels at 200V. After electrophoresis, protein was transferred to a polyvinylidene difluoride (PVDF) membrane (Immobilon-P PVDF Membrane, Merck, Australia) over a 1 hour period. Following transfer, the membrane was washed in Tris-buffered saline with Tween-20 [TBS-T; TBS (10mM Tris, 150mM NaCl, pH 7.4) with 0.05% Tween-20], and blocked for 1 hour in 5% non-fat dried skimmed milk powder in TBS-T (5% milk TBS-T). The membrane was then incubated overnight at 4°C with rabbit polyclonal anti-TJ antibodies (1:1000 dilution in 5% milk TBS-T). Following incubation with primary antibody, the membrane was washed with TBS-T (3 times x 5 minutes) and incubated at room temperature with

horseradish peroxidase (HRP)-conjugated goat anti-rabbit antibody (1:5000 in 5% milk TBS-T) for 1 hour, and then washed with TBS-T. To visualize protein bands, blots were incubated in 1-Step Ultra TMB Blotting Substrate Solution (Thermo Fisher Scientific, Australia) for 1-15 minutes at RT and scanned.

Western blots for TJ proteins were carried out as outlined above using equal amounts of protein from each tissue sampled. As a loading control, total protein was measured. Membranes were incubated with Coomassie Brilliant Blue R-250 staining solution as a modified protocol of that outlined in Welinder and Ekbald (2010). The Coomassie staining solution was combined with 5% MeOH and membranes were stained for ~5 minutes. The membranes were then destained in acetic acid/ethanol/water (1:5:4 ratio respectively), rinsed in water and scanned. TJ protein and total protein abundance were quantified using ImageJ software. Total protein abundance was used for normalizing protein of interest abundance after statistically validating that it did not significantly differ between control and experimental groups.

4.3.10 RNA extraction and cDNA synthesis

Skin samples were homogenised for 3 minutes at 30 Hz with stainless steel beads using a TissueLyser II (Qiagen Pty Ltd, Australia). Total RNA was isolated using an RNeasy Minikit (RNeasy Mini kit, Qiagen Pty Ltd, Australia) as per manufacturer's instructions. First, RLT buffer was added to all samples for homogenization and the homogenates were spun at full speed for 3 minutes (Microfuge 18, Beckman Coulter Pty Ltd, Australia). Then 600 µL of supernatant was removed and mixed with equal parts 70% ethanol. This mixture was pipetted into a spin column and centrifuged at 8,000 g for 15 seconds at RT. The eluted fluid was discarded. Buffer RW1 and buffer RPE (x2) were added to the column sequentially, and the column was centrifuged at 8,000

g for 15 seconds at RT between steps. The flow through from each centrifugation step was discarded. Finally, after transferring the spin column into a sterile collection tube, 50 μL of RNAse-free water was added to the column, the column was spun at top speed for 1 minute at RT and the eluant was flash frozen on dry ice and stored at -80°C. RNA purity (absorbance at 260/280) was assayed by spectrometry, and RNA was quantified using a Qubit fluorometer (ThermoFisher Scientific). RNA was then reverse transcribed into cDNA using the QuantiTech Reverse Transcription Kit (Qiagen Pty Ltd, Australia). First, 2 μL gDNAse wipeout buffer from the kit was added to 1 μg of RNA and this was incubated for 2 minutes at 42°C in the S1000™ Thermal Cycler (Bio-Rad Laboratories, Australia). Subsequently, Quantiscript reverse transcriptase and RT primer mix were added to the samples, and then the samples were incubated at 42°C for 15 minutes. Reverse transcriptase was inactivated at 95°C for 3 minutes and the samples were stored at -20°C. Negative controls (no template control, no reverse transcriptase control) were used to confirm that no contamination was present.

4.3.11 Analysis of TJ protein mRNA by PCR and qPCR.

For PCR, the Taq PCR Master Mix Kit (Qiagen Pty Ltd, Australia) was used. The following reaction conditions were utilized: 1 cycle of initial denaturation (95^{o} C, 10 min), then 40 cycles of denaturation (95^{o} C, 30 sec), annealing (56-60^{o}C, 30 sec) and extension (72^{o} C, 30 sec), followed by a final single extension cycle (72^{o} C, 5 min). PCR generated amplicons were visualized by agarose gel electrophoresis (1.5%, 120V separation for 1 hour).

Gene specific primers were designed for *Litoria caerulea* using the transcriptome of a closely-related species (*Pseudacris regilla*) and confirmed to be homologous. Sequence identity has been confirmed, but the sequences have yet to be submitted the NCBI for annotation. TJ protein

mRNA primers, listed in **Table 4.1**, were used for qPCR. Cldn protein mRNA abundance was examined by qPCR using a Mini Opticon real-time PCR detection system (MJ Mini Cycler, Bio-Rad Laboratories, Inc.) and using PowerSYBR Supermix (Applied Biosystems, Foster City, CA, USA) under the following conditions: 1 initial cycle of denaturation (95 C, 10 min), followed by 40 cycles of denaturation (95^{o} C, 30 sec), annealing (58-61^{o} C, 15 sec) and extension (60^{o} C, 45 sec). A melting curve was constructed after each qPCR run, ensuring that a single product was synthesized during each reaction. For all qPCR analyses, transcript abundance was normalized to *ef-1α* transcript abundance after determining by statistical analysis that *ef-1α* did not significantly alter (P=0.413) in response to infection. *L. caerulea ef-1α* mRNA was amplified using primers reported in **Table 3.1.**

Table 4.1. Primer sets, PCR annealing temperatures, amplicon size, and gene accession numbers for *Litoria caerulea* tight junction proteins and elongation factor-1α.

Tight Junction Protein	Gene	Primers	T_a	Amplicon size (bp)
Elongation factor-1α	*ef-1α*	F: GGCAAGTCCACAACAACC R: GTCCAGGGGCATCAATAA	56	229
Claudin-1	*cldn-1*	F:TGGCTTGTATAGGGTGGATTG R: ACCTTGGCTTTCATCACCTC	60	316
Claudin-4	*cldn-4*	F:TGCCTTCATCGGTAACAACA R: AACTCCCAGGATAGCCACAA	60	187
Occludin	*ocln*	F: TGCTATTGTTCTGGGGTTCC R: CCTTCTCGTTGTATTCGGACA	60	218
Tricellulin	*tric*	F: TAAGCGGATACATTCCAGCA R: CAGCGTTCCTTTTTCTCCAA	60	316
Zonula-Occludens 1	*zo-1*	F: GGGATGAGCGAGCAACTCTA R: GCACCAGGCTTTGACACTC	60	265

4.3.12 Statistical analyses

All data are expressed as mean values ±SEM (n), where n represents the number of frogs sampled, or as individual data points depending on the nature of the data. Significant differences ($P \leq 0.05$)

between groups were determined using the Student's t-test. All statistical analyses were performed using SigmaPlot 12.5 (Systat Software Inc., San Jose, CA, USA).

4.4 Results

4.4.1 Permeability of FITC-dextran through the dorsal and ventral skin of Australian green tree frog, *L. caerulea*.

FITC-dextran is a fluorescent marker that travels solely through the paracellular pathway. In control frogs, no permeability of FITC-dextran was detectable after 24 hours (**Figure 4.1a**). Examining a cross-section of the skin revealed that the fluorescent marker was unable to pass through the epidermis (**Figure 4.1b**). To observe whether perturbing the TJ complex would increase paracellular permeability, skin was incubated with the Ca^{++} chelator EDTA to "open" TJs (**Figure 4.1c**). Exposure to EDTA increased the permeability of the dorsal and ventral skin by 11.2 and 18.2 fold, respectively.

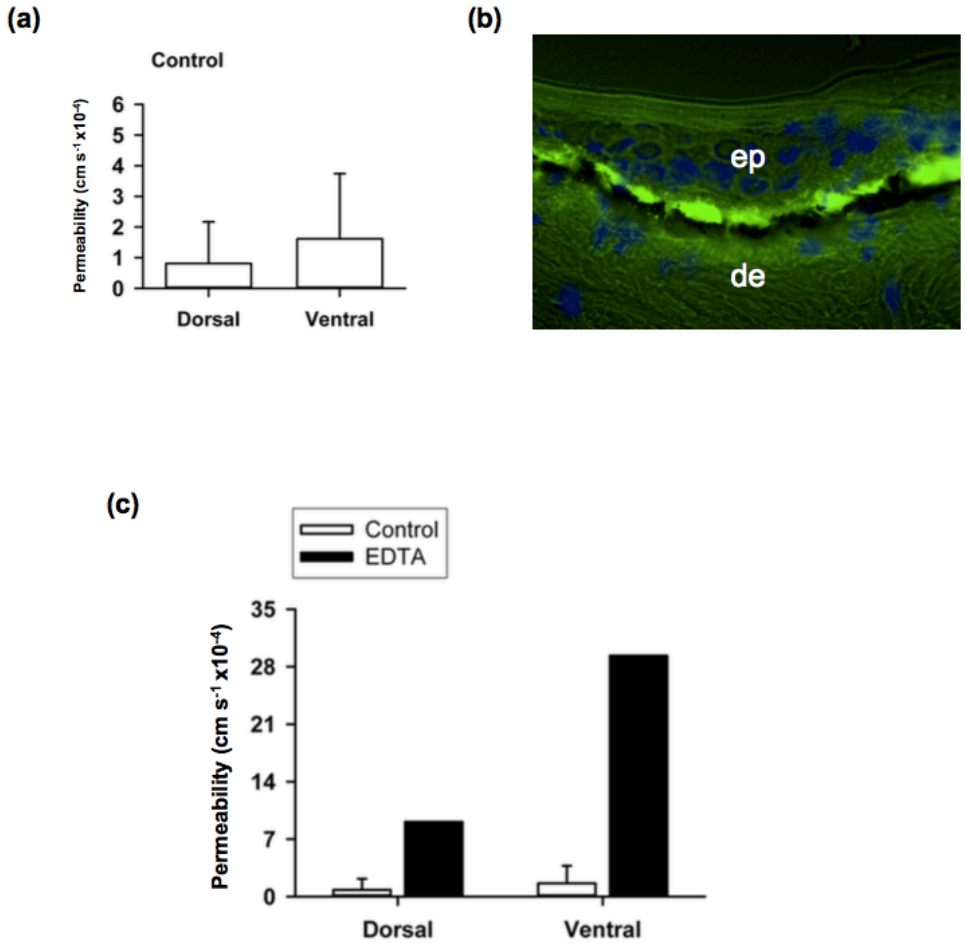

Figure 4.1. Permeability of 4 kDa FITC-dextran in the dorsal and ventral skin of control *Litoria caerulea*. Panel (a) depicts dorsal and ventral skin permeability in control frogs (n=3). Panel (b) shows a cross section of the skin, visualizing FITC-dextran (in green) being trapped under the epidermis. Panel (c) shows the change in dorsal and ventral skin permeability following the addition of EDTA, a TJ opener (control n=3; EDTA n=1). Permeability was measured after 24 hours for control and EDTA-exposed samples. ep= epidermis, de=dermis.

4.4.2 Permeability of FITC-dextran through the ventral skin of *Bd*-infected *L. caerulea*.

The permeability of *L. caerulea* skin altered with infection load (**Figure 4.2**). Ventral skin permeability correlated with zoospore count in a linear fashion, with a linear regression R value of 0.95. The skin of infected animals ranged from 36 to 588 times more permeable that the skin of control organisms.

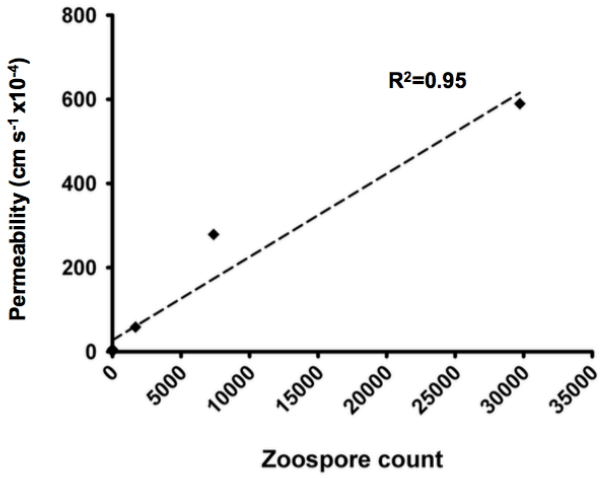

Figure 4.2. Permeability of 4 kDa FITC-dextran through the ventral skin of green tree frog, *Litoria caerulea*, with infection load. Graph depicts the skin permeability of individual animals of various infection loads, with a linear regression overlaying the points. Permeability assays were conducted for 24 hours using Franz cells.

4.4.3 Localization of TJ proteins in the ventral skin of control and *Bd* -infected *L. caerulea.*

Cldn-1, -10, Tric, and ZO-1 localized to the epidermis of control *L. caerulea* (**Figure 4.3a-b**). In control animals, Cldn-1 exhibited peri-junctional staining, whereas Cldn-10 and ZO-1 exhibited cytosolic staining. Transverse sections of the skin were taken to visualize Tric staining in the epidermis, and localization was found to be punctate. Ocln localization was also examined in the skin, however staining was not visible at a dilution factor of 1:100 (not shown).

Brightfield images of infected animal skin revealed that the overall integrity of the skin was compromised; i.e. it was thinner and the margins were disrupted (**Figure 4.3b**). In infected animals, Cldn-1, -10, and ZO-1 fluorescence was diminished. Additionally, Cldn-10 and ZO-1 staining became peri-junctional. Alternatively, Tric fluorescence increased in infected animals and localized to cells that were close to disrupted epidermal margins.

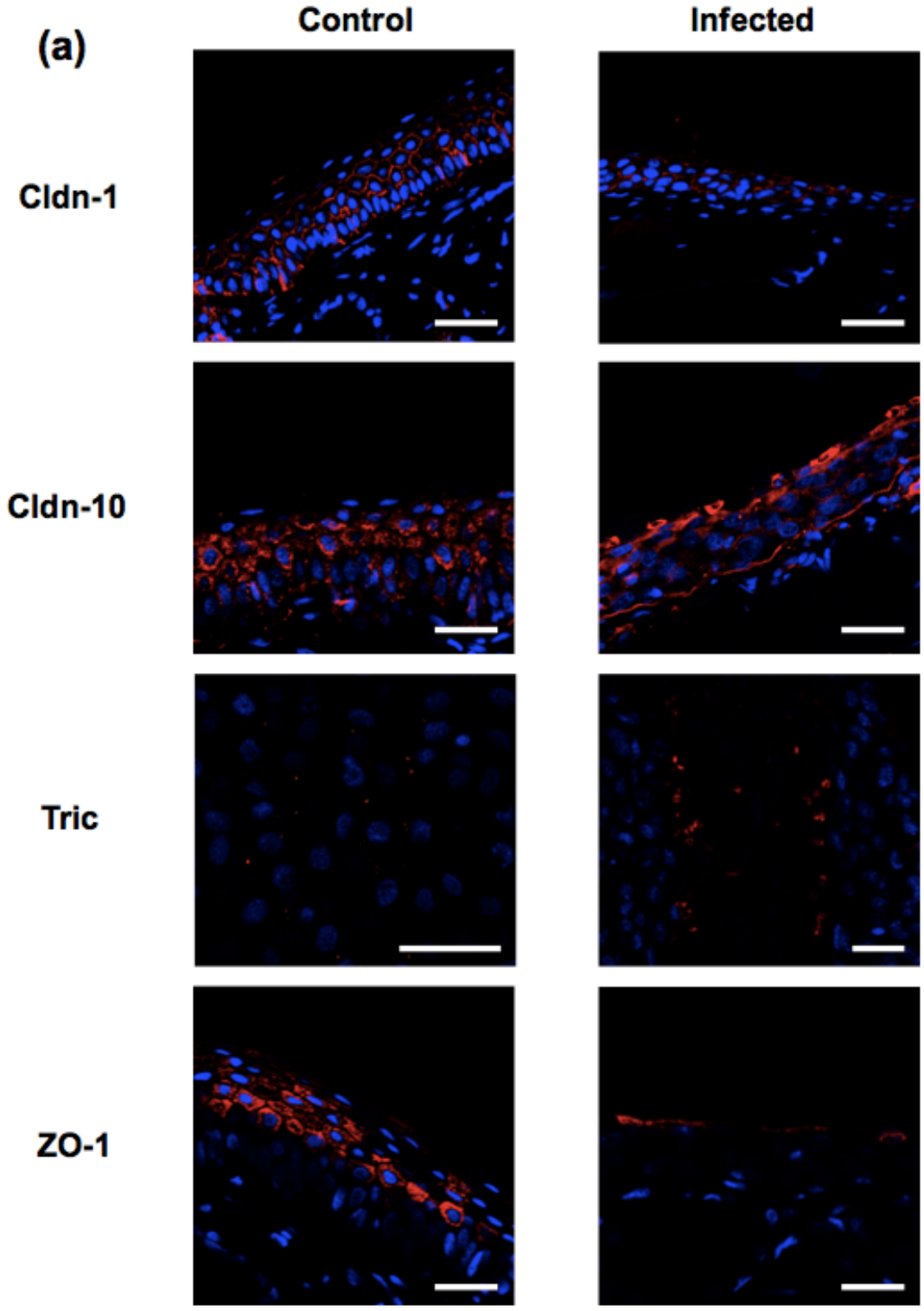

Figure 4.3. Localization of Cldn-1, -10, Tric and ZO-1 in the ventral skin of *Litoria caerulea*. Panel (a) shows fluorescent images only, and panel (b) is an overlay of fluorescence and Brightfield images. TJ protein fluorescence is depicted in red, nuclear staining is in blue. Scale bar= 20 µm

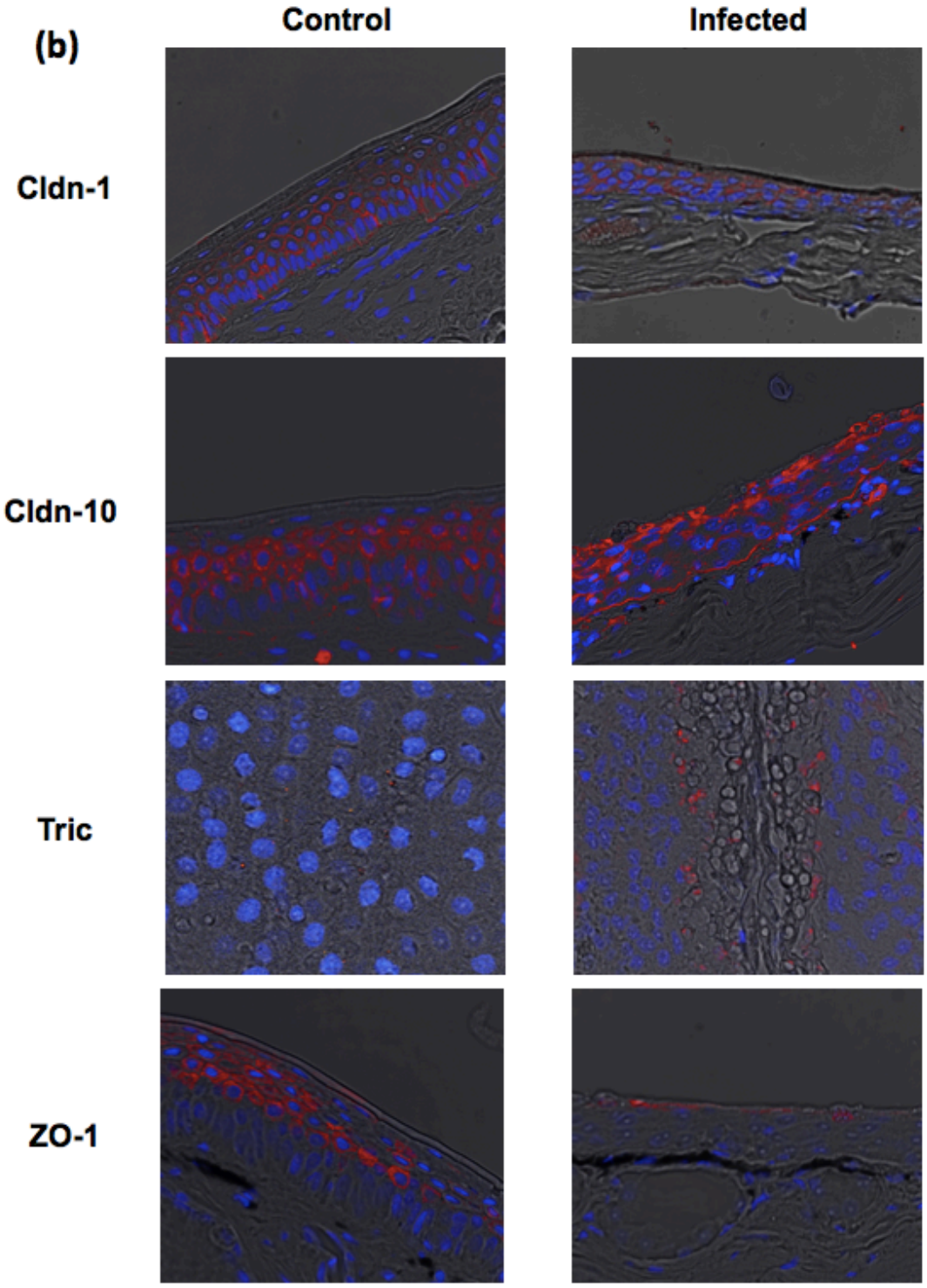

Figure 4.3. Caption on previous page.

4.4.4 Heterologous antibodies tested against *L. caerulea* skin protein extracts.

Rainbow trout, *Oncorhynchus mykiss*, anti-Cldn-10c (*L. caerulea* Cldn-10) exhibited bands of appropriate size in the skin of *L. caerulea* (**Figure 4.4)**. Commercial anti-Cldn-1, -Ocln, and -Tric antibodies also showed single bands of appropriate size (**Figure 4.4**). One thing to note is that the rainbow trout anti-Cldn-10c antibody detected Cldn-10 protein in the green tree frog, as there appears to be only one isoform of this protein in the transcriptome (not shown).

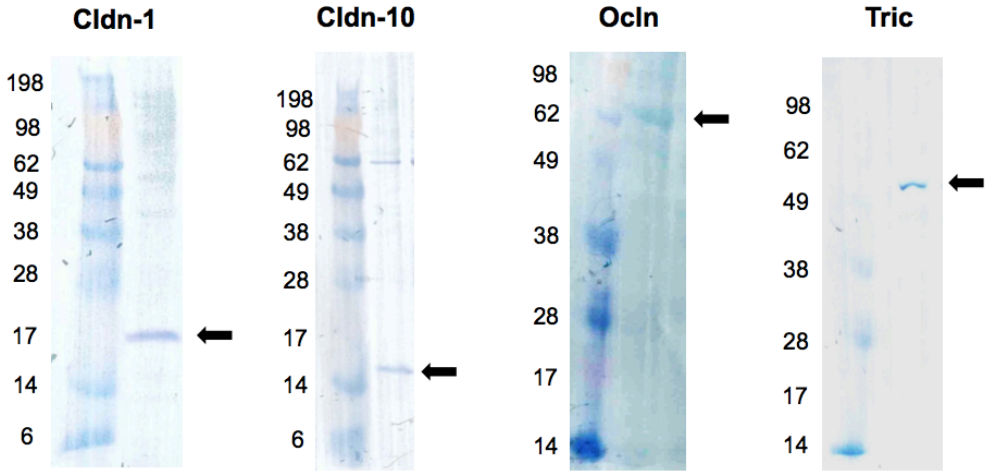

Figure 4.4 Representative Western blots of Claudin (Cldn)-1, -10, Occludin (Ocln) and Tricellulin (Tric) in the skin of Australian green tree frog, *Litoria caerulea*. Heterologous antibodies were used for Western blotting: commercial rabbit polyclonal C-terminal antibodies raised against human Cldn-1, Ocln and Tric and a custom-synthesized rabbit polyclonal antibody raised against rainbow trout, *Oncorhynchus mykiss,* Cldn-10c.

4.4.5 Effect of clinical *Bd* infection on TJ proteins in the ventral skin of *L. caerulea*.

Cldn-1, -10, Ocln, and Tric protein abundance was examined in the ventral skin of control and infected green tree frogs (**Figure 4.5**). Cldn-1 and Cldn-10 protein abundance decreased with infection, whereas Tric protein abundance increased. Ocln protein abundance remained unaltered with *Bd* infection.

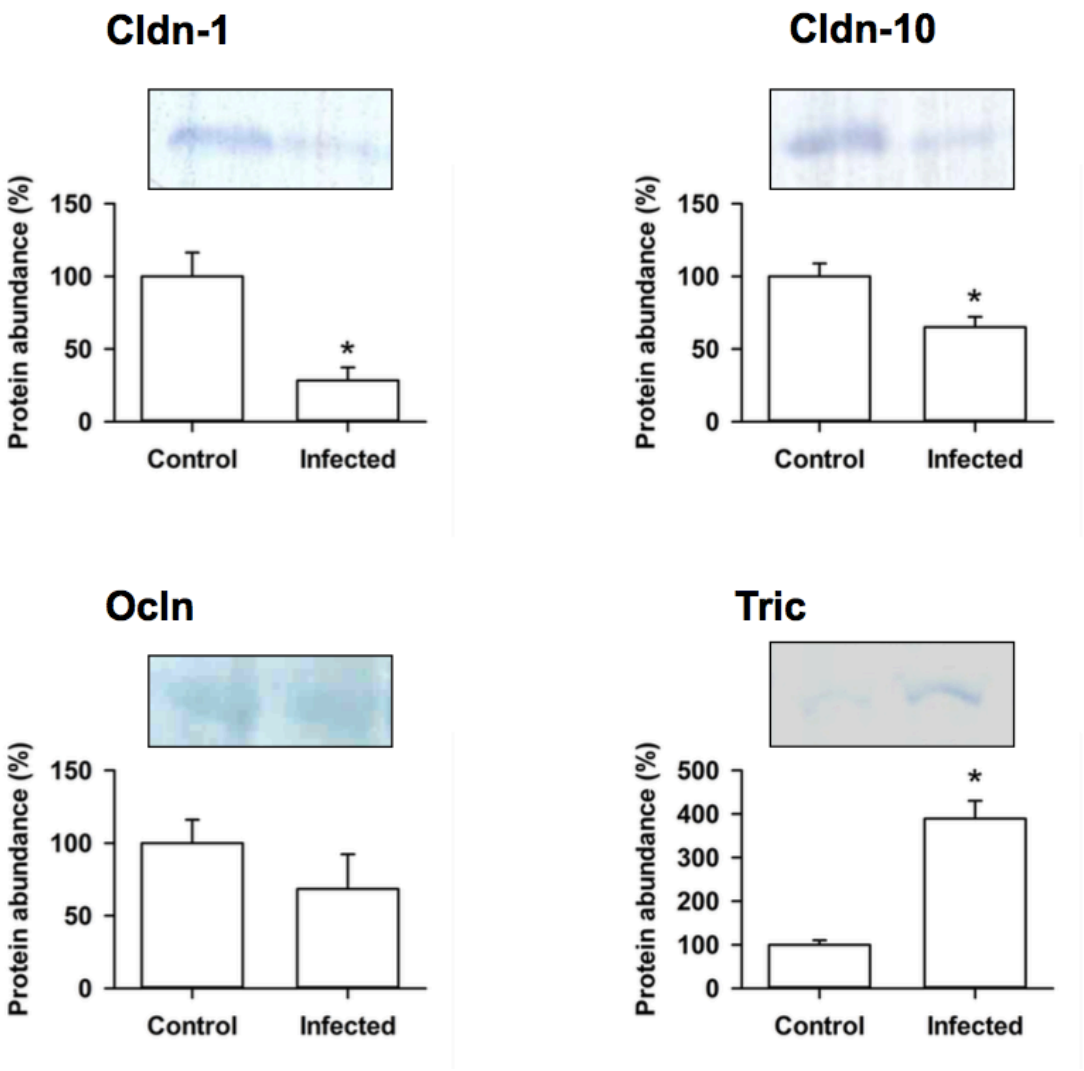

Figure 4.5. Effect of *Batrachochytrium dendrobatidis* infection on Claudin (Cldn)-1, -10, Occludin (Ocln), and Tricellulin (Tric) protein abundance in Australian green tree frog (*Litoria caerulea*) skin. All data are mean values ± SEM (n=8). Asterisks indicate a significant difference between control and infected frogs as determined by a Student's t-test. Total protein was used to normalize data. Representative blots are visualized above each graph.

4.4.6 Effect of clinical *Bd* infection on TJ protein mRNA abundance in the ventral skin of *L. caerulea*.

Transcript abundance of *cldn-1, -4, ocln, tric,* and *zo-1* were examined in the skin of green tree frog and showed single bands with gel electrophoresis (**Figure 4.6**). All TJ gene transcripts examined in the skin at least doubled with *Bd* infection (**Figure 4.7**).

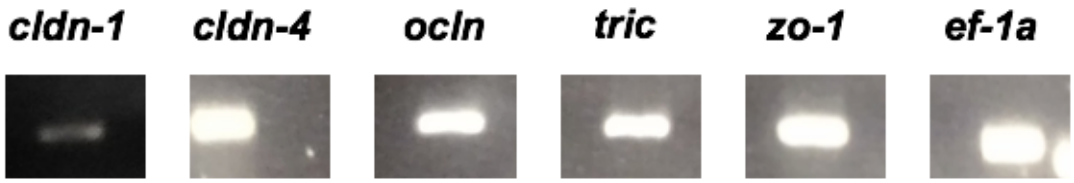

Figure 4.6. mRNA Expression of claudin-1 (*cldn-1*), -4 (*cldn-4*), occludin (*ocln*), tricellulin (*tric*), zonula-occludens 1 (*zo-1*), and elongation factor 1α (*ef-1α) in the* ventral skin of Australian green tree frog *(Litoria caerulea)*. Transcripts were examined in the skin with PCR and visualised with 1.5% agarose gel electrophoresis. Negative control was run under the same conditions but contained only sterile water (not shown).

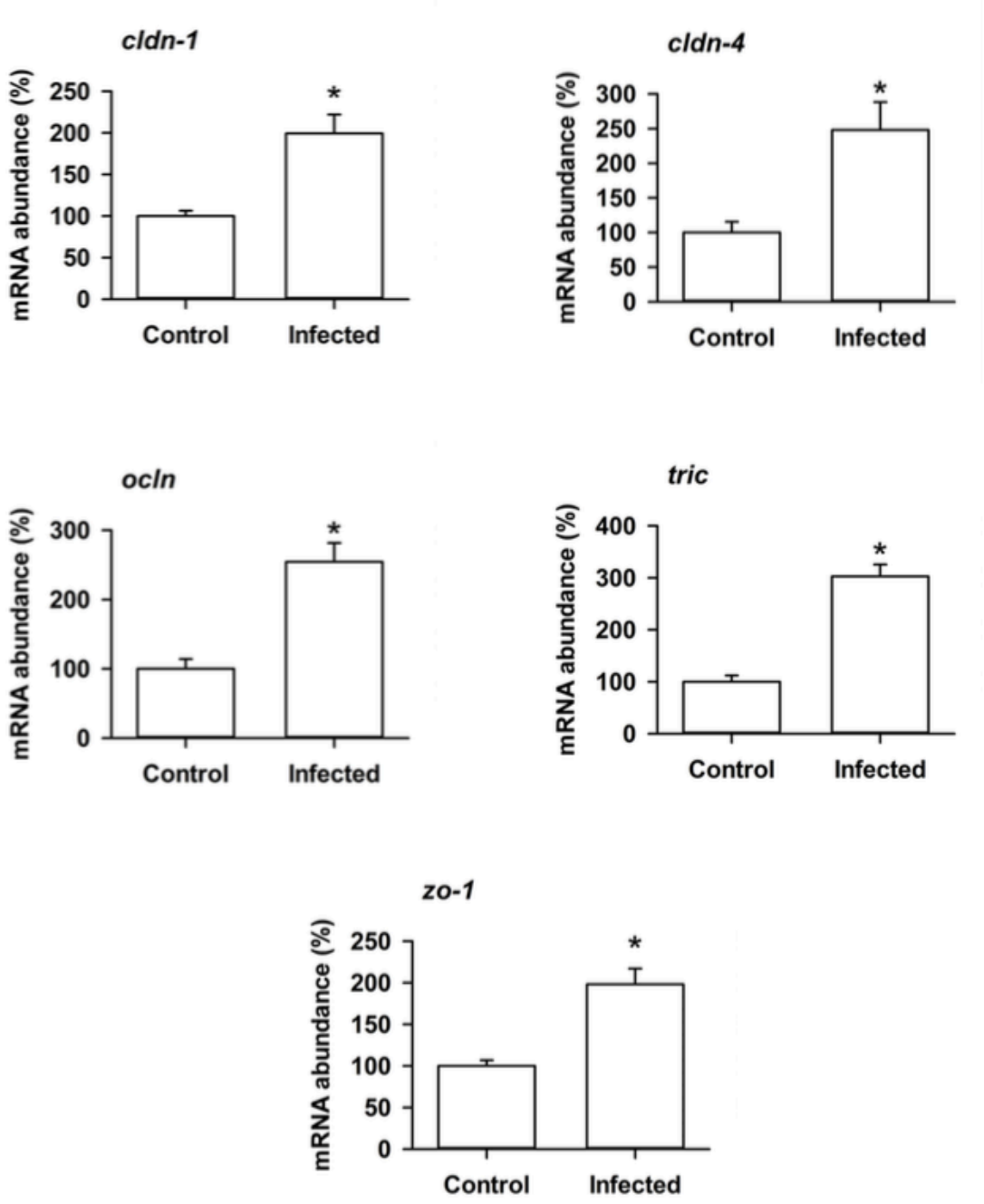

Figure 4.7. Effect of *Batrachochytrium dendrobatidis* infection on claudin (*cldn*)-1, -10, occludin (*ocln*), tricellulin (*tric*), and zonula occludens 1 (*zo-1*) mRNA abundance in Australian green tree frog (*Litoria caerulea*) skin. All data are mean values ± SEM (n=8). Asterisks indicate significant difference between control and infected frogs as determined by a Student's t-test. *ef-1α* was used as a reference gene.

4.5 Discussion

4.5.1 Overview

This study provides a first look at skin permeability in conjunction with the molecular physiology of the TJ complex in the skin of an amphibian infected with *Bd*. The hypothesis that the Chytrid fungus is able to alter TJ protein abundance and the paracellular permeability of *L. caerulea* skin can be accepted. Clinical infection with *Bd* fungus increased the paracellular permeability of the skin linearly with infection load. Additionally, various epidermal TJ proteins altered in abundance with *Bd* infection, indicating that paracellular permeability may have increased due to a change in TJ protein abundance. Finally, *Bd* infection resulted in an increase in abundance of all examined TJ protein transcripts, suggesting that mRNA may be upregulated as part of a whole-body stress response.

4.5.2 TJs maintain the barrier properties of the skin of *L. caerulea*.

In the present study, FITC-dextran was unable to move through either the dorsal or ventral skin of control animals (at least over a 24 h flux period; **Figure 4.1a**). Indeed, FITC-dextran became "trapped" immediately under the epidermis as it moved from the basolateral solution (**Figure 4.1b**). This is not surprising given that *L. caerulea* skin was found to have a transepithelial resistance (TER) of over 900 $\Omega.cm^2$ (Voyles et al., 2009), which is considered to be comparatively "tight" (Claude and Goodenough, 1973). However, to see whether TJs in the basal epidermal layers were responsible for blocking FITC-dextran movement, EDTA was added to the skin. EDTA is a calcium chelator that is known to reversibly open TJs (Deli, 2009). Therefore, in the present study the increased permeability in the dorsal and ventral skin regions with EDTA addition could be attributed to the TJ complex.

4.5.3 *Bd* infection affects the paracellular permeability of *L. caerulea* skin.

Due to the fact that *Bd* mainly colonizes and infects the ventral skin of amphibians (Berger et al., 2005), only the ventral skin was examined for subsequent experiments that focused on experimental *Bd* infection. *Bd* infection linearly increased the permeability of the ventral skin (**Figure 4.2**), indicating that integrity of the skin was compromised with increasing zoospore count. The change in permeability with infection was greater than that seen with the addition of EDTA only, therefore other junctional components, in addition to TJs, must be affected by *Bd* infection. This is in agreement with the study by Brutyn et al. (2012), which found that *Bd* was able to disrupt non-occluding junctional components such as desmosomes. Therefore, *Bd* is able to disrupt the barrier properties of the skin in a zoospore-dependent manner.

4.5.4 TJ protein abundance alters with *Bd* infection.

To examine if the infection-induced changes in skin permeability were linked to TJs at the molecular level, TJ protein and mRNA abundance was examined. Cldn-1, -10, Tric, and ZO-1 proteins localized to the epidermis, which directly interfaces with the external environment (**Figure 4.3**). Therefore, any changes in the abundance of these proteins has a potential to affect the paracellular permeability of the skin. Protein abundance of Cldn-1, -10, Tric and ZO-1 altered with infection, which could be observed qualitatively with immunolocalization (**Figure 4.3**) or quantitatively with Western blots (**Figure 4.5**). Cldn-1 is well known to be a barrier-forming TJ protein (Günzel and Yu, 2013), and specifically so in the skin of mammals (Brandner, 2009). For example, knockdown of CLDN-1 in mice resulted in substantial transepidermal water loss, which led to death within 1 day of birth (Furuse et al., 2002). CLDN-1 is also known to be important for cutaneous wound healing in humans (Volksdorf et al., 2017). So far, no work has been conducted

on Cldn-1 in the skin of amphibians, however, Cldn-1 has been shown to play a role in regulating ion movement in renal epithelial cells of *Xenopus* (Tokuda et al., 2010). Therefore, the decrease of Cldn-1 protein abundance in the skin of *L. caerulea* with *Bd* infection may contribute to the increased paracellular permeability of the skin (see **section 4.5.3**).

Unlike Cldn-1, Cldn-10 isoforms in vertebrates are believed to be pore-forming (Gunzel and Fromm, 2012; Kolosov et al., 2013; Bui and Kelly, 2014). Although it may seem contradictory that a decrease in a pore-forming Cldn leads to "leakier" skin, it may be that the Cldn-10 decrease is part of a larger downregulation of Cldn proteins. If more barrier-forming Cldns (like Cldn-1) are depleted, this could account for the reported increase in paracellular permeability. Because, this fungus was found to express protease genes (Rosenblum et al., 2008), proteases released by *Bd* may be degrading the Cldn proteins. Therefore, *Bd* may be expressing proteases that lead to a general decrease in Cldn abundance.

Contrary to the Cldn abundance, Tric levels increased following *Bd* infection. Tric is known to be a barrier-forming protein in other vertebrates (Günzel and Fromm, 2012) and is concentrated at the tricellular contacts between adjacent epithelial cells (Ikenouchi et al., 2005). Given its tricellular localization, this protein belongs to a different junctional structure and is regulated by different regulatory networks compared to its bicellular counterparts (e.g., Masuda et al., 2010; Krug et al., 2017; reviewed in Mariano et al., 2011). It is possible that *Bd* was not able to degrade Tric due to its structure/regulation, and the increased protein abundance may be a result of the increased mRNA abundance that occurs with infection (see **section 4.5.5; Figure 4.6**). However, because Tric fluorescence increased around disrupted epidermal margins in infected animals (**Figure 4.3**), there may be another explanation for the increase in Tric protein abundance with *Bd* infection. In other vertebrates, several infectious agents have been found to target Tric as a

mechanism for invasion into the tissue without depleting it (Sakaguchi et al., 2002; Fukumatsu et al., 2012; Morampudi et al., 2017). For example, bacterial *Shigella flexneri* infection was reported to decrease Cldn-1, Ocln, and ZO-1 protein abundance, but targeted tricellular junctions for entry into MK2 cells (Sakaguchi et al., 2002; Fukumatsu et al., 2012). When Tric was artificially depleted prior to infection, the spread of *Shigella* was reduced (Fukumatsu et al., 2012). Thus, there is a possibility that the *Bd* fungus is targeting Tric to enter the tissue.

Ocln abundance did not alter with *Bd* infection, but Ocln protein was generally not very abundant in the skin in either control or infected frogs. A concentration of 1:100 detected no Ocln signal with immunohistochemistry, and a faint band with Western blotting. It is possible that *Bd* was able to degrade Ocln, but given the relatively small abundance of Ocln in the skin, an upregulation of Ocln transcription with infection (see **section 4.5.5**; **Figure 4.6**) may have compensated for any degradation in Ocln protein, resulting in no detectable change in protein abundance.

A qualitative decrease in ZO-1 abundance (**Figure 4.3**) indicated that *Bd* infection affected scaffolding proteins in addition to transmembrane proteins. Given that ZO-1 links the transmembrane proteins to the actin cytoskeleton, a decrease in ZO-1 abundance indicates that the structural integrity of the TJ complex may have been disrupted with *Bd* infection. This is consistent with the finding that *Bd* infection was correlated to increased paracellular permeability of the skin (see **section 4.5.3**; **Figure 4.2**). Therefore, the qualitative decrease in ZO-1 abundance may have contributed to the loss of skin integrity with Chytridiomycosis.

4.5.5 TJ protein mRNA abundance in the skin increased uniformly with *Bd* infection.

Despite the differential effects of *Bd* infection on protein abundance, *Bd* uniformly increased the transcript abundance of all TJ genes (*cldn-1, -4, ocln, tric, ZO*-1) examined in this study (**Figure 4.6**). This may have been due to the fact that a stress response was triggered in the host animal with infection. Indeed, blood corticosterone levels have been found to increase in *Bd*-infected amphibians, including *L. caerulea*, suggesting a stress response (Gabor et al., 2013; Peterson et al., 2013). Glucocorticoids have been shown to alter TJ mRNA and protein abundance in various vertebrates (Nguyen and Neville, 1998; Chasiotis and Kelly, 2011; Kielgast et al., 2016), therefore, increased systemic levels of corticosterone in *L. caerulea* with infection may have increased TJ protein transcript abundance en masse.

The observed increases in mRNA abundance of Cldn-1 and ZO-1 were in opposition to their quantitative (Cldn-1) and qualitative (ZO-1) decreases in protein abundance (**Figures 4.3 and 4.5**). This may imply that Cldn-1 and ZO-1 proteins were being degraded faster than their mRNA could be translated. Thus, the increase in mRNA abundance was not sufficiently high to compensate for the protein degradation. Consequently, the net decrease in Cldn-1 and ZO-1 protein abundance with infection may have led to the observed disruption of skin barrier properties.

4.6 Conclusions and future perspectives

Overall, *Bd* infection altered the permeability of *L. caerulea* skin, and evidence suggests that this is in part as a result of TJ proteins being targeted. *Bd* infection did not uniformly affect TJ protein levels; it decreased Cldn abundance, increased Tric abundance and had no effect on Ocln levels. Despite the different effects on protein abundance, *Bd* infection resulted in a uniform upregulation of TJ protein transcript levels, possibly due to an organ inflammatory response.

Only a few TJ proteins were examined in this study due to the short timeframe within which the studies could be conducted. In this regard, it would be useful for future studies to examine all of the TJ proteins expressed in the skin of *L. caerulea* and how they are affected by *Bd*. This is important because TJ proteins are present as part of a "protein mosaic" with each component possessing different properties that collectively contribute to the function of an epithelium. Thus, examining all skin TJ proteins will provide a clearer image of the effects of infection. Additionally, it would be valuable to compare the response of TJ proteins to infection in a frog that is highly susceptible to *Bd,* such as *L. caerulea,* and in a frog that is a subclinical carrier of *Bd*, such as *Xenopus laevis* (Van Rooij et al., 2015). This would provide insight into how important TJ proteins are to the disruption of the skin barrier function with infection. For example, if *Xenopus* has more TJ proteins compared to *L. caerulea*, perhaps there is a potential of certain TJ proteins to compensate for the degradation of other proteins, allowing *Xenopus* to cope more effectively with the infection. Finally, because *L. caerulea* regularly moults its skin, it would be interesting to examine TJ protein abundance during the different sloughing stages (pre-moult, intermoult, and post-moult). Sloughing in another amphibian, the cane toad *Rhinella marina*, was found to increase the loss of ions from the skin (Wu et al., 2017), therefore it would be valuable to see if the loss of TJ integrity is involved in this process.

4.7 References

Berger, L., Speare, R., Skerratt, L.F., 2005. Distribution of *Batrachochytrium dendrobatidis* and pathology in the skin of green tree frogs *Litoria caerulea* with severe chytridiomycosis. Dis. Aquat. Organ. 68, 65–70.

Baltzegar, D.A., Reading, B.J., Brune, E.S., Borski, R.J., 2013. Phylogenetic revision of the claudin gene family. Mar. Genomics 11, 17–26.

Bouhet, S., Oswald, I.P., 2005. The effects of mycotoxins, fungal food contaminants, on the intestinal epithelial cell-derived innate immune response. Vet. Immunol. Immunopathol. 108, 199–209.

Boutilier, R.G., Stiffler, D.F. & Toews, D.P. 1992. Exchange of respiratory gases, ions, and water in amphibious and aquatic amphibians. Environmental Physiology of the Amphibians (eds M.E. Feder & W. Burggren). The University of Chicago Press, Chicago. pp. 100–107.

Boyle, D., Boyle, D., Olsen, V., Morgan, J. & Hyatt, A., 2004. Rapid quantitative detection of chytridiomycosis (*Batrachochytrium dendrobatidis*) in amphibian samples using real-time Taqman PCR assay. Dis. Aquat. Organ. 60, 141–148.

Brandner, J.M., 2009. Tight junctions and tight junction proteins in mammalian epidermis. Eur. J. Pharm. Biopharm. 72, 289–294.

Brutyn, M., D'Herde, K., Dhaenens, M., Rooij, P. Van, Verbrugghe, E., Hyatt, A.D., Croubels, S., Deforce, D., Ducatelle, R., Haesebrouck, F., Martel, A., Pasmans, F., 2012.

Batrachochytrium dendrobatidis zoospore secretions rapidly disturb intercellular junctions in frog skin. Fungal Genet. Biol. 49, 830–837.

Bruus, K., Kristensen, P., Larsen, E.H., 1976. Pathways for chloride and sodium transport across toad skin. Acta Physiol. Scand. 97, 31–47.

Bui, P., Kelly, S.P., 2014. Claudin-6, -10d and -10e contribute to seawater acclimation in the euryhaline puffer fish *Tetraodon nigroviridis*. J. Exp. Biol. 217, 1758–67.

Campbell, C.R., Voyles, J., Cook, D.I., Dinudom, A., 2012. Frog skin epithelium: Electrolyte transport and chytridiomycosis. Int. J. Biochem. Cell Biol. 44, 431–434.

Cardellini, P., Davanzo, G., Citi, S., 1996. Tight junctions in early amphibian development: Detection of junctional cingulin from the 2-cell stage and its localization at the boundary of distinct membrane domains in dividing blastomeres in low calcium. Dev. Dyn. 207, 104–113.

Castillo, G.A., Coviello, A., Orce, G.G., 1991. Effect of theophylline on the electrolyte permeability of the isolated skin of the toad *Bufo arenarum*. Arch. Int. Physiol. Biochim. Biophys. 99, 257–264.

Chang, D.J., Hwang, Y.S., Cha, S.W., Chae, J.P., Hwang, S.H., Hahn, J.H., Bae, Y.C., Lee, H.S., Park, M.J., 2010. Xclaudin 1 is required for the proper gastrulation in *Xenopus laevis*. Biochem. Biophys. Res. Commun. 397, 75–81.

Chasiotis, H., Kelly, S.P., 2009. Occludin and hydromineral balance in *Xenopus laevis*. J. Exp. Biol. 212, 287–296.

Chasiotis, H., Kelly, S.P., 2011. Effect of cortisol on permeability and tight junction protein transcript abundance in primary cultured gill epithelia from stenohaline goldfish and euryhaline trout. Gen. Comp. Endocrinol. 172, 494–504.

Chasiotis, H., Kolosov, D., Bui, P., Kelly, S.P., 2012. Tight junctions, tight junction proteins and paracellular permeability across the gill epithelium of fishes: a review. Respir. Physiol. Neurobiol. 184, 269–81.

Chuong, C., Nickoloff, B., Elias, P., Goldsmith, L., Macher, E., Maderson, P., Sundberg, J., Tagami, H., Plonka, P.M., K, T.P., 2002. What is the "true" function of skin? Exp. Dermatol. 11, 159–187.

Claude, P., Goodenough, D.A., 1973. Fracture faces of zonulae occludentes from "tight" and "leaky" epithelia. J. Cell Biol. 58, 390–400.

Cordenonsi, M., Mazzon, E., De Rigo, L., Baraldo, S., Meggio, F., Citi, S., 1997. Occludin dephosphorylation in early development of *Xenopus laevis*. J. Cell Sci. 110, 3131–3139.

Deli, M.A., 2009. Potential use of tight junction modulators to reversibly open membranous barriers and improve drug delivery. Biochim. Biophys. Acta - Biomembr. 1788, 892–910.

Ehrenfeld, J., Klein, U., 1997. The key role of the H+ V-ATPase in acid-base balance and Na+ transport processes in frog skin. J. Exp. Biol. 200, 247–256.

Fesenko, I., Kurth, T., Sheth, B., Fleming, T.P., Citi, S., Hausen, P., 2000. Tight junction biogenesis in the early *Xenopus* embryo. Mech. Dev. 96, 51–65.

Fisher, M.C., Garner, T.W.J., Walker, S.F., 2009. Global emergence of *Batrachochytrium dendrobatidis* and amphibian chytridiomycosis in space, time, and host. Annu. Rev. Microbiol. 63, 291–310.

Fukumatsu, M., Ogawa, M., Arakawa, S., Suzuki, M., Nakayama, K., Shimizu, S., Kim, M., Mimuro, H., Sasakawa, C., 2012. *Shigella* targets epithelial tricellular junctions and uses a noncanonical clathrin-dependent endocytic pathway to spread between cells. Cell Host Microbe 11, 325–336.

Furuse, M., Hata, M., Furuse, K., Yoshida, Y., Haratake, A., Sugitani, Y., Noda, T., Kubo, A., Tsukita, S., 2002. Claudin-based tight junctions are crucial for the mammalian epidermal barrier: A lesson from Claudin-1-deficient mice. J. Cell Biol. 156, 1099–1111.

Gabor, C.R., Fisher, M.C., Bosch, J., 2013. A non-invasive stress assay shows that tadpole populations infected with *Batrachochytrium dendrobatidis* have elevated corticosterone levels. PLoS One 8, 1–5.

Günzel, D., Fromm, M., 2012. Claudins and other tight junction proteins. Compr. Physiol. 2, 1819–1852.

Günzel, D., Yu, A.S.L., 2013. Claudins and the modulation of tight junction permeability., Physiol Rev. 93, 525-569.

Ikenouchi, J., Furuse, M., Furuse, K., Sasaki, H., Tsukita, S., Tsukita, S., 2005. Tricellulin constitutes a novel barrier at tricellular contacts of epithelial cells. J. Cell Biol. 171, 939–945.

Jorgensen, C.B., 1949. Permeability of the Amphibian Skin. Acta Physiol. Scand. 18, 171–180.

Kielgast, F., Schmidt, H., Braubach, P., Winkelmann, V.E., Thompson, K.E., Frick, M., Dietl, P., Wittekindt, O.H., 2016. Glucocorticoids regulate tight junction permeability of lung epithelia by modulating Claudin 8. Am. J. Respir. Cell Mol. Biol. 54, 707–717.

Kilpatrick, A.M., Briggs, C.J., Daszak, P., 2010. The ecology and impact of chytridiomycosis: an emerging disease of amphibians. Trends Ecol. Evol. 25, 109–118.

Klein, S.L., Strausberg, R.L., Wagner, L., Pontius, J., Clifton, S.W., Richardson, P., 2002. Genetic and genomic tools for *Xenopus* research: The NIH *Xenopus* initiative. Dev. Dyn. 225, 384–391.

Kolosov, D., Bui, P., Chasiotis, H., Kelly, S.P., 2013. Claudins in teleost fishes. Tissue Barriers 1, 1–15.

Kolosov, D., Donini, A., Kelly, S.P., 2017. Claudin-31 contributes to corticosteroid-induced alterations in the barrier properties of the gill epithelium. Mol. Cell. Endocrinol. 439, 457–466.

Kolosov, D., Kelly, S.P., 2017. Claudin-8d is a cortisol-responsive barrier protein in the gill epithelium of trout. J. Mol. Endocrinol. 59, 1–12.

Krug, S.M., Bojarski, C., Fromm, A., Lee, I.M., Dames, P., Richter, J.F., Turner, J.R., Fromm, M., 2017. Tricellulin is regulated via interleukin-13-receptor a2, affects macromolecule uptake, and is decreased in ulcerative colitis. Nat. Publ. Gr.

Mandel, L.J., Curran, P.T., 1972. Chloride flux via a shunt pathway in frog skin: apparent exchange diffusion. Biochim. Biophys. Acta 282, 258–264.

Mariano, C., Sasaki, H., Brites, D., Brito, M.A., 2011. A look at Tricellulin and its role in tight junction formation and maintenance. Eur. J. Cell Biol. 90, 787–796.

Martinez-Palomo, A., Erlij, D., Bracho, H., 1971. Localization of permeability barriers in the frog skin epithelium. J. Cell Biol. 50, 277–287.

Masuda, R., Semba, S., Mizuuchi, E., Yanagihara, K., Yokozaki, H., 2010. Negative regulation of the tight junction protein Tricellulin by snail-induced epithelial-mesenchymal transition in gastric carcinoma cells. Pathobiology 77, 106–113.

Meyer, E.A., Cramp, R.L., Franklin, C.E., 2010. Damage to the gills and integument of *Litoria fallax* larvae (Amphibia: Anura) associated with ionoregulatory disturbance at low pH. Comp. Biochem. Physiol. Part A 155, 164–171.

Morampudi, V., Graef, F.A., Stahl, M., Dalwadi, U., Conlin, V.S., Huang, T., Vallance, B.A., Hong B. Yu, Jacobson, K., 2017. Tricellular tight junction protein Tricellulin is targeted by the enteropathogenic *Escherichia coli* effector EspG1, leading to epithelial barrier disruption. Infect. Immun. 85, 1–20.

Nguyen, D. a, Neville, M.C., 1998. Tight junction regulation in the mammary gland. J. Mammary Gland Biol. Neoplasia 3, 233–246.

Ohmer, M.E.., Cramp, R.L., White, C.R., Franklin, C.E., 2014. Skin sloughing rate increases with chytrid fungus infection load in a susceptible amphibian. Funct. Ecol. 29.

Parsons RH, Mobin F., 1991. Water flow across the pectoral and ventral pelvic patch in *Rana catesbeiana.* Physiol Zool. 235, 812–22.

Pessier, A.P., Nichols, D.K., Longcore, J.E., Fuller, M.S., 1999. Cutaneous chytridiomycosis in poison dart frogs (*Dendrobates* spp.) and White's tree frogs (*Litoria caerulea*). J. Vet. Diagn. Invest. 11, 194–199.

Peterson, J.D., Steffen, J.E., Reinert, L.K., Cobine, P.A., Appel, A., Rollins-Smith, L., Mendonça, M.T., 2013. Host stress response is important for the pathogenesis of the deadly amphibian disease, chytridiomycosis, in *Litoria caerulea*. PLoS One 8, 1–7.

Rosenblum, E.B., Stajich, J.E., Maddox, N., Eisen, M.B., 2008. Global gene expression profiles for life stages of the deadly amphibian pathogen *Batrachochytrium dendrobatidis*. Proc. Natl. Acad. Sci. USA 105, 17034–9.

Saharinen, P., Helotera, H., Miettinen, J., Norrmen, C., D'Amico, G., Jeltsch, M., Langenberg, T., Vandevelde, W., Ny, A., Dewerchin, M., Carmeliet, P., Alitalo, K., 2010. Claudin-like protein 24 interacts with the VEGFR-2 and VEGFR-3 pathways and regulates lymphatic vessel development. Genes Dev. 24, 875–880.

Sakaguchi, T., Köhler, H., Gu, X., McCormick, B.A., Reinecker, H.C., 2002. *Shigella flexneri* regulates tight junction-associated proteins in human intestinal epithelial cells. Cell. Microbiol. 4, 367–381.

Stuart, S.N., Chanson, J.S., Cox, N. a, Young, B.E., Rodrigues, A.S.L., Fischman, D.L., Waller, R.W., 2004. Status and trends of amphibian declines and extinctions worldwide. Science 306, 1783–1786.

Sun, J., Wang, X., Li, C., Mao, B., 2015. *Xenopus* Claudin-6 is required for embryonic pronephros morphogenesis and terminal differentiation. Biochem. Biophys. Res. Commun. 462, 178–83.

Tokuda, S., Miyazaki, H., Nakajima, K., Yamada, T., Marunaka, Y., 2010. NaCl flux between apical and basolateral side recruits Claudin-1 to tight junction strands and regulates paracellular transport. Biochem. Biophys. Res. Commun. 393, 390–396.

Van Rooij, P., Martel, A., Haesebrouck, F., Pasmans, F., 2015. Amphibian chytridiomycosis: A review with focus on fungus-host interactions. Vet. Res. 46, 1–22.

Volksdorf, T., Heilmann, J., Eming, S.A., Schawjinski, K., Zorn-Kruppa, M., Ueck, C., Vidal-y-Sy, S., Windhorst, S., Jücker, M., Moll, I., Brandner, J.M., 2017. Tight junction proteins Claudin-1 and Occludin are important for cutaneous wound healing. Am. J. Pathol. 1–13.

Voyles, J., Berger, L., Young, S., Speare, R., Webb, R., Warner, J., Rudd, D., Campbell, R., Skerratt, L.F., 2007. Electrolyte depletion and osmotic imbalance in amphibians with chytridiomycosis. Dis. Aquat. Organ. 77, 113–118.

Voyles, J., Young, S., Berger, L., Campbell, C., Voyles, W.F., Dinudom, A., Cook, D., Webb, R., Alford, R.A., Skerratt, L.F., Speare, R., 2009. Pathogenesis of chytridiomycosis, a cause of catastrophic amphibian declines. Science. 326, 582–585.

Welinder, C., Ekblad, L., 2010. Coomassie staining as loading control in western blot analysis. J. Proteome Res. 10, 1416–1419.

Wu, N.C., Cramp, R.L., Franklin, C.E., 2017. Living with a leaky skin: upregulation of ion transport proteins during sloughing. J. Exp. Biol. 220, 2026–2035.

Yamagishi, M., Ito, Y., Ariizumi, T., Komazaki, S., Danno, H., Michiue, T., Asashima, M., 2010. Claudin5 genes encoding tight junction proteins are required for *Xenopus* heart formation. Dev. Growth Differ. 52, 665–675.

Zhang, J., Ni, C., Yang, Z., Piontek, A., Chen, H., Wang, S., Fan, Y., Qin, Z., Piontek, J., 2015. Specific binding of *Clostridium perfringens* enterotoxin fragment to Claudin-b and modulation of zebrafish epidermal barrier. Exp. Dermatol. 24, 605–610.

5. Chapter Five: Conclusions and Future Directions

5.1 Summary

The present studies examined the paracellular permeability, and the molecular components that regulate paracellular permeability, of vertebrate skin from three perspectives: (1) exposure to different salinity, (2) natural fluctuation during a 12 hour- LD cycle, and (3) exposure to fungal infection. Alterations in the TJ complex in the skin were able to help maintain salt and water balance with salinity change (**Chapter 2**) and during natural fluctuations caused by the LD cycle (**Chapter 3**). Conversely, dysregulation of TJ proteins in the skin resulted in clear and drastic disruption of the skin barrier properties (**Chapter 4**). Therefore, the results from these studies confirmed that the vertebrate skin is an indispensable barrier to external abiotic and biotic factors. Studies enclosed also indicated that the vertebrate skin is a highly dynamic barrier, which can exhibit spatial and temporal differences in its response to disturbances in order to maintain hydromineral homeostasis. Additionally, this work, for the first time, provided a comparison of the response of the molecular components of the skin TJ complex to extrinsic disturbances in aquatic and semi-aquatic vertebrates.

5.2 Cldn proteins in the skin of fishes and amphibians.

The suite of Cldn proteins expressed in the skin of teleost fishes and amphibians could differ in number and abundance due to their different evolutionary histories. Teleost fishes underwent a lineage-specific whole genome duplication (WGD) event during their evolution. This, in addition to tandem gene duplications, led to an expansion of their Cldn gene family (Loh et al., 2004). In addition to this WGD event that occurred in teleosts, salmonids, such as rainbow trout, underwent another WGD event, further expandin their suite of Cldn genes (Berthelot et al., 2014). Conversely,

in amphibians, polyploidy has evolved independently in many families and species (Schmid et al., 2015). For example, the family to which the Australian green tree frog (GTF) *Litoria caerulea* belongs to, *Hylidae*, possesses multiple species of varying ploidy (Schmid et al., 2015). The ploidy of the GTF has not been determined to date, however, the difference in ploidy between the GTF and rainbow trout could influence the number of unique TJ proteins and isoforms that are present in the skin, and genome, of these animals. For example, given that the GTF skin transcriptome only contained one Cldn-10 trancript, whereas trout expressed multiple Cldn-10 isoforms in the skin (Kolosov et al., 2014: Gauberg et al, 2017), could indicate that the GTF did not undergo as many WGD events as rainbow trout.

Recall that Cldn-10 localized to the epidermis of the GTF skin, whereas Cldn-10c localized to the scale pocket (dermis) of trout skin (see **Chapters 2 and 4**). In previous studies, Cldn-10c, -10d, and -10e were found to be cell-specific in several teleosts (Bui and Kelly, 2014; Kolosov et al., 2014). This may indicate that the various Cldn-10 isoforms in rainbow trout may have specialized to have unique functions and localizations in the rainbow trout skin. It would be valuable to investigate the different properties of the Cldn-10 isoforms in the trout skin and compare them to the properties of Cldn-10 in the GTF, or other vertebrates expressing only one Cldn-10 isoform. Additionally, rainbow trout skin has been found to express Cldn-3, -27, -28, -29, -30, and -31 protein transcripts and isoforms (Gauberg et al., 2017) which have been shown, in the pufferfish *Fugu rupribes*, to be orthologues of the mammalian CLDN-3 and -4 genes (Loh et al., 2004). Therefore, it appears that this set of Cldn genes arose from a duplication of the ancestral Cldn-3 and -4 genes. Thus, like the Cldn-10 isoforms, these proteins may have specialized functions in the skin of rainbow trout. The GTF expressed *cldn-4* mRNA in the skin, therefore it would be interesting to investigate whether fewer Cldn genes are expressed in the skin of this frog.

It would also be interesting to determine the number of Cldn proteins expressed in the skin of amphibians of differing ploidy, and how this contributes to the regulation of the barrier properties of the skin. Therefore, it is possible that rainbow trout possess more Cldn proteins with more derived functions compared to the GTF, and this may influence the regulation of the barrier properties of the skin of these animals.

5.3 Examining the barrier properties of the vertebrate integument.

In the past, insights have been made into certain aspects of the role of vertebrate skin in maintaining homeostasis (e.g. TJ protein localization, immune function), but the majority of these studies have been conducted on mammalian skin (Proksch et al., 2008). Such state of affairs leaves us with many diverse, prevalent, and evolutionarily successful vertebrate clades unstudied when it comes to skin barrier function. Importantly, the skin of vertebrates differs with habitat, lifestyle and ecto/endothermy. Therefore, it is important to examine the various functions of the skin in vertebrates other than mammals. Fishes, specifically teleost fishes, are the largest group of extant vertebrates that are economically important, with worldwide aquaculture production surpassing $150 billion in 2015 (Globefish database, http://www.globefish.org/, FAO Fisheries and Aquaculture Department, accessed 31 July 2017). Therefore, understanding the physiology of teleost skin could greatly benefit the sustainability of fish farming and the maintenance of fish health. For example, aquaculture vaccination practices already involve the immersion of fishes in hyperosmotic water to more effectively uptake vaccines (Huising et al., 2003). However, the mechanisms behind how a salinity change can increase vaccine uptake are not fully understood. In addition to this, due to human anthropogenic activities, heavy metal concentrations have increased in lakes, rivers, and other bodies of water around the world (Wood et al., 2011). Fishes

are known to bioaccumulate heavy metals from the surrounding water through osmoregulatory organs, including the skin (Kennedy, 2011; Wood et al., 2011). Indeed, the skin of various teleosts was found to bioaccumulate zinc, copper, and iron in a region-specific manner and the bioaccumulation of these metals in the skin was higher than in the muscle (Singh et al., 1991). Heavy metals have been found to be far less toxic to fishes in FW and they have been found to affect TJ protein abundance in the intestine of the grass carp, *Ctenopharyngodon idella* (Wood et al., 2011; Jiang et al., 2016). Despite these data, the role of the skin, and of skin TJ proteins, in heavy metal bioaccumulation has not been investigated. Thus, studying the molecular components of the skin barrier function can help elucidate the mechanisms behind heavy metal bioaccumulation, as well as vaccinations in fishes that may employ skin as a conduit.

In addition to the effects of salinity on the skin, it is important to understand the downstream effects of photoperiod on skin barrier function. Data from the present thesis (**Chapter 3**), indicated that peripheral organs, such as the skin, can exhibit circadian-like rhythms in TJ protein transcript abundance. Examining the effect of photoperiod is important for aquaculture because fishes can be farmed outside of their usual habitat (e.g. in indoor tanks). These different farming conditions may result in different photoperiods that the fish skin is exposed to. Indeed, multiple studies on fishes have found that artificially adjusting photoperiod could control the growth, reproduction, and feeding of various teleosts (Hansen et al., 2001; Taylor et al., 2006; Crovatto-Veras et al., 2013). However, the effects of different photoperiod conditions on the skin barrier function has received little attention. A study by Valenzuela et al. (2012) found that altering the LD cycle to 24:0 LD or 14:10 LD for 60 days led to increased infection from commensal bacteria and development of lesions on the skin. Despite the known effects of photoperiod on farmed fishes, how the alteration of photoperiod can influence skin barrier properties is not fully

understood. The oscillation of TJ proteins in the skin with photoperiod (**Chapter 3**) may be linked to skin barrier dysregulation with exposure to altered LD cycles, but more studies should be conducted in this area.

Another aquaculture-relevant application to the study of photoperiod on skin barrier properties is feeding regulation. If skin permeability fluctuates during the LD cycle, fish can be fed during the day at a time when their skin is less permeable to ion loss. Consequently, they can be fed less food at this time and will need to spend less energy to uptake ions from FW in order to maintain homeostasis. Instead, they can spend this energy on growth. Considering the fact that the LD cycle can alter feeding behaviour (Taylor et al., 2006; Crovatto-Veras et al., 2013), an optimal time point can be established for when the fish are likely to feed voraciously and retain most of the ingested ions. Therefore, studying the barrier function of the skin with changes in photoperiod is an important avenue of research that should be explored further.

Like teleost fishes, amphibians are valuable indicators of environmental health. In addition to this, many amphibians are semi-aquatic and thus provide an insight into skin barrier function in the aquatic and terrestrial environments. Despite being terrestrial air-breathers, many amphibians require an aquatic environment to osmoregulate. To date, TJ proteins of amphibians have been examined mostly in the context of development (Fesenko et al., 2000; Yamagishi et al., 2010; Sun et al., 2015), and very few studies have examined the osmoregulatory role of TJ proteins in amphibians, especially in the skin. Therefore, understanding the function of TJ proteins in regulating the barrier properties of amphibian skin is a logical next step in amphibian osmoregulation research. This is even more relevant given that large emphasis is being placed on controlling the spread of *Bd* infection among amphibian species and no preventative treatments, such as immunization, have been effective at inhibiting its spread to date (Stice and Briggs, 2010).

Interestingly, the permeability of epithelial tissues has been gaining attention as a target of disease prevention (Bischoff et al., 2014). Therefore, understanding how the permeability of amphibian skin is regulated, and how *Bd* affects skin permeability, may help prevent the spread of this disease in the future.

Another interesting avenue of study with amphibians is to compare the skin of fully aquatic amphibian larvae to that of semi-aquatic or terrestrial adults, especially in the context of *Bd* infection. Recall that the skin of adult frogs is keratinized, meaning that keratin proteins, intermediate filaments that provide structure and strength to skin cells, accumulate in the outermost layers of the skin (Colville and Bassert, 2002). Thus, keratins also help to establish the barrier properties of the skin. Unlike adult amphibian skin, larval skin is not keratinized, therefore *Bd* is unable to infect it (Olsen et al., 2004). Larval amphibians have keratinized mouthparts, which is the only location that the fungus takes root, and the larvae do not die with infection (Marantelli et al., 2004). Instead, amphibians infected as larvae die following metamorphosis, when the infection spreads to the keratinized skin (Berger et al., 1998). Therefore, it is the disruption of skin function in amphibians that leads to the death of the animal. However, although research groups have observed the translocation of *Bd* from the mouthparts of larvae to the skin of adults (Marantelli et al., 2004; McMahon and Rohr, 2015), no studies have examined the molecular mechanisms behind this transition and the interaction of *Bd* with keratin. Amphibians have recently been found to express dozens of keratin proteins (Suzuki et al., 2017), but their individual functions and interaction with *Bd* have yet to be examined. Additionally, in mammals, one type of keratin protein has been found to interact with Cldn-1 (DiTomasso et al., 2014), which suggests that there may also be a link between keratins and Cldns in the skin of amphibians. Therefore, *Bd* infection may

alter the complex interplay between different barrier-forming proteins in the adult amphibian skin, which would need to be investigated further.

5.4 Development of barrier properties in the dorsal and ventral skin regions

A difference in dorsoventral skin permeability has been observed in vertebrates such as amphibians (Bentley and Yorio, 1976; see **Chapter 3**), mammals (Bronaugh et al., 1983), and now in fishes (**Chapter 2**). It is interesting to see this trend persist throughout vertebrate classes, regardless of their habitats (aquatic/terrestrial) and skin modifications (e.g. fur, scales). It would be interesting to examine different animal models to understand why inherent difference in dorsal and ventral skin permeability exist in vertebrates.

One potential explanation for these spatial differences in skin permeability is that they are a result of vertebrate development. During development, cells in the vicinity of the dorsal and ventral epidermis could affect the differential development of these two regions and provide them with different properties. For example, the dorsal skin is always closer to the developing spinal cord, whereas the ventral skin is closer to the developing gastrointestinal tract. Cells within these regions may release specific cytokines that influence the regional differences in dorsal and ventral skin properties. A recent review by Sriram et al. (2015) on dermal fibroblasts, multifunctional cells that form the extracellular matrix and aid in skin healing, reported that this phenomenon may indeed be occurring. Dermal fibroblasts develop in a region-specific manner and possess varying functions that influence epidermal differentiation and morphogenesis (Sriram et al., 2015). For example, in birds, when epidermis from a scale-forming area (e.g. feet) is placed onto the dermis of a feather-forming area of the body during development, feathers develop instead of scales (Sriram et al. 2015). Therefore, the present work could be translated into a different field of

comparative studies—developmental biology—that may explain the differences in dorsal and ventral skin barrier properties of vertebrates.

5.5 Development of epidermal cell culture models

Given that the epidermis is a heterogeneous tissue, it is difficult to attribute responses to external stimuli to a particular cell type in *ex vivo* and *in vivo* experiments. Although cell culture models have been created for the human epidermis (Netzlaff et al., 2005), cell culture models have yet to be developed for the skin of other vertebrates that allow for the measure of permeability. A fish skin cell culture model has been developed in the past (Eyngor et al., 2007), however, the peak resistance of this model was only ~160 $\Omega*cm^2$, whereas typical peak resistance of the primary cultured gill epithelium is about 1000-3000 $\Omega*cm^2$, and freshwater fish skin has been reported to have >2000 $\Omega*cm^2$ resistance (Foskett et al., 1981). Therefore, cell culture models of the epidermis for vertebrates such as fishes and amphibians still need to be elucidated in order to effectively measure skin barrier properties. With the development of skin cell culture models the function of specific TJ proteins can be elucidated using knockdown studies. Although similar loss-of-function studies have been performed in other cultured epithelia (e.g., the gill epithelium; Kolosov and Kelly, 2017; Kolosov et al., 2017), the TJ makeup of these tissues is different from that of the skin. Therefore, a compensatory response mounted by the TJ protein mosaic to individual Cldn knockdowns in the cultured gill epithelium may be different to the compensatory response mounted in cultured skin. Additionally, the effects of external factors (e.g. salinity, photoperiod, infection) and endogenous factors (e.g. hormones) on particular cell types and proteins can be better delineated. It would also be prudent to create cell culture models of both the dorsal and ventral skin, given that their response to one factor could differ drastically. For example, cell

culture models of *Xenopus* dorsal and ventral epidermis have been developed by the Katzenback lab at the University of Waterloo (Dr. Barb Katzenback, personal communication). Therefore, the development of cell culture models for the skin could greatly advance the understanding of skin barrier properties.

5.6 The skin as a model organ: practical considerations

Vertebrate skin is a flat structure, which makes it easy to work with in *ex vivo* experiments, such as mounting it in a diffusion chamber and measuring its permeability. In the past, the flat structure of the skin has been exploited with the use of the opercular skin (i.e. skin covering the operculum which overlays the gills), as a model for the gills (Karnaky and Kinter, 1977; Marshall et al., 1997). Opercular skin possesses ion transporters similar to those found in the fish gill epithelium, however, the structure of the operculum is not as architecturally complex as the gills. Therefore, it was much easier to measure ion flux across the operculum, prior to the development of the primary cultured gill epithelial models (Wood and Pärt, 1997).

Of all vertebrate skin structures, the skin of fishes is useful to work with in particular, because it possesses live cells at the surface, allowing for whole-mount imaging and visualization of epidermal cells. In this thesis, TJ proteins in the fish epidermis were much easier to visualize from a "top down" view than those in the frog skin. Fish skin required only fixation and incubation with antibodies, whereas the frog epidermis had to be sectioned sagittally to obtain a "whole mount" view of the *stratum granulosum*, which expressed TJ proteins (**Illustration 5.1**). The challenge of visualising the live cell layers in amphibian skin can be circumvented by utilising epidermal cell culture models of amphibian skin, however, those have yet to be developed.

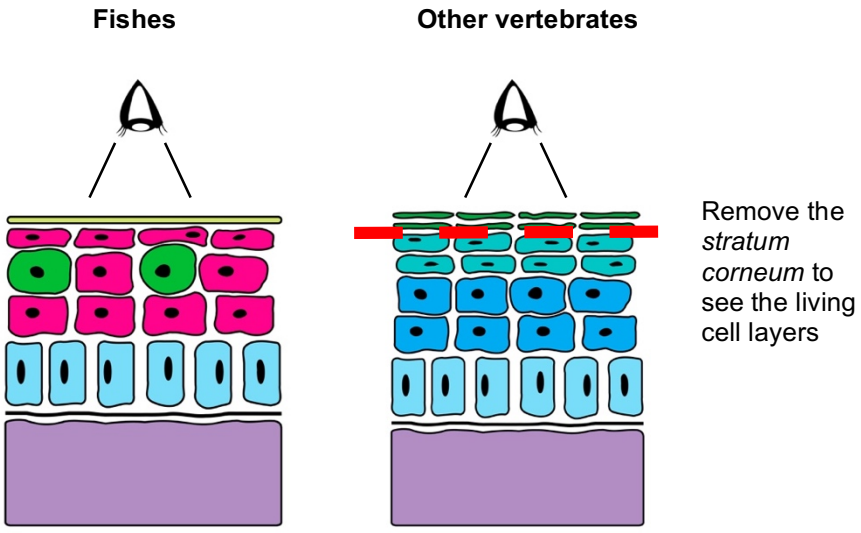

Illustration 5.1 The live cells of the fish epidermis can be visualized directly, whereas the *stratum corneum* must be removed from skin of other vertebrates to visualize the live epidermal cells.

In addition to visualising TJ proteins in fish skin, live cell staining could be performed on the skin to observe living cells in real time. Indeed, live cell staining has already been performed on neuromasts, which are mechanosensory structure in the skin of fishes (Nakae et al., 2012). Therefore, the ease of visualization of cells and proteins in the fish skin makes it an especially useful skin model to work with.

The studies presented in the previous chapters are also important for future osmoregulatory research. Given that the teleost skin was able to respond dynamically to a salinity change (see **Chapter 2**), this organ should be taken into consideration whenever whole-animal osmoregulation is examined. The results in this thesis, and in the published work examining the region-specific response of fish skin to an osmoregulatory hormone (i.e. cortisol; Gauberg et al., 2017), indicate that an osmoregulatory response in fishes will include physiological and molecular changes to the skin. Additionally, future studies on TJ proteins in the fish skin, and on other osmoregulatory

organs such as the gills (Cuciureanu, A., unpublished findings), should consider the time of day that the fishes were sampled because TJ protein transcript abundance may change over a 24-hour period (see **Chapter 3**). Ideally, all animals in a cohort should be sampled at the same time of day to avoid variation in TJ protein mRNA abundance. Additionally, control and experimental animals must be sampled within 4 hours of each other, avoiding times where the lights turn on/off, to ensure that any observed changes are the result of the experimental conditions and not due to normal circadian fluctuations. Finally, future studies on vertebrate skin should examine both dorsal and ventral regions when exposing the skin to an exogenous or endogenous factor. Therefore, the current work has significance on future studies in the field of osmoregulatory research and illustrates practical considerations that should be taken into account when working with vertebrate skin.

5.7 References

Bentley, P.J., Yorio, T., 1976. The passive permeability of the skin of anuran amphibia: a comparison of frogs (*Rana pipiens*) and toads (*Bufo marinus*). J. Physiol. 261, 603-l5.

Berger, L., Speare, R., Daszak, P., Green, D. E., Cunningham, A. A., Goggin, C. L., Slocombe, R., Ragan, M. A., Hyatt, A. D., McDonald, K. R., Hines, H. B., Lips, K. R., Marantelli, G. and Parkes, H., 1998. Chytridiomycosis causes amphibian mortality associated with population declines in the rain forests of Australia and Central America. Proc. Natl. Acad. Sci. USA 95: 9031~036.

Berthelot, C., Brunet, F., Chalopin, D., Juanchich, A., Bernard, M., Noël, B., Bento, P., Da Silva, C., Labadie, K., Alberti, A., Aury, J.-M., Louis, A., Dehais, P., Bardou, P., Montfort, J., Klopp, C., Cabau, C., Gaspin, C., Thorgaard, G.H., Boussaha, M., Quillet, E., Guyomard, R., Galiana, D., Bobe, J., Volff, J.-N., Genêt, C., Wincker, P., Jaillon, O., Roest Crollius, H., Guiguen, Y., 2014. The rainbow trout genome provides novel insights into evolution after whole-genome duplication in vertebrates. Nat. Commun. 5, 3657.

Bischoff, S.C., Barbara, G., Buurman, W., Ockhuizen, T., Schulzke, J.-D., Serino, M., Tilg, H., Watson, A., Wells, J.M., 2014. Intestinal permeability – a new target for disease prevention and therapy. BMC Gastroenterol. 14, 189.

Bronaugh, R.L., Stewart, R.F., Congdon, E.R., 1983. Differences in permeability of rat skin related to sex and body site. J. Soc. Cosmet. Chem 34, 127–135.

Bui, P., Kelly, S.P., 2014. Claudin-6, -10d and -10e contribute to seawater acclimation in the euryhaline puffer fish *Tetraodon nigroviridis*. J. Exp. Biol. 217, 1758–67.

Colville, T.P., Bassert, J.M., 2002. Clinical anatomy and physiology for veterinary technicians. St. Louis: Mosby. pp. 149-156.

Crovatto-Veras, G., Solis-Murgas, L.D., Vieira-Rosa, P., Gilberto-Zangeronimo, M., da Silva-Ferreira, M.S., Solis-De Leon, J.A., 2013. Effect of photoperiod on locomotor activity, growth, feed efficiency and gonadal development of Nile tilapia. Rev. Bras. Zootec. 42, 844–849.

DiTommaso, T., Cottle, D.L., Pearson, H.B., Schlüter, H., Kaur, P., Humbert, P.O., Smyth, I.M., 2014. Keratin 76 is required for tight junction function and maintenance of the skin barrier. PLoS Genet. 10.

Eyngor, M., Chilmonczyk, S., Zlotkin, A., Manuali, E., Lahav, D., Ghittino, C., Shapira, R., Hurvitz, A., Eldar, A., 2007. Transcytosis of *Streptococcus iniae* through skin epithelial barriers: an in vitro study. FEMS Microbiol. Lett. 277, 238–48.

Fesenko, I., Kurth, T., Sheth, B., Fleming, T.P., Citi, S., Hausen, P., 2000. Tight junction biogenesis in the early *Xenopus* embryo. Mech. Dev. 96, 51–65.

Foskett, J.., Logsdon, C.D., Turner, T., Machen, T.E., Bern, H.A., 1981. Differentiation of the chloride extrusion mechanisms during seawater adaptation of a teleost fish, the cichlid *Sarotherodon mossambicus*. J. Exp. Biol. 93, 209–224.

Gauberg, J., Kolosov, D., Kelly, S.P., 2017. Claudin tight junction proteins in rainbow trout (*Oncorhynchus mykiss*) skin: Spatial response to elevated cortisol levels. Gen. Comp. Endocrinol. 240, 214–226.

Hansen, T., Karlsen, Ø., Taranger, G.L., Hemre, G.I., Holm, J.C., Kjesbu, O.S., 2001. Growth, gonadal development and spawning time of Atlantic cod (*Gadus morhua*) reared under different photoperiods. Aquaculture 203, 51–67.

Huising, M.O., Guichelaar, T., Hoek, C., Verburg-van Kemenade, B.M.L., Flik, G., Savelkoul, H.F.J., Rombout, J.H.W.M., 2003. Increased efficacy of immersion vaccination in fish with hyperosmotic pretreatment. Vaccine 21, 4178–4193.

Jiang, W.D., Qu, B., Feng, L., Jiang, J., Kuang, S.Y., Wu, P., Tang, L., Tang, W.N., Zhang, Y.A., Zhou, X.Q., Liu, Y., 2016. Histidine prevents Cu-induced oxidative stress and the associated decreases in mRNA from encoding tight junction proteins in the intestine of grass carp (*Ctenopharyngodon idella*). PLoS One 11, 1–19.

Karnaky, K.J., Kinter, W.B., 1977. Killifish opercular skin - flat epithelium with a high-density of chloride cells. J. Exp. Zool. 199, 355–364.

Kennedy, C.J., 2011. The toxicology of metals in fishes, in Encyclopedia of Fish Physiology: From Genome to Environment. In: Farrell, A.P. (Ed.), 3. Academic Press, San Diego, Calif, USA, pp. 2061–2068.

Kolosov, D., Chasiotis, H., Kelly, S.P., 2014. Tight junction protein gene expression patterns and changes in transcript abundance during development of model fish gill epithelia. J. Exp. Biol. 217, 1667–81.

Kolosov, D., Donini, A., Kelly, S.P., 2017. Claudin-31 contributes to corticosteroid-induced alterations in the barrier properties of the gill epithelium. Mol. Cell. Endocrinol. 439, 457–466.

Kolosov, D., Kelly, S.P., 2017. Claudin-8d is a cortisol-responsive barrier protein in the gill epithelium of trout. J. Mol. Endocrinol. 59, 1–12.

Lillywhite, H.B., 2006. Water relations of tetrapod integument. J. Exp. Biol. 209, 202–26.

Loh, Y.H., Christoffels, A., Brenner, S., Hunziker, W., Venkatesh, B., 2004. Extensive expansion of the claudin gene family in the teleost fish , *Fugu rubripes*. Genome Res. 1248–1257.

Marantelli, G., Berger, L., Speare, R., Keegan, L., 2004. Distribution of the amphibian chytrid *Batrachochytrium dendrobatidis* and keratin during tadpole development. Pacific Conserv. Biol. 10, 173–179.

Marshall, W.S., Bryson, S.E., Darling, P., Written, C., Patrick, M., Wilkie, M., Wood, C.M., Buckland-Nicks, J., 1997. NaCl transport and ultrastructure of opercular epithelium from a freshwater-adapted euryhaline teleost, *Fundulus heteroclitus*. J. Exp. Zool. 277, 23–37.

McMahon, T.A., Rohr, J.R., 2015. Transition of chytrid fungus infection from mouthparts to hind limbs during amphibian metamorphosis. Ecohealth 12, 188–193.

Nakae, M., Asaoka, R., Wada, H., Sasaki, K., 2012. Fluorescent dye staining of neuromasts in live fishes: an aid to systematic studies. Ichthyol. Res. 59, 286–290.

Netzlaff, F., Lehr, C.M., Wertz, P.W., Schaefer, U.F., 2005. The human epidermis models EpiSkin, SkinEthic and EpiDerm: An evaluation of morphology and their suitability for testing phototoxicity, irritancy, corrosivity, and substance transport. Eur. J. Pharm. Biopharm. 60, 167–178.

Olsen, V., Hyatt, A.D., Boyle, D.G., Mendez, D., 2004. Co-localisation of *Batrachochytrium dendrobatidis* and keratin for enhanced diagnosis of chytridiomycosis in frogs. Dis. Aquat. Organ. 61, 85–88.

Proksch, E., Brandner, J.M., Jensen, J.M., 2008. The skin: An indispensable barrier. Exp. Dermatol. 17, 1063–1072.

Schmid, M., Evans, B.J., Bogart, J.P., 2015. Polyploidy in Amphibia. Cytogenet. Genome Res. 145, 315–330.

Singh, J.G., Chang-Yen, I., Stoute, V.A., Chatergoon, L., 1991. Distribution of selected heavy metals in skin and muscle of five tropical marine fishes. Environ. Pollut. 69, 203–215.

Sriram, G., Bigliardi, P.L., Bigliardi-Qi, M., 2015. Fibroblast heterogeneity and its implications for engineering organotypic skin models in vitro. Eur. J. Cell Biol. 94, 483–512.

Stice, M.J., Briggs, C.J., 2010. Immunization is ineffective at preventing infection and mortality due to the amphibian chytrid fungus *Batrachochytrium dendrobatidis*. J. Wildl. Dis. 46, 70–7.

Sun, J., Wang, X., Li, C., Mao, B., 2015. *Xenopus* Claudin-6 is required for embryonic pronephros morphogenesis and terminal differentiation. Biochem. Biophys. Res. Commun. 462, 178–83.

Suzuki, K. ichi T., Suzuki, M., Shigeta, M., Fortriede, J.D., Takahashi, S., Mawaribuchi, S., Yamamoto, T., Taira, M., Fukui, A., 2017. Clustered *Xenopus* keratin genes: A genomic, transcriptomic, and proteomic analysis. Dev. Biol. 426, 384–392.

Taylor, J.F., North, B.P., Porter, M.J.R., Bromage, N.R., Migaud, H., 2006. Photoperiod can be used to enhance growth and improve feeding efficiency in farmed rainbow trout, *Oncorhynchus mykiss*. Aquaculture 256, 216–234.

Valenzuela, A., Campos, V., Yañez, F., Alveal, K., Gutiérrez, P., Rivas, M., Contreras, N., Klempau, A., Fernandez, I., Oyarzun, C., 2012. Application of artificial photoperiod in fish: A factor that increases susceptibility to infectious diseases? Fish Physiol. Biochem. 38, 943–950.

Wilkie, M.P., Morgan, T.P., Galvez, F., Smith, R.W., Kajimura, M., Ip, Y.K., Wood, C.M., 2007. The African lungfish (*Protopterus dolloi*): Ionoregulation and osmoregulation in a fish out of water. Physiol. Biochem. Zool. 80, 99–112.

Wood, C. M.; Part, P., 1997. Cultured branchial epithelia from freshwater fish gills. J. Exp. Biol. 200:1047-1059.

Wood, C.M., Farell, A., Brauner C.J., 2011. Fish Physiology: Homeostasis and Toxicology of Essential Metals, Volume 31A. Academic press. pp.24-27.

Yamagishi, M., Ito, Y., Ariizumi, T., Komazaki, S., Danno, H., Michiue, T., Asashima, M., 2010. Claudin5 genes encoding tight junction proteins are required for *Xenopus* heart formation. Dev. Growth Differ. 52, 665–675.